MECHANISMS OF GENE REGULATION IN NEMATODE VULVAL DEVELOPMENT

THE ROLE OF CHROMATIN REMODELING AND SIGNAL TRANSDUCTION IN *C. ELEGANS* AND *C. BRIGGSAE* VULVAL DEVELOPMENT

By

Philip Cumbo, B.Sc

A Thesis

Submitted to the School of Graduate Studies

in Partial Fulfillment of the Requirements

for the Degree

Master of Science

McMaster University

MASTER OF SCIENCE (2010) McMaster University

(Biology) Hamilton, Ontario

TITLE: The Role of Chromatin Remodeling and Signal Transduction In *C. elegans* and *C. briggsae* Vulval Development

AUTHOR: Philip Cumbo, B.Sc (McMaster University)

SUPERVISOR: Professor Bhagwati P. Gupta

NUMBER OF PAGES: ix, 131

Abstract

The *C. elegans* vulva is an established model system to understand how genes and pathways function to control organ formation. The precise mechanisms underlying vulval development are complex and require multiple layers of integration. These regulatory networks range from direct regulation of gene transcription through chromatin modification to activation or repression of downstream targets of signaling pathways. At the level of chromatin modification the *C. elegans* histone deacetylase, *hda-1*, plays an important role in repressing gene transcription. This work shows that *hda-1* mutants have defects in vulval invagination, morphogenesis, and gonadogenesis. Consistent with these phenotypes, *hda-1* is expressed in vulval cells and gonadal lineage cells in both *C. elegans* and *C. briggsae*. Furthermore, *hda-1* was found to regulate the expression of two transcription factors involved in uterine formation, *lin-11* and *egl-13*, and one gene involved in AC specification, *zmp-1*. *hda-1* also regulates *fos-1b* in vulval cells. With regards to cellular signaling we focused on the Wnt pathway component, *pry-1/Axin*. *pry-1* mutants are Muv and these ectopically induced VPCs in both *C. elegans* and *C. briggsae* adopt a secondary cell fate. This fate specification is independent of the gonad derived and LIN-12/Notch mediated lateral signals, indicating activated Wnt signaling alone can specify cell fates. *pry-1* mutants also exhibit a P7.p induction failure defect in both species. This defect is likely caused by LIN-12 signaling resulting in persistent expression of the MAP kinase phosphatase, *lip-1,* in P7.p and P8.p. Further examination revealed that P7.p induction in *pry-1; lip-1* and *pry-1; lin-12* double mutants was significantly increased. These results are consistent with our hypothesis that crosstalk

between Wnt and LIN-12/Notch are crucial to proper vulval formation. These experiments provide evidence that vulval development is regulated by a complex regulatory network that is evolutionary conserved between *C. elegans* and *C. briggsae*.

Acknowledgements

First and foremost, I would like to thank my supervisor Dr. Bhagwati P. Gupta for this wonderful experience and the opportunity to learn and work in his lab. Thank you for your guidance, support, and advice. I would also like to thank my committee members, Dr. Roger Jacobs and Dr. Andre Bedard for helpful comments and guidance.

This thesis is dedicated to the important people in my life. Mom, Dad, Monica, and Johncarlo thank you for your support and all that you have done for me. Steph, you inspire me and encourage me to be the best I can be. Words cannot describe the gratitude you deserve from me and I will be forever grateful to you, thank you.

I am indebted to my colleagues in the lab who have always been helpful and understanding. Anyone who has passed through our lab has helped me and made lab life exciting and fun. Your advice and ideas have enabled me to be successful and innovative.

Thanks to all of my friends, of which there are too many to name, but you know who you are. Although you may not have contributed to what is written here, you have helped maintain my sanity throughout this process.

Last but not least, I would like to thank the Phoenix Crew for making Graduate School enjoyable and exciting everyday. What you have done for me cannot be measured in numbers or letters. I will cherish the crazy ideas and random banter over the most useless topics. You have all become great friends to me and I look forward to many more "Friday" afternoons.

Figure Legend

Table Legend

Appendix Figure Legend

List of Abbreviations

Cel- Caenorhabditis elegans
Cbr- Caenorhabditis briggsae
AC- Anchor cell
VPC- Vulval precursor cell
Pn.p- Ventrolateral P cell epidermal progeny
L1 to L4- Larval stages
hyp7- Hypodermal syncitium 7
utse- Uterine-seam cell connection
HAT- Histone acetyltransferase
HDAC- Histone deacetylase
HMT- Histone methyltransferase
NuRD- Nucleosome remodeling and HDAC complex
SynMuv- Synthetic Multivulva
Vul- Vulvaless
Muv- Multivulva
GFP- Green Fluorescent Protein
Pvl- Protruding vulva
Unc- Uncoordinated
PCR- Polymerase Chain Reaction
RNAi- RNA interference
hsp- Heat shock promoter
TAP- Tandem Affinity Protein
qRT-PCR- Quantitative Real Time Polymerase Chain Reaction
VU- Ventral Uterine precursor

Chapter 1- Introduction

1.1 Background

There is a vast range of diversity among all living organisms which can be ultimately attributed to a single universal molecule, deoxyribonucleic acid (DNA). DNA is common to all organisms and encodes the very elements that control the size, shape, structure, and function of a living organism. Genes are made of nucleotides which are connected together in a double helix structure that is further wound and compacted to fit within the nucleus of a single cell. Millions of nucleotide bases are bound to each other in a very specific and complex order, which comprise the genes that encode proteins. Proteins are the building blocks of life, from contributing to cellular stability to providing enzymatic activity to catalyze reactions within the cell. Proteins are produced when genes are transcribed into ribonucleic acid (RNA) and that single stranded RNA molecule is translated into protein. To coordinate the transcription of millions of genes and regulate the temporal expression of specific genes during developmental processes requires a complex system of regulatory mechanisms. This regulation takes place at the DNA, RNA, and protein level. Two major components of gene regulatory networks occur at the level of DNA modification by chromatin remodelers and at the level of transcription by gene specific transcription factors (TFs). The characterization of gene regulatory networks requires an in depth dissection and perturbation of many important signaling pathways which cannot be fully achieved in humans due to the high degree of complexity associated with human development. To address this issue the widespread use of model

organisms has been implemented, which offer solutions to many of the problems associated with using a mammalian system.

1.2 *Caenorhabditis elegans* as a Model Organism

The study of living organisms, biology, would not have been able to progress to its current level of knowledge had it not been for the widespread use of genetic model organisms. Model organisms have been utilized to study everything from human diseases to fundamental biological processes, such as, cell commitment, cell proliferation, and cell division. Many key discoveries have been made in model organisms, such as the programmed cell death pathway in *C. elegans* that led to the discovery of the homologs that regulate the same pathway in humans (Conradt and Xue, 2005).

C. elegans was chosen as a model by Sydney Brenner (1974) for numerous reasons, including its ease of culturing and maintenance (Brenner, 1974). This hermaphroditic species of nematode thrives in laboratory conditions and is able to produce upwards of 300 progeny (substantially more when males are present) within very short period of time. In total, the *C. elegans* life cycle is complete within 3 days of hatching. A self fertilized egg is laid and hatches to form the L1 larva, which proceeds through the L2, L3, and L4 stages prior to becoming an adult worm in a normally growing culture that has plenty of *E. coli* as a food source. Under certain conditions where there is a lack of food or overcrowding of the culture, *C. elegans* is able to transition into a dauer stage before it enters into the L3 stage, where they can survive for

months, then re-enter the normal life cycle when conditions improve (Brenner, 1974). Adding to its many positive attributes, *C. elegans* can be frozen in liquid nitrogen for many years for preservation, and can be thawed to establish a growing culture when needed. Another attribute to *C. elegans* as a model organism is one that not many models possess, it is transparent and single cells can be visualized using differential interference contrast (DIC) microscopy. The ability to observe single cells has allowed for easy manipulations that could otherwise not be possible, including single cell laser ablation and visualization of cell migrations (Kimble and Hirsh, 1979; Sulston and White, 1980).

This particular soil nematode is the first and only animal to have its complete cell lineage known and mapped (Kimble and Hirsh, 1979; Sulston and Horvitz, 1977b; Sulston et al., 1983). After the somatic, gonadal, and embryonic lineages were characterized and counted, minus the 131 cells in the hermaphrodite that undergo programmed cell death, the final number of cells in an adult hermaphrodite was determined to be 959, while in the adult male the total was determined to be 1031 cells (Sulston and Horvitz, 1977a). To further complement the absolute number of cells determined by the cell lineage, Sulston and Horvitz (1977) discovered that this lineage was invariant in both number of cells and the position of those cells (Sulston and Horvitz, 1977a). This laid the groundwork for the use of this organism as a model for many developmental processes. This crucial work is important because when a cell divides, where it migrates, and where its position is in the adult is known. Since this information is

the same in every wildtype animal, it allowed researchers to study how mutations in a variety of genes affected the position and morphology of cells.

1.3 *C. elegans* Vulval Development

The invariant cell lineage and position was particularly important in the establishment of the hermaphrodite vulva as model for organogenesis. At hatching 12 ventrolateral P (Pn) cells lie along the larvae, 6 on each side and during the L1 stage these 12 Pn cells migrate to the ventral nerve cord (Sulston et al., 1983). At the mid-L1 stage the Pn cells divide to give an anterior daughter cell (Pn.a) and a posterior daughter cell (Pn.p) which give rise to neuronal cells and hypodermal cells, respectively (Sulston et al., 1983). Of the 12 Pn.p cells, P(1-2).p and P(9-11).p fuse to the hypodermal syncitium, hyp7, in the late L1 stage and the remaining P(3-8).p cells remain unfused and become the vulval precursor cells (VPCs), which are the vulval competence group (Sulston and Horvitz, 1977b). In 50% of animals P3.p fuses to hyp7 in the L2 stage, while P4.p and P8.p normally fuse to hyp7 in the L3 stage (Sulston and Horvitz, 1977b). These six VPCs are called the vulval competence group because they are all able to respond to inductive vulval signaling to form the adult vulva, yet in wildtype animals only P(5-7).p undergo divisions to form the adult vulva (Sulston and Horvitz, 1977b) (Figure 1). The ability to respond to inductive signaling to form the adult vulva was tested by means of laser ablation of each VPC and finding that any of P(3-8).p can form vulval cells (Kimble, 1981; Sternberg and Horvitz, 1986; Sulston and White, 1980). The VPCs, through signaling interactions, adopt either a 1^{o}, 2^{o}, or 3^{o} cell fate, where 3^{o} cells only divide once

then fuse to the hyp7, while 1^{o} and 2^{o} cells divide 3 times to form the adult vulva (Sternberg, 2005). These fates are acquired in a specific and invariant pattern of 3^{o}-3^{o}-2^{o}-1^{o}-2^{o}-3^{o}, corresponding to P(3-8).p (Sternberg, 2005). Through these subsequent divisions, P(5-7).p form the adult vulva consisting of 22 cells comprising 7 different cell types, vulA to vulF in a symmetrical manner (Sternberg, 2005). vulE and vulF cells comprise the 1^{o} lineage as daughter cells of P6.p, while vulA, B, C, and D cells comprise the 2^{o} lineage as daughters of P5.p and P7.p (Sternberg, 2005) (Figure 1). The mid-L4 stage represents a specific stage to clearly visualize all 7 cell types in different focal planes that form a clear Christmas tree like shape (Figure 2). Following the invasion of the anchor cell (AC) (a gonadal cell involved in vulval morphogenesis) into the vulval epithelium, the adult vulval cells fuse with their corresponding partners to form 7 toroidal rings which attach to vulval muscles and undergo extensive morphogenetic changes resulting in the formation of the adult hermaphrodite vulva (Sherwood and Sternberg, 2003; Sternberg, 2005). Another aspect critical to vulval development lies physically above the vulva in the vulva-uterine connection. Crucial to the ability to properly mate and lay eggs is the formation of a thin membrane called the uterine-seam cell (utse) connection (Sternberg, 2005). This membrane is formed by the fusion of the AC with the uterine π progeny, which results in a fully functioning organ that is able to lay eggs and mate proficiently (Sternberg, 2005). The ability to temporally coordinate these events and specify cell fates in a highly regulated manner is a complex yet elegant process. This complex process is buried beneath multiple layers of regulation, which include chromatin remodeling and cell signaling events.

1.4 Signaling Crosstalk during Vulval Development

Integration of multiple signals is necessary for the proper development of tissues and organs. Complex cellular processes that underlie development involve numerous inputs that interact with each other and play essential roles in specifying and determining cell fate. *C. elegans* vulva development provides a tool to study the integration of these signals. Three conserved signaling pathways converge during vulval development and interact with one another to produce the stereotypical and robust vulval phenotype seen in *C. elegans* and *C. briggsae*. Ras, Notch, and Wnt signaling all play roles in vulval development as described above, and their interactions with one another have also been characterized. The Ras-Notch interaction during vulval development has been the most investigated, while the Wnt-Ras interaction has been described in lesser detail, and finally the Notch-Wnt interaction has not been investigated in vulval development.

1.4.1 Ras-Notch pathway crosstalk in vulval development

The AC emits a LIN-3 graded signal to the underlying VPCs to induce the activation of the Ras signaling pathway. Other than activating 1^{o} fate specific genes in P6.p, Ras signaling is crucial in activating the lateral signal from P6.p to the neighbouring P5.p and P7.p. Ras signaling induces the transcription of LIN-12 DSL family ligands (Delta, Serrate, and Lag family). Specifically, *lag-2, apx-1,* and *dsl-1* are upregulated in response to Ras signaling in P6.p (Chen and Greenwald, 2004). The upregulation of these genes is dependant on the activity of the Mediator complex component SUR-2 (Chen and Greenwald, 2004). Furthermore, expression of the DSL ligands is not sufficient to induce

the proper lateral signaling between P6.p and its neighbours. LIN-12 must be internalized by P6.p to prevent an autocrine signaling cascade from taking place within P6.p. LIN-12 has an intracellular downregulation targeting sequence (DTS) that is required for the proper internalization and endocytosis of LIN-12 (Shaye and Greenwald, 2002). Shaye and Greenwald show that if the DTS is removed and LIN-12 is stabilized in the cell membrane of P6.p, lateral signaling is compromised (2002). The proper degradation of LIN-12 requires the action of SUR-2, and lateral signaling is reduced when SUR-2 function is inhibited (Shaye and Greenwald, 2002). Although LIN-12 is degraded in P6.p after internalization in wildtype animals, the internalization of LIN-12 is the required step in order to permit lateral signaling (Shaye and Greenwald, 2005). Animals expressing an altered LIN-12 protein that allows for the internalization, but not degradation of LIN-12 results in proper lateral signaling, which provides evidence that internalization is the limiting step in lateral signaling between P6.p and its neighbours (Shaye and Greenwald, 2005). Once the *lin-12* signaling pathway is activated by the DSL ligands in P5.p and P7.p, certain genes that are known to be repressors of the Ras pathway are upregulated in these VPCs. Two groups have shown that there are numerous genes that are upregulated in response to the *lin-12* signal and many of these genes act as negative regulators of the EGFR-MAPK pathway in presumptive 2^{o} fate cells (Berset et al., 2001; Yoo et al., 2004). These two groups have identified seven genes that have the ability to suppress Ras signaling, namely, *ark-1, dpy-23, lst-1, lst-2, lst-3, lst-4,* and *lip-1* (Berset et al., 2001; Yoo et al., 2004). This allows for the *lin-12* pathway to properly assign the 2^{o} fate on

VPCs by activating the transcription of target genes by interacting with the transcription factor, LAG-1.

1.4.2 Wnt-Ras pathway crosstalk in vulval development

The HOX gene, *lin-39*, is involved the proper development of the *C. elegans* vulval by maintaining VPC competence which allows the VPCs to respond to the inductive and lateral signals required to pattern the hermaphrodite vulva. Since *lin-39* plays an essential role in vulva development, it is not surprising that its expression is regulated by multiple signaling pathways, including Ras and Wnt. Maloof and Kenyon (1998) were able to show that *lin-39* is upregulated in response to the Ras signaling pathway in P(5-7).p. They were also able to show that reduction of the Ras signaling pathway in P(5-7).p results in downregulation of *lin-39* in these VPCs (Maloof and Kenyon, 1998). Eisenmann and colleagues (1998) described the upregulation of *lin-39* in response to Wnt signaling in P(3-8).p using *pry-1* mutants that have a constitutive activation of the Wnt signaling pathway. Conversely, they were able to show that when Wnt signaling is compromised by eliminating *bar-1*/β-catenin activity, *lin-39* expression was accordingly downregulated (Eisenmann et al., 1998). To connect the two pathways Eisenmann and colleagues performed epistasis experiments with *bar-1(ga80)* loss of function mutants and *let-23*/RTK loss of function mutants (1998). *bar-1(ga80); let-23(sy1)* double mutants showed an increase in the adoption of the F fate in P(5-7).p when compared to either the *bar-1(ga80)* or *let-23(sy1)* mutants alone (Eisenmann et al., 1998). This experiment shows the overlapping function of Wnt and Ras signaling in vulval development where both pathways play partial roles in regulating *lin-39* levels and maintaining VPC competence.

1.5 The Role of Chromatin Remodeling in Gene Expression and Vulva Development

Each cell of every living organism contains millions of nucleotides bound to each other and paired with a complimentary strand in an anti-parallel fashion then wound into a double helix structure called DNA. DNA encodes thousands of genes that are essential to producing a fully functioning organism. The sheer length and size of an entire eukaryotic genome would make it impossible to fit it into a single cell, let alone a single nucleus. To aid in the compaction of DNA the cell has devised an intricate and complex framework to wind the DNA around proteins, which are further compacted into high order structures through interactions between the proteins that the DNA is wound around. This condensed and packaged DNA is called chromatin, which not only provides an efficient way to package DNA, but also bestows ultimate control DNA mediated processes within the cell since the higher order structure of chromatin hinders the access of proteins that are required to transcribe the DNA.

Eukaryotic nuclei contain genomic DNA that is packaged as chromatin through the use of histone proteins. 147 base pairs (bp) of DNA are wrapped almost twice around a complex of histones to form the nucleosome, which is the basic structure of chromatin (Peterson and Laniel, 2004). The histone complex forms in an octamer composed of a heterotetramer of histones H3 and H4, and two heterodimers of histones H2A and H2B (Peterson and Laniel, 2004). Each of these histone proteins have an amino terminal tail rich in basic residues of approximately 25-40 bases, while histone H2A has an additional

carboxy terminal tail of 37 bp (Cui and Han, 2005; Peterson and Laniel, 2004). Although these tails do not provide stability or structure to the nucleosomes, they are very important to modulating the higher order folding of nucleosomes and regulating access of transcription factors to the DNA. The compaction of chromatin can be altered through post-translational modifications of the histone tails described above. These modifications include acetylation and methylation of lysines (K) and arginines (R), phosphorylation of serines (S) and threonines (T), and ubiquitylation and sumoylation of lysines (Peterson and Laniel, 2004). Each of these post-translational marks serves to facilitate the binding of specific non-histone proteins to specific marks in order to allow or prevent the access of transcriptional proteins to the DNA (Peterson and Laniel, 2004). The binding of these non-histone proteins has been shown to require specific domains for specific types of marks, for instance, proteins with chromodomains bind to methylated lysines, while bromodomains bind to acetylated lysines (Peterson and Laniel, 2004). Four enzyme groups have been identified that are involved in regulating the placement of these post-translational modifications. These groups include histone acetyltransferases (HATs), histone deacetylases (HDACs), histone methyltransferases (HMTs), and histone kinases (Peterson and Laniel, 2004). Generally acetylation and phosphorylation are associated with transcriptional activation, while methylation and deacetylation are associated with repression. These modifications are specific to certain amino acids in the histone tails and can act differently between different amino acids, for instance, trimethylation of H3K4 is known to be associated with gene activity. Different outcomes that result from

modification of specific residues clearly show that chromatin modification is highly regulated.

To date, 18 HDACs have been identified in humans and are separated into four families, Class I, II, III, and IV (Johnstone, 2002). There are 4 members of class I, 6 members of class II, 7 members of class III, and a single member of class IV (Gao et al., 2002; Johnstone, 2002). Class I HDACs are known to be exclusively expressed within the nucleus and are the major components of two transcriptional repressor complexes, the SIN3-HDAC and NuRD-Mi2-NRD complexes (Johnstone, 2002). They are also classified based on their similarity with yeast deacetylase RPD3 (Fischle et al., 2001). Class II HDACs have been shown to shuttle between the nucleus and the cytoplasm and thus are not a constituent of either the SIN3-HDAC or NuRD-Mi2-NRD complexes (Fischle et al., 2001). Based on sequence similarity to the yeast Sir2 transcriptional repressor, class III HDACs were identified and shown to require the cofactor NAD^+ to perform its deacetylation activities (Imai et al., 2000). Finally, the single member of class IV, HDAC11, was identified through a databank search for homology with the yeast HOS3 protein, which is a unique member of the HDAC family but carries deacetylase motifs that are shared between class I and II HDACs (Gao et al., 2002). Of these identified human HDACs, many homologs have been identified in *C. elegans*. Currently there are 12 known *C. elegans* HDACs, consisting of 3 class I, 4 class II, 4 class III, and one putative class IV HDAC (Gregoretti et al., 2004).

1.5.1 Chromatin remodeling and the *C. elegans* vulva

The action of chromatin remodeling in relation to *C. elegans* vulva development was first realized through a set of elegant experiments which led to the discovery of the synthetic multivulva, SynMuv, phenotype. SynMuv is a phenotype that is described as requiring two discrete mutations in two separate genes that act synergistically to produce a multivulva phenotype, while either mutation on its own is not capable of producing a Muv phenotype (Ferguson and Horvitz, 1985; Horvitz and Sulston, 1980; Sulston and Horvitz, 1981). Since their discovery, numerous members of the SynMuv family have been identified and grouped into three distinct classes, A, B, and C. In most cases a member of one group must be mutant along with a member from another group to produce a Muv phenotype, while having two members of the same group being mutant does not produce this phenotype (Fay and Yochem, 2007). To date 34 SynMuv genes have been reported, 6 class A, 24 class B, and 4 class C type (Fay and Yochem, 2007). The overwhelming theme across all classes of SynMuv genes is transcriptional regulation, particularly in class B which contains multiple members involved in chromatin remodeling and histone modifications (Fay and Yochem, 2007). The majority of class B genes are known to be involved in transcriptional repression, while class C genes have been shown to be associated with transcriptional activation (Fay and Yochem, 2007). Class A genes are also implicated in regulating transcription through protein modification (Fay and Yochem, 2007). Of the SynMuv B genes, a few are of particular interest to vulva development because they have been shown to cause vulva morphogenesis and development defects.

Key components of important complexes known to regulate chromatin remodeling and histone modification are among the identified SynMuv B genes. All members that form the *C. elegans* DRM (DP, Rb, MyB) complex, which is orthologous to the *Drosophila* dREAM (RBF, E2F, and Myb interacting protein), are members of the SynMuvB class of genes (Harrison et al., 2006). Although the DRM complex does not have any members that are directly involved in chromatin remodeling or histone modification, it has been suggested that it requires histone deacetylase activity to deacetylate histone tails, thus allowing the DRM complex to bind to the unmodified histone tails to maintain transcriptional repression of local genes (Harrison et al., 2006). Fitting with this model is that among the identified SynMuv B genes are 3 components of the Nucleosome Remodeling and histone Deacetylase (NuRD) complex. These components are histone deacetylase 1 (*hda-1*), RbAp48 (Rb associated protein) (*lin-53*), and Mi-2 (CHD3 ATP dependent nucleosome remodeling protein) (*let-418*) (Lu and Horvitz, 1998; von Zelewsky et al., 2000). A unique aspect of the NuRD complex is that it embodies both a histone modifier in *hda-1* and an ATP dependent nucleosome remodeler in *let-418*/Mi-2 (Xue et al., 1998). Other components of the *C. elegans* NuRD complex are another histone deacetylase, HDAC2 (*hda-2*), the Rb associated protein RbAp46 (*rba-1*) and the human metastasis tumor associated gene MTA1 (*egl-27*), as well as other unidentified proteins (Solari and Ahringer, 2000).

1.5.2 The role the histone deacetylase, *hda-1*, in nematode development

hda-1 is a class I histone deacetylase that, as previously mentioned, is a core component of the NuRD complex. HDA-1 has been identified to play a role in endoderm differentiation during embryogenesis in conjunction with the acetyltranserase CBP-1 (Shi and Mello, 1998). This connection was made when researchers described a situation where CBP-1 is mutated, thus endoderm differentiation is defective, yet in the same mutant when HDA-1 is inhibited, endoderm differentiation is restored suggesting that CBP-1 promotes differentiation by counteracting HDA-1 (Shi and Mello, 1998). During early embryogenesis two cells are formed, the MS and E cells, which give rise to the mesoderm and the endoderm, respectively (Priess, 1994). Within the E lineage CBP-1 has been shown to overcome HDA-1 to activate a critical endoderm determining gene, *end-1* (Calvo et al., 2001). While within the MS lineage, the TCF/LEF factor POP-1 acts as a transcriptional repressor by recruiting the co-repressors HDA-1 and UNC-37 (Groucho) to inhibit *end-1* transcription, thus preventing the MS lineage from acquiring the E fate (Calvo et al., 2001). POP-1 is a member of the highly conserved Wnt signaling pathway, which, in the absence of a Wnt signal, acts as a transcriptional repressor by binding to DNA and recruiting its co-repressor Groucho (UNC-37), which has been shown to interact with HDA-1 in *Drosophila* (Calvo et al., 2001; Chen et al., 1999). Further work has been done showing the role *hda-1* plays in *C. elegans* in postembryonic development in gonadogenesis and axon pathfinding (Dufourcq et al., 2002; Zinovyeva et al., 2006). In *hda-1(e1795)* mutants gonad development is severely defective, thus causing sterility

(Dufourcq et al., 2002). *hda-1* was also found in the germline and knockdown of *hda-1* through RNAi results in embryonic lethality, thus identifying *hda-1* as being maternally contributed (Dufourcq et al., 2002). Another mutant, *hda-1(cw2),* was identified in a screen for candidates involved in nervous system development (Zinovyeva et al., 2006). *hda-1(cw2)* mutants are severely uncoordinated and have prominent defects in axon pathfinding and fasciculation, which was also found to be present in *hda-1(e1795)* mutants (Zinovyeva et al., 2006). Unlike *hda-1(e1795)* mutants, *hda-1(cw2)* homozygotes are viable and not sterile, but do have a smaller brood size than wildtype (Zinovyeva et al., 2006). Both mutations cause gonad defects along with defects in vulval morphogenesis and vulval induction, although the phenotype in *hda-1(cw2)* mutants is much weaker (Dufourcq et al., 2002; Zinovyeva et al., 2006). Interestingly, Dufourqc and colleagues also placed *hda-1* in the Notch pathway due to its derepression of the Notch ligand, *lag-2* (Dufourcq et al., 2002). They found that *lag-2* expression, which is normally expressed only in the distal tip cells and a few vulval cells, was globally expressed (Dufourcq et al., 2002). Using qRT-PCR they were able to measure the transcript levels of *lag-2* and found that in *hda-1* mutant animals, *lag-2* transcript levels increased significantly (Dufourcq et al., 2002).

Genetic analysis of vulval development has identified the role that SynMuv genes play in regulating vulval development through the repression of the Ras signaling pathway. In wildtype animals the AC produces an EGF-like inductive signal in the form of LIN-3, which binds to the LET-23 receptor in the underlying VPCs (Sternberg, 2005).

Through LET-23 signaling, the LET-60/Ras pathway is activated in VPCs that receive the LIN-3 inductive signal in a gradient dependent fashion, specifically, P6.p receives the greatest amount of LIN-3, while P5.p and P7.p receive a lesser amount, and an even lesser amount reaches the other VPCs (Figure 1). Once activated, the LET-60/Ras pathway transduces the signal through the MAP Kinase MPK-1, which negatively regulates the transcriptional repressors LIN-31 and LIN-1, and allows for the transcription of the target genes *lin-39* and *egl-17*. Cui and colleagues have investigated the role of *lin-3*, and found that double mutants for SynMuv A and SynMuv B that were exposed to *lin-3(RNAi)* showed a strong suppression of the SynMuv phenotype (Cui et al., 2006). Further analysis revealed that while the SynMuv B genes are expressed in the hyp7, they act to inhibit ectopic expression of *lin-3* to other VPCS and maintain the wildtype induction pattern of P(5-7).p (Cui et al., 2006). It has been shown that the SynMuv phenotype is due to the ectopic expression of *lin-3* which causes multiple inductions in normally uninduced VPCs (Cui et al., 2006). Thus, upstream of the Ras pathway in *C. elegans*, it is clear that the chromatin remodeling and histone modifiers of the SynMuvB class act to negatively regulate *lin-3* expression, thus repressing ectopic cellular proliferation, and subsequently vulval induction. The suppression of the Ras pathway by SynMuv genes is essential to maintain the correct VPC induction pattern, while other conserved signaling pathways, such as Wnt and Notch, play crucial roles in maintaining competence and specifying cell fates of VPCs. Studies of the regulation of Ras pathway suppression by SynMuv genes have been thorough, while Wnt interaction studies are

beginning to advance but require a more extensive characterization of the Wnt pathway itself before any significant progress can be made.

1.6 The Role of Wnt Signaling in Nematode Vulva Development

As mentioned above, the Wnt signaling pathway is a crucial regulator of vulval development. The canonical Wnt signaling pathway acts through the transcriptional regulator β-catenin. When the Wnt ligand interacts with the Frizzled receptor, β-catenin is stabilized and able to accumulate in the cytoplasm, then translocate to the nucleus, and interact with the TCF/LEF factors, which will modulate the transcription of its target genes. In the absence of the Wnt ligand, β-catenin is bound by the destruction complex, consisting of APC, Axin, GSK3-β, and CKI, and then is phosphorylated, ubiquitinated, and sent to the proteosome for degradation (Figure 3) (Eisenmann, 2005). Wnt signaling has been identified in *C. elegans* to control multiple processes throughout development in multiple tissues. Embryonic patterning has been shown to require Wnt signaling from the P2 cell to the EMS cell in order for the EMS to divide properly into the MS and E lineage as described above (See *hda-1* in development section) (Rocheleau et al., 1997; Thorpe et al., 1997). This signaling persists in the MS and E cell to correctly specify cell fate through the TCF/LEF factor, POP-1 as described previously (see The role of chromatin remodeling in gene expression and vulva development). Although this type of Wnt signaling utilizes a non-canonical pathway, it is still essential to maintain proper development of the animal. Other non-canonical Wnt signaling pathways are involved in the development of the gonad and T-cell polarity (Herman, 2001; Miskowski et al., 2001;

Rocheleau et al., 1999; Siegfried and Kimble, 2002; Sternberg and Horvitz, 1988). The canonical Wnt signaling pathway is also involved in numerous processes throughout development, including neuronal differentiation, male hook formation, and vulval development (Eisenmann and Kim, 1994; Gleason et al., 2002; Maloof et al., 1999; Salser and Kenyon, 1992; Yu et al., 2009).

There are several genes that encode Wnt components in *C. elegans* and they include the ligands, *lin-44, egl-2-, mom-2, cwn-1,* and *cwn-2*, the frizzled family of receptors, *lin-17, mom-5, mig-1,* and *cfz-2*, and Disheveled homologs, *mig-5, dsh-1,* and *dsh-2*. Other members found in *C. elegans* are the Porcupine homolog *mom-1*, the Casein Kinase I-α *kin-19*, and the GSK-3β homolog *gsk-3*. Unlike humans, the *C. elegans* genome is known to possess 4 β-catenins, *bar-1, wrm-1, hmp-2,* and *sys-1*, while only a single TCF/LEF factor *pop-1,* a single APC, *apr-1*, and a single Axin, *pry-1*, have been identified (Eisenmann, 2005; Gleason et al., 2002; Gleason et al., 2006; Inoue et al., 2004). The major targets of the Wnt signaling pathway are the Hox genes *lin-39* (*Deformed/Sex combs reduced, Dfd/Scr family), mab-5* (*Antennapedia/Ultrabithorax/Abdominal-A, Antp/Ubx/Abd-A family),* and *egl-5* (*Abdominal-B, Abd-B family*).

The competence of VPCs to respond to inductive signals is dependent on the expression of *lin-39.* In the L1 stage *lin-39* is expressed in P(3-8).p to prevent their fusion to the hyp7, then expressed again in the L2 stage in P(5-7).p, while P(3-4).p and P8.p fuse

to the hyp7. The L2 stage expression of *lin-39* is positively regulated by the BAR-1 mediated canonical Wnt signaling pathway. In *bar-1* loss of function mutants, *lin-39* expression is down regulated, causing VPCs to adopt the fused cell fate, which is essentially the result of the loss of the Wnt signaling pathway in those cells (Eisenmann et al., 1998). Since the VPCs in *bar-1* mutants adopt a fused fate, there is little to no vulval induction, resulting in a vulvaless phenotype (Vul), which also occurs in *lin-39* and *pop-1* loss of function mutants (Eisenmann et al., 1998). In contrast, in *pry-1*/Axin loss of function mutants *lin-39* expression is up regulated and causes extra VPCs to adopt an induced vulval fate, referred to as multi-vulva (Muv), which is due to the constitutive activation of the Wnt pathway (Eisenmann et al., 1998).

The prevention of fusion of the VPCs to the hyp7 is what allows them to respond to the inductive signal, LIN-3/EGF, in order to activate the LET-60/Ras signal cascade. Subsequently, P6.p adopts a 1^{o} cell fate due to its close proximity to the AC and the LIN-3 signal (Figure 4). This activates lateral signaling between P(5-7).p through the LIN-12/Notch signaling pathway. Upon activation of the LET-60/Ras signal transduction cascade in P6.p, the LIN-12 secreted ligand, DSL-1 is released to the neighbouring P5.p and P7.p, which binds to the LIN-12 receptor. This induces the LIN-12/Notch signaling transduction pathway in P5.p and P7.p to promote a 2^{o} cell fate in these cells, while inducing the production of LIP-1 (MAPK phosphatase) to antagonize the EGF/Ras/MPK signal in the presumptive 2^{o} lineage cells (Figure 5). This essentially promotes 2^{o} cell fate and inhibits 1^{o} cell fate in P5.p and P7.p, which results in the typical 2^{o}-1^{o}-2^{o} pattern

formation of the *C. elegans* vulva (Greenwald, 2005; Sternberg, 2005; Sundaram, 2005). This delicate interplay between the Ras, Notch, and Wnt signaling pathways is crucial to the proper pattern and formation of the vulva. Reduction of the level of LIN-3/EGF signal to the VPCs from the AC results in the LIN-12/Notch pathway overpowering the Ras pathway transduction, causing P(5-7).p to all adopt a 2^{o} cell fate. While a dominant *lin-12* mutation cause all VPCs P(3-8).p to become induced and adopt a 2^{o} cell fate, a null *lin-12* mutation results in P(5-7).p all adopting a 1^{o} cell fate due to the overwhelming Ras signaling and lack of lateral inhibition. Even more striking is the loss of Ras pathway function results in the fusion of all VPCs to the hyp7 due to the inability to activate the lateral signal between P(5-7).p. Finally, without the Wnt signaling pathway, no induction is possible because the VPCs fuse to the hyp7 in the L1 stage, while overactivation of the Wnt pathway results in a Muv phenotype due to the failure of P(3-8).p to appropriately fuse to the hyp7. Thus, through these interactions, it is clear that the layering of gene expression and regulation is complex but is crucial to proper development.

1.7 *C. briggsae* and *C. elegans*: A Model to Study Evolutionary Conservation in Vulval Development

C. briggsae is another *Caenorhabitid* species that shares much in common with *C. elegans*. Both species are hermaphroditic, share the same lifestyle and life cycle, and are easy to maintain in a laboratory setting. Although *C. briggsae* is not a sibling species to *C. elegans* and they have diverged from a common ancestor 30 million years ago, their striking similarities make comparative analysis an attractive avenue to study evolutionary networks and differential regulation of conserved genes (Cutter, 2008; Stein et al., 2003).

Through rigorous testing and characterization, it is known that although the formation of the vulva is identical in both species, the underlying regulation of the genes controlling vulva development has diverged (Felix, 2007). Thus, analysis of the genes and modulators of vulval development in *C. briggsae* and in comparison to *C. elegans* allows for the elucidation of the levels of conservation of the underlying mechanism of vulva morphogenesis and induction. Comparing the regulatory networks involved in vulva development in *C. elegans* and *C. briggsae* may discover how genetic redundancy is achieved in order to produce an invariant morphology and how changes in regulation can ultimately affect the health of an organism as a whole. Elucidation of differences in pathway regulation may provide clues to the deregulation of human pathways in a variety of diseases. It is also worth noting that like *C. elegans*, *C. briggsae* could also be independently used to study signaling pathway function and regulation. This is aided by recent genetic and molecular tools to facilitate mutant analysis, gene mapping, and gene interaction studies (Hillier et al., 2007; Koboldt et al., 2010; Stein et al., 2003; Zhao et al., 2010). These tools lend more power to the use of similar but different species when studying genetic networks. Due to its genetic differences from *C. elegans*, *C. briggsae* may help to identify new pathway components and regulators that have not been possible in *C. elegans*.

1.8 The Goal of this Study

The regulation of gene expression is a complex and layered process. To examine the regulation of gene expression in *C. elegans* and *C. briggsae* we utilize the simple egg

laying organ, the hermaphrodite vulva. Numerous studies have shown that vulval development relies on multiple levels of regulation of gene expression, from chromatin remodeling to activation of signaling pathways, and finally the transcription of target genes.

First I examined the regulation of gene expression at the level of chromatin remodeling. My work shows that animals mutant for the histone deacetylase, *hda-1*, a NuRD complex member and SynMuv B gene, exhibit vulval morphogenesis and uterine defects. Using GFP based molecular markers we were able to analyze vulval cell morphology, π cell fate specification, and utse formation. *hda-1* was found to be expressed in the vulva and gonad lineages, consistent with our phenotypic observations. To study the mechanism of *hda-1* function, we focused on target genes identified through a microarray, and transcription factors known to be involved in uterine development. Specifically, we determined that *fos-1* (proto-oncogene *fos* homolog) acts downstream of *hda-1* in vulval morphogenesis, while *lin-11* (LIM sub-family) and *egl-13* (SOX family) act upstream of *hda-1* and mediate *hda-1* function in π cell specification and formation of the vulva uterine connection. Another gene, *zmp-1* (zinc metalloprotease family), was utilized to determine the role *hda-1* plays in AC specification since *zmp-1* is known to be involved in AC fate specification. In *hda-1* mutants, *zmp-1* expression was found to be abnormal, indicating a defect in AC specification. These results provide evidence that *hda-1* and chromatin remodeling play a crucial role in vulval morphogenesis, and a novel role in uterine development.

Next I focused on Wnt signaling to determine its role in vulval development. To achieve this, an Axin mutant in both *C. elegans* and *C. briggsae* was utilized to examine the role of activated Wnt signaling in vulval development. A detailed analysis of the *pry-1* mutant phenotype was undertaken in both *C. elegans* and *C. briggsae*. We show that *Cbr-pry-1* is expressed in vulval cells, while ectopically induced VPCs in *pry-1* mutants adopt 2^{o} cell fates independent of the gonad-derived inductive and LIN-12/Notch mediated lateral signaling pathways. We also found that *Cbr-pry-1* mutants frequently show a failure of P7.p induction. The genetic analysis of the P7.p induction defect revealed that it was caused by altered regulation of the LIN-12/Notch transcriptional target *lip-1* (MAP kinase phosphatase). Thus, our results provide evidence for LIN-12/Notch-dependent and independent roles of Wnt signaling in promoting 2^{o} VPC fates in both nematode species.

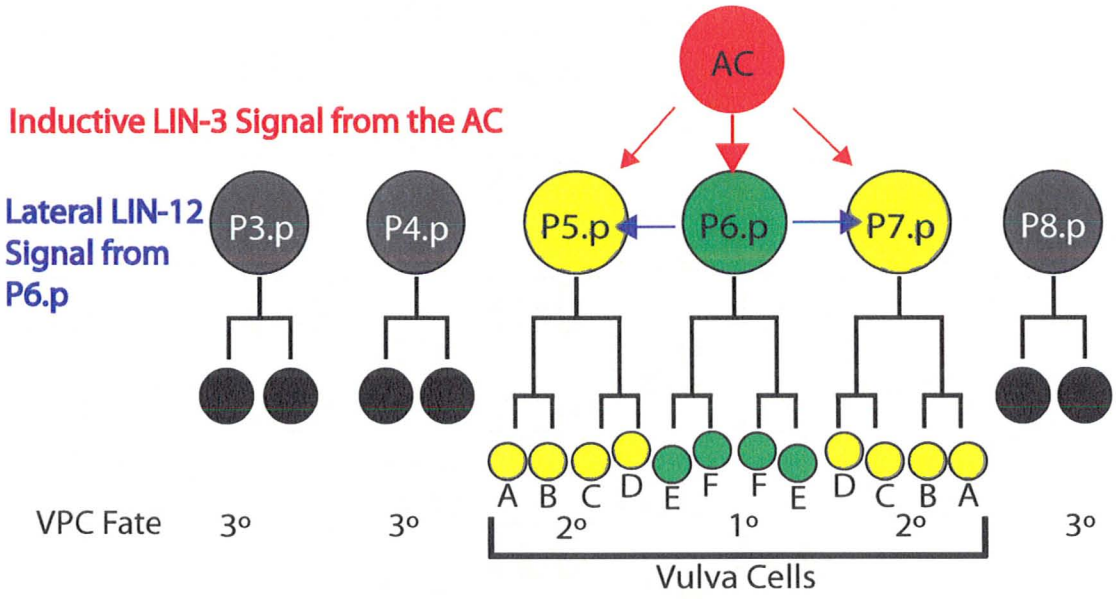

Figure 1- Cellular signaling to mediate vulval development

The LIN-3 inductive signal emanates from the anchor cell to activate the Ras/MPK pathway in P6.p and promotes the acquisition of the 1^{o} fate. Both LIN-3 mediated inductive signaling and LIN-12/Notch mediated lateral signaling confer 2^{o} fate on P5.p and P7.p. In addition Wnt signaling is also involved in VPC induction. P(5-7).p respond to the signaling and divide to form the adult vulva composed of 22 cells grouped into 7 cell types, vulA to vulF.

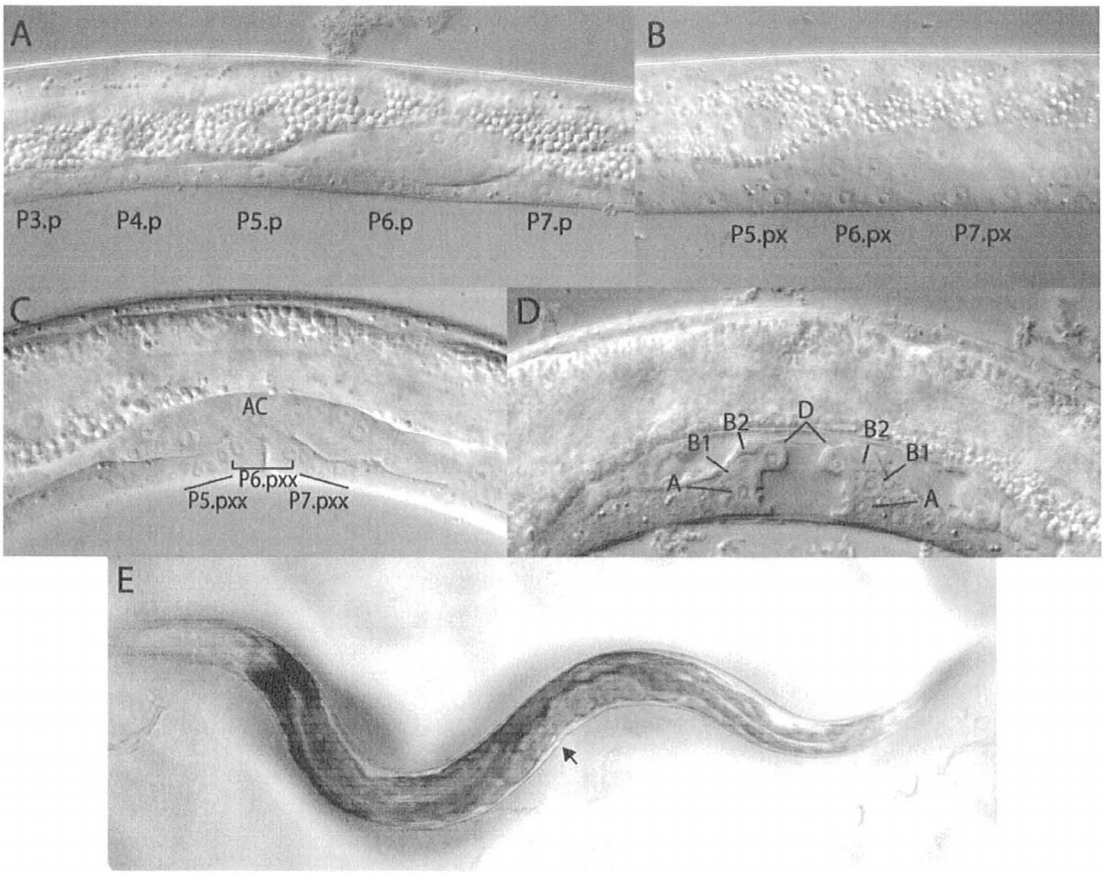

Figure 2- Wildtype *C. elegans* Vulva Development

(A) An L2 stage animal at the Pn.p stage of development. The vulval competence group (P(3-7).p, P8.p is to the left of the field of view) is arranged on the ventral side of the developing animal.

(B) An L3 stage animal at the Pn.px stage. In the early to mid L3 stage the P(3-8).p undergo one round of division to give rise to two daughter cells each, termed Pn.px. P(5-7).px can be observed in this animal

(C) An early L4 animal at the Pnp.xx stage. By this stage of development P(3-4).p and P8.p have fused to the hyp7 and P(5-7).p have undergone three rounds of division to give rise to the 22 cells that will form the adult vulva.

(D) A mid-L4 vulval invagination. The adult vulval cells have taken up their stereotypical positions to form the 'Christmas tree like' shape. In this focal plane only vulA, vulB1/B2, and vulD can be observed. vulC/E/F are out of the focal plane.

(E) An adult wildtype animal. The arrow indicates the location of the adult vulva along the ventral surface. In this particular animal eggs can be seen in the uterus.

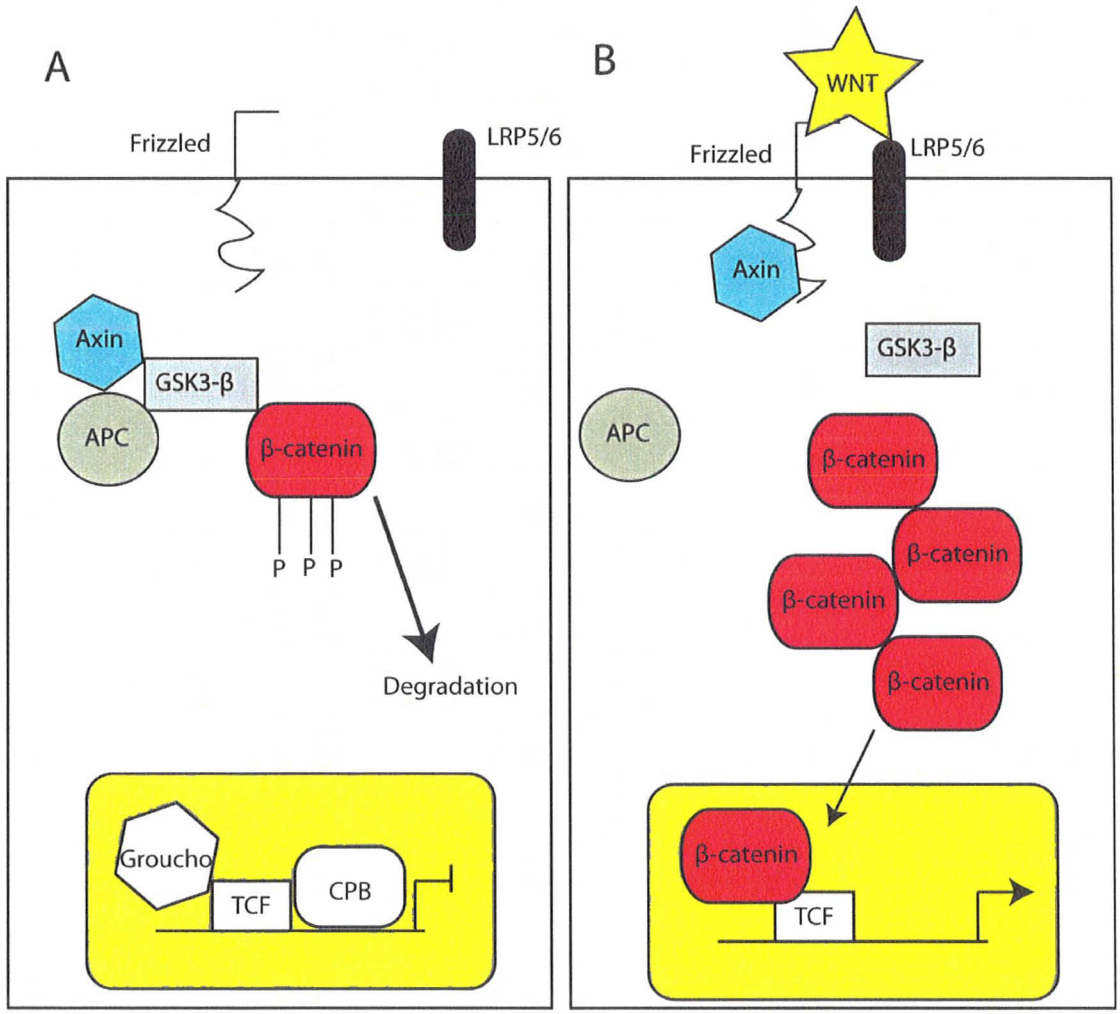

Figure 3- The Canonical Wnt Signaling Pathway

(A) In the absence of a Wnt signaling ligand the pathway is not active. In this situation β-catenin is phosphorylated and ubiquitinylated by the destruction complex (Axin, GSK-3β, APC) which marks it for degradation by the proteosome. The constant degradation of β-catenin results in the block of transcription of target genes by Groucho, TCF/LEF, and CPB.

(B) A Wnt ligand binds to the Frizzled receptor to disrupt the formation of the destruction complex. β-catenin is permitted to accumulate in the cytoplasm, which upon sufficient accumulation, translocates to the nucleus. In the nucleus β-catenin interacts with TCF/LEF to activate transcription of Wnt target genes.

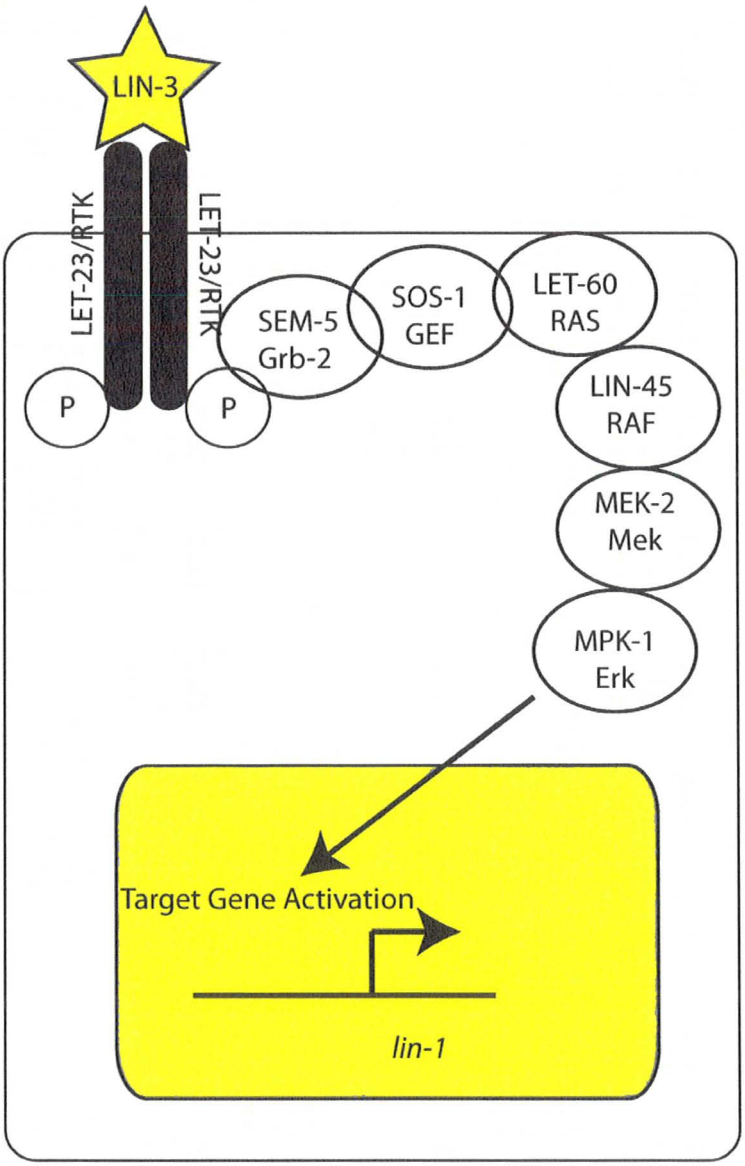

Figure 4- The *C. elegans* RTK/Ras/MPK Signaling Pathway

The EGF ligand, LIN-3 binds to the receptor tyrosine kinase, LET-23, which causes RTK dimerization and autophosphorylation. These phosphorylated residues serve as docking sites for the adapter proteins SEM-5/Grb-2 and SOS-1/GEF which activate LET-60/Ras. LET-60 binds to LIN-45/Raf to activate is kinase domain, which in turn, phosphorylates MEK-2/Mek. Activated MEK-2 interacts with and activates the MAP Kinase, MPK-1/Erk. MPK-1 translocates to the nucleus to promote the transcription of its target genes, such as *lin-1* (Sundaram, 2005).

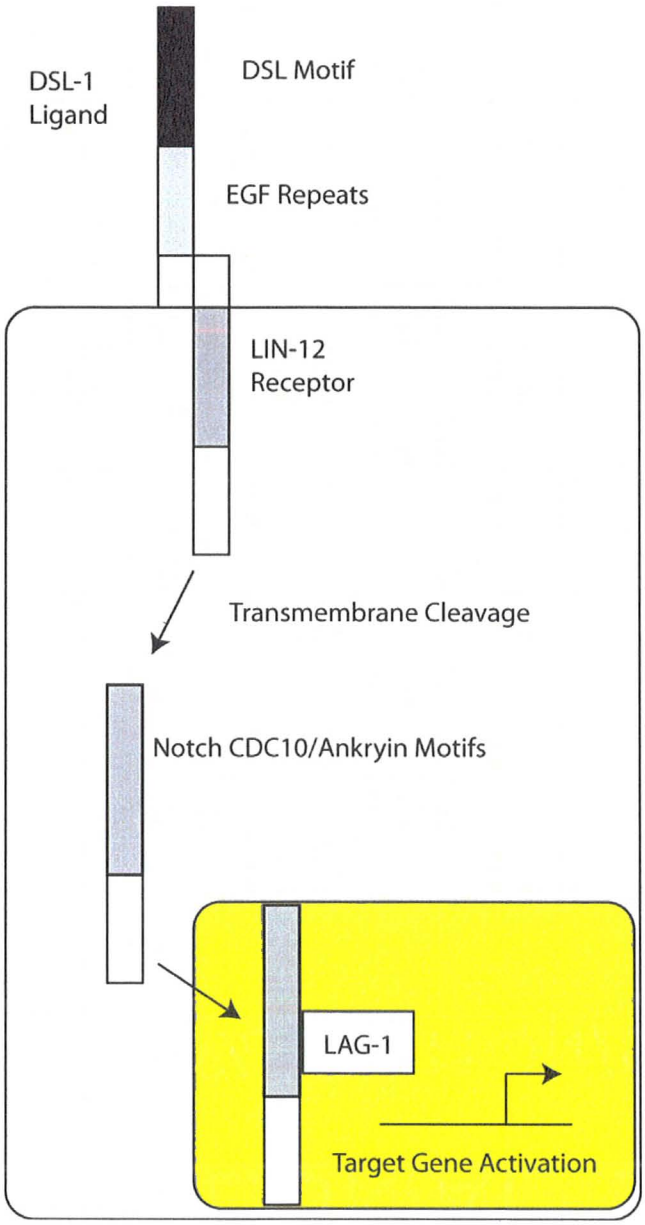

Figure 5- The LIN-12/Notch Signal Transduction Pathway

A DSL family member ligand (DSL-1, LAG-2, APX-1) binds to the LIN-12/Notch receptor extracellular domain. This causes a series of cleavages to release the intracellular LIN-12 domain. The intracellular domain translocates to the nucleus where it interacts with LAG-1, a member of the CSL family (mammalian **C**BF1, *Drosophila* **S**u(H), and *C. elegans* **L**AG-1). This interaction is mediated by the intracellular domain's CDC10/Ankyrin motifs, which activates the transcription of LIN-12 target genes

Chapter 2: Materials and Methods

2.1 Strains and General Methods

The general methods for culturing and genetic manipulations have been previously described (Brenner, 1974). All experiments were carried out at 22°C unless otherwise noted. The staging of animals was primarily based on the gonad morphology as described in Wormatlas (Lints, 2008). The gonad arms initiate turning during mid-L3 stage and by mid-L4 stage arms are in close proximity to the center of vulval invagination formed by P(5-7).p progeny.

Various mutations used in this study are listed below in chromosomal order, followed by transgenic strains (Table 1). Where known, the locations of mutations and transgenic strains are indicated. The '*Cbr*' prefix identifies the *C. briggsae* ortholog of a *C. elegans* gene.

C. briggsae: AF16 (wild type), *Cbr-pry-1 (sy5353) I, Cbr-pry-1(sy5270) I, Cbr-pry -1(sy5411) I, Cbr-unc-119(st20000) III*

C. elegans: N2 (wild type), *pop-1(hu9) I, pry-1(mu38) I, lin-29(n333) II, lin-12(n137) III, lin-12(n952) III, lin-12(n676n909) III, mpk-1(ku1) unc-32(e189) III, sel-5(ok149) III, unc-119(ed4) III, lip-1(zh15) IV, hda-1(cw2) V, hda-1(e1795) V, hbl-1(mg285) X, hbl-*

1(ve18) X

2.2 Genetic Crosses

Genetic crosses to obtain GFP reporter expressing lines in a mutant background were performed in both *C. elegans* and *C. briggsae* by crossing 8-10 wildtype (either N2 or AF16) males and 2-4 GFP reporter expressing hermaphrodites on agar plates. Animals were allowed to mate and produce F1 progeny for 3-4 days at which point the F1 heterozygous males were isolated. F1 heterozygous males were then crossed to the mutant of interest. F1 progeny that were heterozygous for the mutation and the reporter were obtained and cloned. Cloned F1 progeny were allowed to self fertilize and reporter expressing F2 progeny, that were homozygous for the phenotype caused by the mutation of interest, were cloned onto separate plates. These F2 progeny were allowed to self fertilize and clones that produced only reporter expressing progeny were selected. One homozygous population, for both the reporter and mutation, was used as the reference strain and frozen.

hda-1(e1795)/dNT1; syIs80 (or syIs49) animals were made by crossing *e1795/dNT1* hermaphrodites to homozygous GFP males of the desired marker. F1 WT looking males (which carry *e1795*) were subsequently crossed to Unc sibling hermaphrodites (which carry dNT1) in order to increase the chances of obtaining a homozygous GFP F2 generation. 10 F2 Unc hermaphrodites were picked that expressed GFP. From these clones, ones that segregated *e1795* like Pvl hermaphrodites were chosen

and mounted. A single clone that segregated *e1795* and was homozygous for the molecular marker was frozen and used as the reference strain.

To make the *Cel-pry-1(mu38) ayIs4; lin-12(n676n909)* strain, double mutant *n676n909* males were crossed to *mu38 ayIs4* hermaphrodites. F1 wild type looking hermaphrodites of the genotype *mu38 ayIs4/+ +; n676n909/+* were cloned on to separate plates. These hermaphrodites were allowed to self fertilize to produce a heterogeneous population that included *mu38 ayIs4; n676n909* homozygotes, as judged by a large central Pvl phenotype characteristic of a *lin-12* loss of function mutation. These homozygotes were mounted and scored for a muv phenotype and *ayIs4* expression using low magnification Nomarski imaging to avoid bursting the worms. Candidate worms were recovered and single worm PCR of the *lin-12* locus was performed. Successful PCRs were sequenced for the *n676* mutation (*n676* has never been separated from *n909* in any report).

To generate the *pry-1(mu38) ayIs4; lip-1(zh15)* double mutant strain, heterozygous *mu38* males (*mu38 ayIs4/++*) were crossed to *zh15* hermaphrodites. F1 heterozygous progeny were cloned out and multiple lines were set up. These heterozygotes were allowed to self fertilize to produce a heterogeneous population which included *mu38 ayIs4; zh15* homozygotes. Since the *zh15* mutation has no phenotype, F2 muvs were cloned on to separate plates and allowed to self fertilize. From these plates bulk genomic DNA was extracted from numerous worms and sequenced for the *zh15*

mutation. A single line was picked that was Muv (like *mu38*), homozygous for *ayIs4*, and contained the homozygous *zh15* mutation.

The *pry-1(mu38) ayIs4; mpk-1(ku1) unc-32(e189)* double mutant strain was made by crossing heterozygous *mu38 ayIs4* males to *ku1 e189* hermaphrodites. Wild type heterozygous (for all loci) F1 progeny were cloned on to separate plates and allowed to self fertilize. Fluorescing Muvs from the F2 generation were picked, to homozygous *mu38,* and cloned on to separate plates and allowed to self fertilize. F3 *unc-32* Uncs (curler Uncs) that were Muv and fluorescing were picked and subcloned onto separate plates once again. The *mpk-1 (ku1)* locus was sequenced in these animals to confirm the presence of the lesion. A single homozygous line was picked and used as the reference strain.

2.3 Generation of Transgenic Strains

The transgenic animals carrying extrachromosomal arrays were generated by standard microinjection technique (Mello et al., 1991) using *C. elegans unc-119* (Maduro and Pilgrim, 1995) and *myo-2::GFP* (pPD118.33) (S. Q. Xu, B. Kelly, B. Harfe, M. Montgomery, J. Ahnn, S. Getz and A. Fire, personal communication) as transformation markers. The concentrations of plasmids that were injected as part of this study are: ***pGLC29*** *(hsp::Cbr-pry-1)* 50 ng/µl, ***pGCL37*** *(hsp::Cel-pry-1)* 50 ng/µl, ***pGLC41*** *(hsp::Cbr-hda-1::TAP)* 25 ng/µl, ***pGLC43*** *(Cbr-hda-1::GFP)* 50 ng/µl, ***pGLC44*** *(Cel-hda-1::GFP)* 50 ng/µl, ***pGLC47*** *(Cel-hda-1p::Cel-hda-1::TAP)* 50 ng/µl, ***pGLC48*** *(Cbr-*

pry-1-2.4kb::GFP) 50 ng/µl, ***pGLC49*** *(Cbr-pry-1-3.8kb::GFP)* 50 ng/µl, ***pGLC50*** *(Cbr-pry-1-5kb::GFP)* 50 ng/µl.

2.4 Heat-shock Protocol

The synchronized L1 stage *sy5353; bhEx59* and sy5353; *bhEx93* animals were heat shocked at 31°C for 24 hrs and subsequently grown at 20°C until adulthood. *mu38; bhEx79* and *mu38; bhEx81* animals were heat shocked at 38°C for 30 min 27 hrs post synchronization at the L2/L3 molt and subsequently grown at 20°C until adulthood. Cell ablation experiments were performed as described (Avery and Horvitz, 1987). Worms were recovered from slides and allowed to grow until L4 stage.

2.5 Microscopy

Worms were mounted on agar pads. L4 and young adult stage animals were examined under Nomarski optics using Zeiss Axioimager D1 and Nikon Eclipse 80i. For GFP reporter expressing strains, epifluorescence was visualized by using a Zeiss Axioimager D1 microscope equipped with the GFP filter HQ485LP (Chroma Technology). The confocal images were taken on a Leica DMI 6000 B laser scanning microscope using a Leica TCS-SP5 scanner and Leica Application Suite Advanced software. All images were processed using NIH Image J and Adobe Photoshop CS programs.

2.6 Vulval phenotype and induction analysis

Vulva morphology was scored using wildtype N2 and AF16 as a guide. Morphology of mutant and RNAi vulvae was scored at mid-L4 stage as described in Wormatlas (Lints, 2008). We scored VPC competence and induction during the L2-L4 stages. A VPC was considered induced if it gave rise to 4 or more progeny that had invaginated. With the exception of P7.p and P8.p in *pry-1* mutants that appear morphologically similar to P12.pa (referred as P12.pa-like fate), an uninduced VPC can adopt either an F fate (no division and fusion to hyp7 syncytium in L2) or a 3^{o} fate (one division followed by fusion of both daughters to hyp7 in L3). In wild-type animals (*C. elegans* and *C. briggsae*) P4.p and P8.p always adopt a 3^{o} fate, while P3.p does in ~20-50% of cases (F fate in the remainder). Statistical analyses were performed using InStat 2.0 (GraphPad) Software. Two-tailed P values were calculated in unpaired t tests and values less than 0.05 were considered statistically significant. Unlike wild type animals in which P3.p, P4.p and P8.p fuse to hyp7, in *pry-1* mutants these Pn.p cells can be ectopically induced to divide (termed 'Overinduced'). Additionally, *pry-1* mutants frequently show a failure of P7.p induction (termed 'Underinduced'). Thus, the same animal can exhibit both Overinduced and Underinduced phenotypes.

2.7 Molecular Biology

All PCR and sequencing primers are listed in Table 2. The *pry-1(mu38) ayIs4; lin-12(n676n909), pry-1(mu38); lip-1(zh15), pop-1(hu9); muIs32; lin-12(n952),* and *pry-*

1(mu38) ayIs4; mpk-1(ku1) unc-32(e189) strains were confirmed by sequencing *lin-12* (primers GL477/GL478), *lip-1* (GL466/GL467/GL468), *pop-1* (GL508/GL509), and *mpk-1* (GL531/GL532) mutations, respectively.

The *Cbr-pry-1* locus was amplified in two large fragments (excluding intron 7) using primers GL104, GL106 (3.6 kb) and GL107, GL105 (2.2 kb). The *sy5353* and *sy5411* alleles were confirmed by sequencing both strands (Figure 6).

2.7.1 *pGLC48*, *pGLC49*, and *pGLC50- Cbr-pry-1*::GFP

To construct *Cbr-pry-1::GFP*, 2.4 kb, 3.8 kb, and 5 kb 5' UTR fragments were amplified by PCR using primers GL307/218, GL306/GL218, and GL217/GL218, respectively (Figure 6). The PCR products were digested (*Sph*I and *Sal*I for 2.4kb, 3.8 kb, *Pst*I and *Sal*I for 5 kb) and subcloned into pPD95.69 (Fire lab vector, *www.addgene.com*). The *Cbr-lip-1* RNAi construct was made by subcloning a 1.5 kb genomic fragment of *Cbr-lip-1* (GL464/GL465) into a *Sac*I, *Kpn*I digested double-T7 RNAi vector L4440 (Fire Lab vector kit, *www.addgene.com*). The heat-shock promoter driven *Cel-pry-1* construct was made by subcloning the full-length *Cel-pry-1* cDNA (1.7 kb) using GL334/GL335 into the Fire lab pPD49.83 vector.

2.7.2 *pGLC43* and *pGLC44- hda-1*::GFP

The 5' regions of *hda-1* (1.0 kb in *C. elegans* and 1.1 kb in *C. briggsae*) were amplified by PCR using primers GL360/GL363 and GL354/355, respectively. The PCR products were inserted into the Fire lab GFP expression vectors pPD95.69 and pPD95.67,

respectively. The *C. elegans* expression construct, pGLC44, was subcloned by digesting the 5' UTR with HinDIII and NsiI, while the *C. briggsae* expression construct, pGLC43, was subcloned by digesting the 5' UTR with HinDIII and PstI. In the case of pGLC44 we amplified the entire 5' upstream region of *cel-hda-1* leaving ~175 bp region immediately upstream of an RNAi-induced longevity gene *ril-1*. Although this fragment is likely to exclude the *ril-1* promoter, it may contain the *ril-1* enhancer elements. Therefore it is formally possible that *bhEx72* animals also show expression of *ril-1* in addition to *hda-1*. However, *ril-1* has no known function in the development of vulva and uterine cells (Hansen et al., 2005; Lemire, 2005) (BPG, unpublished) and, therefore, is unlikely to affect our interpretation regarding *hda-1* expression in these tissues.

2.7.3 *pGLC47- hda-1p::hda-1*::TAP

The heat shock promoter driven *Cel-hda-1::TAP* construct, pGLC45, was generated by amplifying a 2 kb *hda-1* cDNA fragment using primers GL317/GL366 and digesting with KpnI and NcoI, then subcloning it into pPD49.83. TAP was isolated by digesting the pBS1479 vector with NcoI and EcoRV. A similar version of this construct was created, pGLC47, using the endogenous *Cel-hda-1* promoter in place of the heat shock promoter. pGLC47 was made by amplifying the *Cel-hda-1::TAP* fragment from pGLC45 using primers GL367/373 and subcloning it into pGLC44 in place of the GFP between BamHI and SmaI. All insert-vector junctions were sequenced using GL388, GL323, and GL369 which confirmed the correct reading frame.

2.7.4 *pGLC41- hsp::Cbr-hda-1*::GFP

The heat shock promoter driven *Cbr-hda-1::TAP* construct, pGLC41, was generated by excising the 1.5 kb *Cbr-hda-1* fragment from pGLC35 with KpnI and NcoI then subcloning it, in frame, into pGLC39 in place of *Cel-hda-1.*

2.8 RNAi

Since the wild type *C. briggsae* (AF16) is resistant to environmental RNAi, we used a transgenic strain *mfIs42* that carries wild type copy of the *C. elegans sid-2* gene. *mfIs42* animals are sensitive to environmental RNAi similar to the wild-type *C. elegans* (Winston et al., 2007). RNAi was performed on plates containing 0.6% Na_2HPO_4, 0.3% KH_2PO_4, 0.1% NH_4Cl, 0.5% Casamino Acids, 2% Agar, 1 mM $CaCl_2$, 1 mM $MgSO_4$, 0.0005% cholesterol, 0.2% β-lactose, and 50 µg/ml Carbenicillin. Plates were seeded with 150 µl of overnight grown HT115 bacterial culture in LB and Carbenicillin media that produces dsRNA of the gene of interest. Double RNAi experiments were performed by mixing equal concentrations of each RNAi vector which was calculated using absorbance at 600nm. Three to 5 L4 stage worms were placed on RNAi plates and the phenotypes of F1 progeny were examined. For genes that caused sterility and early stage lethality, animals were subjected to RNAi treatment during the L1 larval stage. All RNAi experiments were repeated at least 3-4 times and batches that produced consistent results were analyzed.

2.9 qRT-PCR

For microarray validation, total RNA was used from the same batch that was used to perform the microarray experiment. Total RNA was also extracted from AF16, *sy5353, sy5411, sy5270,* and *mu38.* RNA was extracted from 3-5 6cm plates of mixed stage well fed worms using the TRIZOL method (Portman, 2005).

To validate the microarray data we performed a quantitative real-time PCR (qRT-PCR) experiment. The housekeeping genes *Cel-rsp-5* was used as an internal control. In general, the qRT-PCR results were qualitatively similar, although fold differences in transcript levels were lower compared to those observed in microarray experiment (Figure 7). This may be due to fundamental differences in the two technologies. We also used qRT-PCR to measure the transcript levels in each of the *Cbr-pry-1* mutant alleles and the *Cel-pry-1* mutant, *mu38. Cbr-gpd-1* was used as the internal control for *C. briggsae* alleles (Guerry et al., 2007). *Cbr-rsp-5* was not used as a control for this experiment due to the inability to obtain a PCR product after testing multiple primer pairs. All qRT-PCR experiments were performed using Biorad iQ SYBR Green Real-Time PCR Supermix with ROX on an Mx3000P qRT-PCR thermocycler. Data were generated using MxPro software and analyzed using Microsoft Excel. A sample reaction mixture for a single gene is included below:

1 µl cDNA
1 µl UP primer
1 µl DOWN primer
12.5 µl 2X SYBR Green Real-Time PCR Supermix

9.5 µl dH_2O
25 µl per well.

2.9 Western Blot

The Western blots were performed using a standard western blot protocol adapted from Sambrook and Russell's Molecular Cloning 3rd Ed. The adapted western blot protocol can be found on the Gupta Lab server. Buffers used in the western blot protocol are listed below:

Electrophoresis running buffer
3g Tris base
14.4g Glycine
1g SDS
dH2O to 1L
pH should be ~8.3

Destain Solution
80% dH2O
10% meOH
10% acetic acid

Coomassie Stain
0.05% CBB
50% meOH
10% acetic acid
39.05% dH2O
Mix with stir bar and filter

Transfer buffer
50 ml meOH
1.514g Tris Base
7.206g Glycine
dH2O to 500 ml

Worm Sample Buffer (5X SDS Loading Buffer)

1M Tris-HCl pH 6.8	100mM
10% SDS	2%
Betamercaptoethanol	5%
60% Glycerol	15%

10% Bromophenol Blue	0.1%

Protein was extracted from a mixed population of worms from 3-4 gravid agar plates. The plates were washed with M9 to isolate worms, and then worms were washed to remove all bacteria from the worm population. Worms were resuspended in RIPA buffer with protease inhibitors and sonicated on 20 second cycles until the majority of worms were broken apart, as judged under a dissecting microscope.

RIPA Buffer	
Tris-HCl pH 8.0	50mM
NaCl	150mM
NP-40	1%
NaDeoxycholate	0.5%
SDS	0.1%

TAP-tag isolation was not attempted, thus is not included in this section. Although TAP-tag isolation was not performed, it is necessary to know that the RIPA buffer used for protein isolation for the western blot is not compatible with tandem affinity purification since the SDS in the buffer will break apart protein complexes. Information regarding the TAP-tag isolation protocol can be found in the Gupta Lab shared folder.

Table 1- List of Transgenic Strains used in this study

Integrant	GFP Reporter	Strain	Chromosome
C.briggsae			
mfIs5	*Cbr-egl-17::gfp*	JU610	II
mfIs8	*Cbr-zmp-1::gfp*	JU613	V
mfIs29	*lip-1::gfp*	JU936	?
mfIs42	*sid-2(+)*	JU1018	?
mfEx33	*dlg-1::gfp*	JU1078	Ex
bhEx59	*hsp::Cbr-pry-1*	DY157	Ex
bhEx83	*Cbr-pry-1-5kb::gfp*	DY225	Ex
bhEx84	*Cbr-pry-1-3.8kb::gfp*	DY226	Ex
bhEx86	*Cbr-pry-1-2.4kb::gfp*	DY228	Ex
bhEx93	*hsp::Cel-pry-1*	DY239	Ex
C. elegans			
ayIs4	*egl-17::gfp*	PS3082	I
muIs32	*mec-7::gfp*	KN562	II
syIs54	*ceh-2::gfp*	PS3504	II
syIs80	*lin-11::gfp*	PS3808	III
syIs137	*fos-1b::CFP-TX*	PS4558	III
zhIs4	*lip-1::gfp*	AH142	III
syIs49	*zmp-1::gfp*	PS3229	IV
syIs101	*dhs-31::gfp*	PS3722	IV
kuIs29	*egl-13::gfp*	MH1317	V
syIs50	*cdh-3::gfp*	PS3352	X
syIs123	*fos-1a::YFP-TL*	PS4411	X
ctIs39	*hbl-1::gfp*	BW1932	?
deIs4	*ajm-1::gfp, lin-39::gfp-TX*	EW61	?
bhEx8	*nhr-91::gfp*	DY23	Ex
bhEx53	*daf-6::YFP*	DY145	Ex
bhEx67	*hsp::Cbr-hda-1::TAP*	DY170	Ex
bhEx68	*Cbr-hda-1::gfp*	DY171	Ex
bhEx72	*Cel-hda-1::gfp*	DY178	Ex
bhEx77	*hda-1p::hda-1::TAP*	DY190	Ex
bhEx79	*hsp::Cbr-pry-1*	DY210	Ex
bhEx81	*hsp::Cel-pry-1*	DY215	Ex
sEx13706	*C53A5.3::gfp*	BC13706	Ex
wyEx3372	*syg-2::gfp*	TV8740	Ex

Table 2- List of Transgenic Strains used in this study

Locus	Oligo	Sequence (5' to 3')
Cbr-pop-1	GL184	ACGAAGAGCTCGGCGATGAGGTGAAG
Cbr-pop-1	GL185	AAAGGTACCAACGCTCTTATCTCTCTTTCTCTTTGG
Cbr-lin-39	GL313	CTAGGTACCATGACCACATCTACATCATCGC
Cbr-lin-39	GL314	CTGGAGCTCGCCTACAATGTTTTCTAAGCTCCC
Cbr-pry-1	GL104	ATGGAGAGTGGACCATCATCTCATCTC
Cbr-pry-1	GL105	ATAGCGAATCTCGGCAGCAATTCTTC
Cbr-pry-1	GL106	GCTAGGTGGTGACAGATTTGATTGGTG
Cbr-pry-1	GL107	GCTAGGTGGTGACAGATTTGATTGGTG
Cbr-pry-1	GL113	GACCAATCAATCAGCATCTGTCAC
Cbr-pry-1	GL118	AGCTACACCGCCGAAACTTTCAAACTC
Cbr-pry-1	GL119	CTAGATTTGGGAATTTCAGATACCG
Cbr-pry-1	GL120	CCGAGATTCTGGAATGTGGAAATTC
Cbr-pry-1	GL141	TTGGAGCTCATGGAGAGTGGACCATCATCTCATCTC
Cbr-pry-1	GL142	TTGGGTACCGACCAATCAATCAGCATCTGTCAC
Cbr-pry-1	GL143	CTCATTTTGAAGCTCTCAATCTCAC
Cbr-pry-1	GL217	CAGCTGCAGCGAGAATTTCCAAGGTGGCCGAG
Cbr-pry-1	GL218	GGGGTCGACTGATGGTCCACTCTCCATATTACC
Cbr-pry-1	GL306	CGCGCATGCGGTTTTTTTTGGAATCAACGGC
Cbr-pry-1	GL325	CTGGAAATACTGTAGCTCC
Cbr-pry-1	GL410	CTCAAAGTTGACAGTGTGGAGGTCC
Cbr-pry-1	GL411	AGTTACGGCCTGAACTGTTTC
Cbr-lip-1	GL464	ATCGAGCTCATGACAACACATTTACCTAGCACATCCCAG
Cbr-lip-1	GL465	ATCGGTACCGTGAAATGACTTGGCTGAGTGATTACTCG
cbr-hda-1	GL354	CTCCCTTGACAGTTTCGGCAGTCCATTTC
cbr-hda-1	GL355	CTCCCTTGACAGTTTCGGCAGTCCATTTC
lip-1	GL466	GATTATCCCTCTCTCACAGCTT
lip-1	GL467	GGTGAAGATCAAGGCGGAAAACAACG
lip-1	GL468	ACTGCAGTTTCGGCTAAAATTCTTG
lin-12	GL477	TCAGCTCTTCGTGTAACTGTCCG
lin-12	GL478	GTGTTGCAGTTCATTTCTTTGCC
pry-1	GL506	TGTTGGTAGGTTTTCGTGGCGAG
pry-1	GL507	GTATACCGACACTCTTCGATATC
pop-1	GL508	AAATTTCCCGCGTCTTTCCCCTCT
pop-1	GL509	ACGGTTCTATGGGCGGAGTTTAGA
hda-1	GL317	ATAGGTACCATGAACTCAAACGGCCCGTTGATG
hda-1	GL360	GATTGAATGCATGTTTGATGGTCGCAGTAGACTG
hda-1	GL363	ATCAAGCTTGTGCGTGCTCGCGGTTGTG
hda-1	GL366	TGCCATGGACTCTGTCTTCTGACGCTTTTC
hda-1::TAP	GL323	GATCCATGGAAAAGAGAAGATGG
hda-1::TAP	GL367	ATAGGATCCATGAACTCAAACGGCCCGTTGATG
hda-1::TAP	GL373	GAGCATGTAGGGATGTTGAAGAGTAATTGGACTTAG
hda-1::TAP	GL388	GCATAACCTGTCTTACACCTTCTC
hda-1::TAP	GL369	GGAGACTTCTACGATGGTGAG

mpk-1	GL531	TTCGCCTATGATTTCCGTCAG
mpk-1	GL532	CGAAGTGTCCGTTGACAGAAT
fos-1	GL328	GACGCTTTCCAGAATCGTTG
fos-1	GL329	CCCTGTACTCTGCGGTGTTT
rsp-5	GL330	TCGTTCACGTACTCCACCAA
rsp-5	GL331	TCACGAACTGGTGATCTGGA
lin-29	GL332	GATCAACTGGATCCACACCA
lin-29	GL333	GTTTGTCGATGAAGCAGCAG
hbl-1	GL336	TGGCTTCCGCATTAGGAGTTG
hbl-1	GL337	TTTCCGCTACTGCTTCTTCTGC
nhr-91	GL340	CCGACACAACAGAAATGATAGACG
nhr-91	GL341	TGCCGAGCACCAGTGATAATC
sel-5	GL342	CGAATGTTCCCAGTATTTCACCAG
sel-5	GL343	TCGGACTTGACTTCCATCAGTTTC

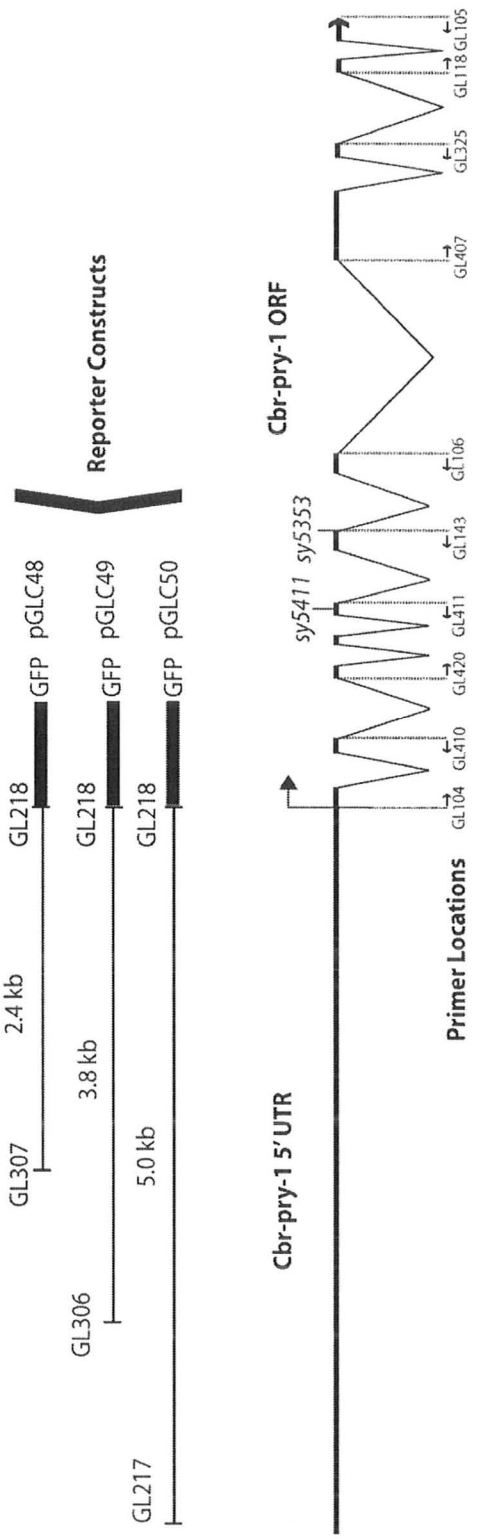
Reporter Constructs
GL307
2.4 kb
GL218
GFP
pGLC48
GL306
3.8 kb
GL218
GFP
pGLC49
GL217
5.0 kb
GL218
GFP
pGLC50
Cbr-pry-1 5'UTR
Cbr-pry-1 ORF
Primer Locations
GL104
GL410
GL420
sy5411
GL411
sy5353
GL143
GL106
GL407
GL325
GL118
GL105

Figure 6- *Cbr-pry-1* open reading frame

GFP reporter constructs pGLC48, pGLC49, and pGLC50 were generated by amplifying 2.4 kb, 3.6 kb, and 5 kb fragments, respectively, and subcloning them into the Fire lab GFP expression vector pPD95.69. Primers used for amplification of the 5'UTR, amplification of the *Cbr-pry-1* genomic region, and sequencing are indicated by GL number, while their orientation is shown by arrows. A table containing the list of primers used in this study can be found in supplementary table 1.

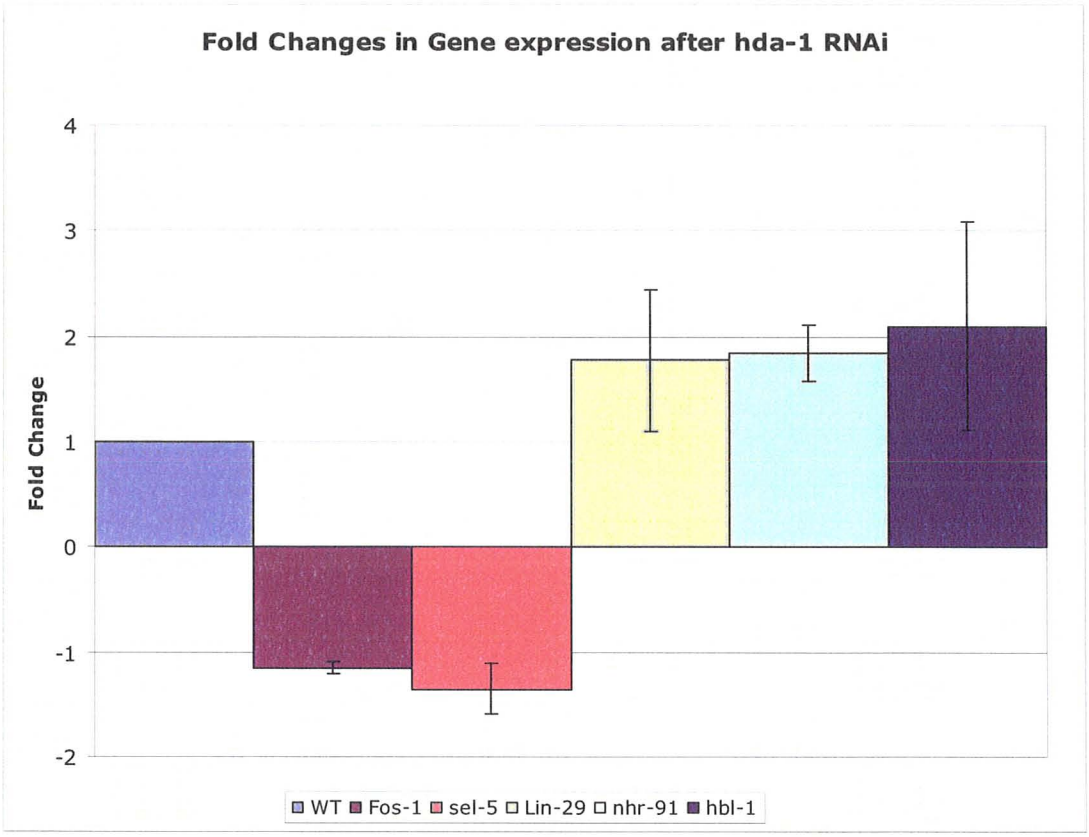

Figure 7- Histogram depicting the fold change detected by qRT-PCR

Two to four independent qRT-PCR experiments were performed for each gene analyzed. The total RNA that was extracted for the microarray was used to synthesize cDNA for the qRT-PCR experiments. The changes in expression detected by qRT-PCR followed the a similar trend as the results obtained by the microarray (Joshi, 2008).

Chapter 3: The Role of *hda-1* in Vulval Development

Genes that are members of chromatin remodeling complexes, such as the NuRD complex, play important roles in regulating gene expression. The class I histone deacetylase, *hda-1*, is known to play a role in gene silencing through the removal of acetyl groups from histone tails. This allows the wound DNA to take a closed confirmation and restrict the access of transcription factors to specific genes, ultimately silencing those genes. In this chapter I focus on the role of *hda-1* in vulval development. Specifically, the *hda-1* mutant phenotypes in both the vulval and the vulva-uterine connection support its role in gene regulation in vulval and vulval related tissues. We show that *hda-1* is expressed in many tissues, including vulval cells and gonadal lineage cells. Finally the identification and characterization of several putative *hda-1* targets in vulval development and uterine development are examined. These results support the hypothesis that *hda-1* plays a role in the maintenance of the proper formation of the hermaphrodite vulva and vulval uterine connection through gene silencing.

3.1 *hda-1* Mutants Exhibit Defects in Vulval Morphology and theV-Uterine Connection

An initial RNAi screen for genes involved in vulval development revealed that *hda-1 (RNAi)* animals exhibited an adult Pvl phenotype (Joshi, 2008; Kim, 2007). This result is consistent with previously reported data that the two viable mutant alleles of *hda-1*, *cw2* and *e1795*, both exhibit prominent Pvl phenotypes (Cumbo et al., 2010; Dufourcq et al., 2002; Zinovyeva et al., 2006) (Figure 8) (Table 3). Upon closer examination using

Nomarski optics, the vulval invagination at the L4 stage was found to be defective (Figure 8). The vulval invagination defect ranges from a mild defect of low penetrance in *cw2* animals to a variably strong defect of mid range penetrance in *hda-1(RNAi)* animals, to a very strong and 100% penetrant defect in *e1795* mutants and *cw2(RNAi)* mutants (Cumbo et al., 2010) (Figure 8) (Table 3). Previous reports suggest that *cw2* is a weaker allele, while *e1795* is a much stronger allele, and our results support these observations since the *e1795* phenotype is more severe and *hda-1(RNAi)* in *cw2* mutants elevates the phenotypic defects to *e1795* levels (Dufourcq et al., 2002; Zinovyeva et al., 2006). At the L4 stage *hda-1* mutant animals lack a significant invagination and they also fail to form typical wildtype morphology, such as the finger-like extensions characteristic of mid-L4 N2 worms (Cumbo et al., 2010) (Figure 8). *hda-1* mutants that have a severe vulval defect also show defects in the formation of a vulva-uterine connection. In wildtype animals the vulva-uterine connection can be seen by the formation of a thin uterine-seam cell (utse) membrane at the L4 stage that acts as passage between the uterus and vulva (Figure 8). In *hda-1* mutants this thin membrane is not formed, instead there is a physical blockage present which may be due to defects in the AC. The AC fails to invade the basement membrane then migrate away from the vulva in many of these animals. Often the AC is situated directly above the vulval apex which may be the reason that the utse is defective (Cumbo et al., 2010) (Figure 8).

To assess the severity of the lack of a significant invagination we used the apical junction associated marker *ajm-1* (Sharma-Kishore et al., 1999). *ajm-1::GFP* is

expressed in apical junctions of unfused cells, which can be used to visualize the formation of the vulval rings. The 7 concentric toroidal rings that form the vulva are formed by the fusion of each of the 7 cell types, vulA to vulF. Each cell type extends processes across the vulval invagination to its corresponding partner(s) and then eventually fuses together to form a ring (Sharma-Kishore et al., 1999). Prior to fusion, but after the extension of processes, the rings can be visualized using *ajm-1::GFP* as a reporter. We found that in L4 *hda-1(RNAi)* animals the toroidal ring pattern was defective (Cumbo et al., 2010) (Figure 8). The rings in *hda-1(RNAi)* animals were flatter, displayed fewer rings than the wildtype, and the fluorescence was greatly reduced (Cumbo et al., 2010) (Figure 8). These results are consistent with the observed phenotypes of the lack of a significant invagination and the defective morphology of *hda-1* mutant animals. Taken together, these results demonstrate that *hda-1* plays an important role in the proper formation and morphogenesis of the vulva.

3.2 *hda-1* is Expressed in Vulval and Gonadal Lineage Cells

Since *hda-1* mutants show defects in vulval morphology and formation of the utse, it is reasonable to assume *hda-1* would be expressed in those tissues. To determine the pattern of *hda-1* expression we generated a transcriptional fusion construct containing a 1kb fragment of the *hda-1* 5' UTR driving the expression of GFP (pGLC44) (Chapter 2: Materials and Methods). This construct was injected into *unc-119(ed4)* animals along with the transformation marker plasmid that contained the wildtype *unc-119* locus to generate a stable line (bhEx72) (Chapter 2: Materials and Methods). We also utilized a

previously generated strain, sEx13706, that contains the entire *hda-1* 5' UTR along with the upstream genes and corresponding regulatory regions of *ril-1* and C53A5.2 (Hunt-Newbury et al., 2007). We generated our own construct and strain to determine if the expression of *hda-1* in sEx13706 animals was true *hda-1* expression, not the resulting expression of all three genes. Both sEx13706 and bhEx72 animals showed similar expression in multiple tissues throughout development, including neurons, epidermal, and hypodermal cells as early as gastrulation, although sEx13706 was generally brighter (Cumbo et al., 2010) (Figure 9).

Vulval expression was first observed in the L3 stage in the descendants of P(5-7).p, but not observed in any other Pn.p lineages (Cumbo et al., 2010) (Figure 9). This expression was persisted into the L4 stage where vulval cell types could be seen fluorescing, such as, vulA, vulB1/B2, and vulD (Cumbo et al., 2010) (Figure 9). Beyond the late L4 stage vulval fluorescence is absent. The expression of *hda-1* begins in early embryos and persists throughout development in multiple tissues, which suggests that it is required in multiple developmental roles. The fact that *hda*-1 is a histone deacetylase and would likely be involved in chromatin remodeling throughout development supports this argument. Early expression data is consistent with the fact that *hda-1* is required for survival since *hda-1(e1795)* mutants are sterile. To further support this claim, when *hda-1* is knocked down in the L4 stage by means of RNAi, embryos that are laid fail to hatch due to a lack of maternal contribution of HDA-1.

Gonadal lineage cell expression was also observed in *hda-1::GFP* animals, but was limited to the AC (Cumbo et al., 2010) (Figure 9). In no case did we find that π cells or π progeny expressed *hda-1::GFP*. GFP expression was first observed in the AC at the early L3 stage and persisted until the early L4 stage (Cumbo et al., 2010) (Figure 9). Since no π lineage expression was detected there is a likely scenario where the observed utse defects in *hda-1* mutants are due to abnormal or absent AC-mediated signaling in the specification of π cells. Normally, one of two cells in the developing gonad, Z1.ppp or Z4.aaa, becomes the AC through a LIN-12-LAG-2 mediated feedback loop (Seydoux and Greenwald, 1989). Whichever cell generates the highest level of *lin-12* activity through this feedback loop will adopt the VU (Ventral Uterine precursor cell) fate and the other will become the AC (Greenwald et al., 1983). Once the AC fate has been assigned, it is involved in a number of processes, one of which is the specification of π cells. This occurs through the transcription of the LIN-12 ligand, *lag-2,* in the AC, in a *lin-29* mediated manner, which then is excreted and interacts with the receptor, LIN-12, on the surface of the π cells (Newman et al., 1999; Newman et al., 1995). The binding of LAG-2 to LIN-12 activates the expression of the transcription factors *lin-11* and *egl-13*, which are required for the formation of the utse (Newman et al., 1999; Newman et al., 1995). Thus, in this situation, where *hda-1* is expressed in the AC, but not in the π cell lineage, it is likely that knockdown of *hda-1* may inhibit the formation of the AC, or it's signaling to the neighbouring π cells.

The ability of a 1 kb fragment of the *hda-1* 5' UTR to drive the expression of *hda-1* in multiple cell types, including vulval cells and the AC, enabled us to test whether the full length *hda-1* cDNA tagged with TAP under the control of the native promoter could rescue the *cw2* mutant phenotype. The tandem affinity purification (TAP) tag was included in this construct to enable us to isolate HDA-1 interacting proteins from *in vivo* protein extracts (See Appendix 1). To achieve this, pGLC44 was digested to insert *hda-1*cDNA::TAP in the place of GFP (pGLC47) (Materials and Methods). This construct was injected, along with a *myo-2::GFP* pharyngeal transformation marker, directly into *cw2* mutant animals and a stable line was obtained (bhEx77) (Materials and Methods). Animals that expressed the *myo-2::GFP* were scored as the experiment, while animals that did not express the *myo-2::GFP* were scored as an internal control, since these animals are *cw2* homozygotes but do not carry the rescue construct. The *hda-1::hda-1cDNA::TAP* construct was able to rescue the Pvl and Unc phenotype of the *cw2* mutants, where 70% (n=340) of the array expressing animals were WT, compared to 40% (n=99) of the animals lacking GFP fluorescence, thus lacking the array (internal control) were WT (Cumbo et al., 2010). A failure to observe rescue in all animals could be due to a variety of reasons, one of which is that the *hda-1::TAP* fusion could be poorly expressed. This provides evidence that the 5' UTR can drive expression of *hda-1* cDNA in the necessary tissues and subsequently rescue the mutant phenotype.

3.3 *Cbr-hda-1* Plays a Conserved Role in Vulval Development

Since *hda-1* seems to play a very important role in *C. elegans* development, we were interested in using similar methods to determine if the role of *hda-1* is evolutionary conserved in a sister nematode species, *C. briggsae*. Previous data has shown that *Cbr-hda-1(RNAi)* causes similar phenotypes in *C. briggsae* (Cumbo et al., 2010; Joshi, 2008). The phenotypes observed in these experiments are defects in vulval morphology and gonadogenesis defects (Cumbo et al., 2010; Joshi, 2008). This RNAi experiment indicates that *hda-1* is playing a role in the vulva, which encouraged us to determine the wildtype *Cbr-hda-1* expression pattern. A 1kb fragment of the *Cbr-hda-1* 5' UTR was cloned into a GFP expression vector and this construct (pGLC43) was injected into wildtype AF16 animals (bhEx68) (Materials and Methods). bhEx68 animals expressed GFP throughout all stages of development starting in early embryos and continuing until adulthood (Cumbo et al., 2010) (Figure 9). Expression could be seen in all vulval cell types but was predominantly expressed in vulA, vulB1/B2, and vulD cells (Cumbo et al., 2010) (Figure 9). This expression is consistent with *Cel-hda-1* expression in both sEx13706 and bhEx72 animals as described above.

3.4 Identification of *hda-1* Targets

Characterization and analysis of the *hda-1* mutant phenotypes and its expression pattern led to a better understanding of its role in vulva morphogenesis. To determine how *hda-1* regulates the acquisition of vulval cell fates, K. Joshi (a former graduate

student) performed a microarray analysis to identify its downstream targets. This microarray revealed 412 genes whose activity was either up or downregulated in *hda-1(RNAi)* treated animals compared to the control (Cumbo et al., 2010; Joshi, 2008). Many of these genes were collagens or transcription factors, while we found that 11% of these genes have been previously associated with vulval development (Cumbo et al., 2010; Joshi, 2008).

Six candidate genes were chosen based on published data that shows their involvement in vulval development. These genes include 3 that were upregulated, *lin-29* (Zn finger, C2H2 type), *hbl-1* (Zn finger, C2H2 type), *nhr-91* (Zn finger, NHR), and 3 that were downregulated, *fos-1* (*fos* proto-oncogene), *sel-5* (Ser-Thr Kinase), and *jac-1* (p120 catenin homolog). *lin-29* is a transcription factor involved in the heterochronic development of the vulva and has been proposed to regulate genes involved in determining vulval cell types, π cell specification, and the vulva-uterine-seam cell connection (Newman et al., 2000). *hbl-1* is the *C. elegans* homolog of the *Drosophila hunchback* (*hb)* gene and is required for the proper organization of seam cells, the proper migration of the P cells (precursors to the Pn.p cells) to the ventral surface in the L1 stage, and the correct execution of Pn.p cell divisions to form the adult vulva (Fay et al., 1999). The adult vulva in both *lin-29* and *hbl-1* mutants develop precociously and are severely deformed, which includes Pvl and Egl phenotypes (Figure 10). *nhr-91* is known to be expressed in vulval cells during the late L4- young adult stage, but mutants do not show any defects and are completely wildtype (Figure 10) (Gissendanner et al., 2004).

The proto-oncogene *fos-1* has been extensively studied and characterized in its role in forming the vulva-uterine connection, π cell differentiation, invasion of the anchor cell into the vulval epithelium, and invagination and morphology of the vulva (Figure 10) (Hwang et al., 2007; Marri and Gupta, 2008; Oommen and Newman, 2007; Seydoux et al., 1993; Sherwood et al., 2005). *sel-5* is a suppressor/enhancer of *lin-12* that is not a core component of the LIN-12/Notch pathway but is involved in the AC/VU fate decision (Figure 10) (Fares and Greenwald, 1999). Last, *jac-1* is a member of the cadherin-catenin complex in at apical junctions that is non-essential in epithelial morphogenesis, but plays a minor role, similar to the *Drosophila* p120 catenin (Myster et al., 2003; Pettitt et al., 2003).

To validate the microarray data we performed a quantitative real-time PCR (qRT-PCR) experiment. qRT-PCR utilizes the foundation of PCR with some modifications to allow the quantification of the amount of PCR product produced. To accomplish this, fluorescently tagged nucleotides are used that, when incorporated into a PCR product, emit a particular wavelength of light which is measured and quantified by a computer. The fluorescence measured is correlated to the amount of product produced. Since the cDNA used as a template for the experiment is generated from total RNA from mutant or RNAi treated worms, the quantity of PCR product produced for genes that are regulated by the mutant gene will be directly affected. Of these six genes all but *jac-1* showed the same trend in either up or down regulation as the microarray and were validated as being regulated by *hda-1* (Cumbo et al., 2010) (Figure 7).

The interaction of *hda-1* with the remaining 5 genes was further validated and characterized using a combination of genetic and RNAi techniques. By combining *hda-1(RNAi)* and known mutant alleles or RNAi of each of the candidate genes, we were able to confirm or reject the interactions indicated from the microarray. *fos-1(ar105), hbl-1(mg285),* and *lin-29(n333)* mutants are known to have vulval morphology defects. We observed subtle invagination defects in *nhr-91(RNAi)* (no mutant currently exists for *nhr-91*) and *sel-5(ok149)* animals, suggesting that these genes are involved in vulval development (Figure 10), although weak phenotypes may be caused by other factors, such as, genetic redundancy or gene inactivation. We examined interactions of these genes with *hda-1* and found that the penetrance of vulval morphology defects in *hda-1(RNAi); nhr-91(RNAi)* and *hda-1(RNAi); sel-5(ok149)* mutants showed no difference from control *hda-1(RNAi)* animals (Table 4) (Cumbo et al., 2010). *hda-1(RNAi); fos-1(ar105)* animals displayed an increase in vulval morphological defects when compared to *hda-1(RNAi)* animals alone and the defect was morphologically similar to *hda-1(RNAi)* animals (Table 4) (Figure 10) (Cumbo et al., 2010). While *fos-1* appears to be interacting with *hda-1* in the vulva, it is clear that *nhr-91* and *sel-5* are not. The difference between microarray and phenotypic analysis results could be explained by tissue specific gene regulation in other non-vulval tissues. *hbl-1* and *lin-29* are epistatic to *hda-1* since *hda-1(RNAi)* in these mutant backgrounds neither affected the penetrance nor the vulval morphology of the mutants alone (Table 4) (Figure 10) (Cumbo et al., 2010). Since both *hbl-1* and *lin-29* are heterochronic and are important in regulating developmental timing in *C. elegans*, it is possible that they act much earlier than *hda-1* in determining vulval morphology.

We further characterized the interaction of the above genes with *hda-1* by examining GFP reporter expression in the vulval cell lineage at the L4 stage in *hda-1(RNAi)* animals. *hbl-1::GFP* expression was observed in vulval muscle cells at the L4 stage, but was not observed in any of the 22 cells that comprise the vulva thus, *hda-1(RNAi)* did not reveal any changes in vulval expression. *nhr-91::GFP* is expressed in many cell types including neuronal cells, seam cells, the spermatheca, and vulval cells as reported earlier (Gissendanner et al., 2004). *hda-1(RNAi); nhr-91::GFP* animals showed a slight overall reduction in expression in all cell types, even though the microarray and qRT-PCR experiments predicted *nhr-91* would be upregulated in *hda-1* mutants (Joshi, 2008). The RNA for the microarray and qRT-PCR was extracted from L2 stage animals, which could be a reason for this inconsistent result. *hda-1* may be regulating *nhr-91* at the L2 stage, which would be detected by the microarray and qRT-PCR, but may not be a target of *hda-1* at the L4 stage when we examined *nhr-91* expression. Thus, it is possible that *nhr-91* is a target of *hda-1* regulation early in development, but this needs to be carefully tested to be confirmed.

The expression of a splice variant of *fos-1, fos-1b,* was found to be downregulated in *hda-1(RNAi)* treated animals. Previous reports have described the expression of both *fos-1a* and *fos-1b* in gonadal lineage cells, where *fos-1a* is exclusively expressed in the AC, while *fos-1b* is expressed in the AC and other uterine cells (Oommen and Newman, 2007; Sherwood et al., 2005). Upon closer examination a former summer student, V. Raghavan, observed *fos-1b::CFP* expression in the vulval cell lineage, specifically vulD,

vulE, and vulF cells (Cumbo et al., 2010). *hda-1(RNAi)* treated animals showed a significant decrease in *fos-1b::CFP* expression in all of these cell types with the greatest reduction in vulE and vulF cells where no expression was typical, while a faint level of expression was typically observed in vulD (Cumbo et al., 2010). While *hbl-1::GFP* fluorescence was not observed in vulval cells and *nhr-91::GFP* expression was ambiguous, it is clear that *fos-1b* expression was down regulated in *hda-1(RNAi)* animals. These results are consistent with *hda-1* regulating the expression of *fos-1b* in vulval cells.

3.5 *hda-1* Regulates *lin-11* and *egl-13* Expression In π Cells and Their Progeny

We found that *hda-1* was expressed in the AC in *sEx13706* animals and observed an AC migration defect in *hda-1* mutants (Figure 8) (Cumbo et al., 2010). Although no expression of *hda-1* was observed in π cells, we frequently observed a defective vulva-uterine connection in *hda-1* mutants implicating its role in regulating gonadal cell fates (Figure 8) (Cumbo et al., 2010). In order to determine the role of *hda-1* in gonadal cells we utilized two reporter genes that are known to express in and are necessary in determining the fates of π cells and their progeny, *lin-11* (LIM-HOX family) and *egl-13* (SOX family) (Hanna-Rose and Han, 1999; Newman et al., 1999). *lin-11::GFP* (*syIs80*) and *egl-13::GFP* (*kuIs29*) expression can be seen as early as the L3 stage in π cells, which persists through a round of division in the L4 stage to give rise to 12 π cell progeny (6 on each side of the animal) and begins to express in the AC (Gupta and Sternberg, 2002; Hanna-Rose and Han, 1999) (Figure 11). *hda-1(RNAi)* animals show a significantly decreased or absent level of expression in both *lin-11::GFP* and *egl-13::GFP* animals,

but animals that had low levels of expression of either *lin-11::GFP* or *egl-13::GFP* had excess numbers of π progeny-like cells (Figure 11) (Cumbo et al., 2010). Examined *lin-11::GFP* animals ranged between 1 and 9 π progeny-like cells, while *egl-13::GFP* animals ranged between 3 and 13 π progeny like cells (Table 5) (Cumbo et al., 2010). Extra cells could be due to extra divisions at the L4 stage or due to abnormal specification of gonadal cells at the L3 stage. To determine which of these scenarios is the case, *hda-1(RNAi)* L3 animals were examined and were frequently found to have more than 3 π cells compared to control animals (Table 6) (Cumbo et al., 2010). To distinguish between these possibilities we generated *hda-1(e1795); syIs80 (lin-11::GFP)* and *hda-1(cw2); kuIs29 (egl-13::GFP)* strains. Nearly all *e1795; syIs80* animals had no gonadal or vulval cell expression and significantly decreased levels of expression in all other cells, such as ventral cord neurons, which is comparable to *hda-1(RNAi)* fed animals (Figure 12) (Table 5) (Cumbo et al., 2010). *hda-1(cw2); kuIs29* animals showed a less penetrant reduction of gonadal expression, but clearly had extra cells expression the *egl-13::GFP* marker. These results are consistent with *hda-1* regulating the expression of *lin-11* and *egl-13* in π lineage cells leading to the formation of the vulval-uterine connection.

3.6 *hda-1* Regulates the Expression of *zmp-1* in the AC

Our *hda-1::GFP* expression and phenotypic analysis indicates that *hda-1* plays a role in the AC since it is expressed there and there is a visible migration defect (Figure 8) (Cumbo et al., 2010). *zmp-1* is known to be expressed in the AC, uterine, and vulval cells throughout development, so we were interested in whether its expression was regulated

by *hda-1* (Inoue et al., 2005). *e1795; zmp-1::GFP (syIs49)* animals have significantly reduced or absent expression in the AC, and an overall decrease in vulval expression (n=10; Faint AC expression= 4, Absent AC expression= 6) (Figure 13) (Cumbo et al., 2010). Reduced or absent expression of *zmp-1* in the AC indicates an AC fate specification defect. It is possible that *zmp-1* and other genes play an important role in specifying the AC fate, thus failure to specify this fate would result in abnormal uterine development. Furthermore, reduced expression of *zmp-1* in the AC may affect its ability to specify uterine cell fates, which would subsequently cause a defect in the formation of the vulval uterine connection. We observe increase in π lineage cells and it is known that *lin-11* and *egl-13* mutants do not affect π cell number, yet we observe the abnormal expression of these two transcription factors in supernumerary π-like cells. This indicates that *hda-1* likely functions upstream of *lin-11* and *egl-13* in π cell specification. Further experiments such as *zmp-1(RNAi)* or using a *zmp-1* mutant allele in a wildtype and *hda-1* mutant background will help to clarify the exact role *hda-1* plays in regulating *zmp-1* expression.

3.7 Summary and Discussion

This chapter demonstrates the importance of *hda-1* in both *C. elegans* and *C. briggsae* vulval development. *hda-1* mutant animals have gonadal, vulval, and uterine defects that were characterized using the cell junction maker *ajm-1*, the uterine π cell markers *lin-11* and *egl-13*, and the AC marker *zmp-1*. The cell junction marker revealed abnormal vulval ring formation, while the uterine and AC markers showed decreased and

abnormal expression. These observations prompted us to examine the expression of *hda-1*, which was found to be expressed in vulval and uterine lineage cells, consistent with our observations that *hda-1* is involved in vulval development. This expression was observed in *C. briggsae* animals also, while the *C. briggsae hda-1(RNAi)* phenotype was similar to that of *C. elegans* suggesting a conserved role in development. K. Joshi (a former graduate student) performed a microarray to identify target and examine genes that *hda-1* may interact with in vulval development. A number of putative targets were identified and we tested 5 of these targets that have implicated roles in vulval development (Joshi, 2008). We validated these 5 genes by qRT-PCR, but only 1 gene was able to be characterized using expression analysis. *fos-1b*, a transcript of *fos-1* that expresses in the vulva, was found to have aberrant expression in vulval cells in *hda-1(RNAi)* fed animals.

These experiments show that chromatin modifications are crucial to gene regulation. This layer of regulation is conserved between *C. elegans* and *C. briggsae* vulval development, and in fact, chromatin modifications are highly prevalent from yeast to humans. The role of *hda-1* in vulval morphogenesis is consistent with the roles of HDACs in yeast and mice, where they are required for sporulation, meiosis, and embryonic development. HDA-1 is a component of the NuRD complex and interacts with other NuRD complex proteins, all of which are involved in regulating gene expression through chromatin modification. These results provide support for the role of *hda-1* in vulval development, specifically morphogenesis. NuRD complex components are conserved in many eukaryotes and understanding the mechanism of gene regulation in

vulval development through chromatin mediated modifications will provide insight to the mechanisms of morphogenetic processes in other eukaryotes. By uncovering this layer of gene regulation in vulval development we are able to better understand how developmental processes are affected at the level of chromatin modification.

Table 3- *hda-1* mutant phenotypes

Genotype	Vulval Invagination Defect (L4)	Adult Pvl Phenotype
N2	0% (n>100)	0% (n>100)
hda-1(cw2)	68% (n=45)	1.4% (n=152)
hda-1(e1795)	100%(n=43)	100% (n=30)
N2; hda-1(RNAi)	79% (n=261)	79% (n=36)
hda-1(cw2)(RNAi)	95% (n=43)	ND
mfIs42	0%	0%
mfIs42; Cbr-hda-1(RNAi)	27% (n=56)	ND

ND= Not Done

Table 4- *hda-1* putative target phenotypic analysis

Genotype	L4 Def	Adult Pvl
hda-1(RNAi)	79% (n=261)	79% (n=36)
fos-1(RNAi)	76% (n=66)	39% (n=83)
hda-1(RNAi); fos-1(RNAi)	76% (n=74)	ND
lin-29(n333)	100% (n=16)	100 %(n=100)
lin-29(RNAi)	42% (n=69)	ND
hda-1(RNAi); lin-29(RNAi)	55% (n=62)	ND
hbl-1(mg285)	100%(n=14)	100% (n=50)
hbl-1(RNAi)	90% (n=79)	ND
hda-1(RNAi); hbl-1(RNAi)	74% (n=88)	ND
nhr-91(RNAi)	29% (n=69)	0% (n>100)
hda-1(RNAi); nhr-91(RNAi)	69% (n=72)	ND
sel-5(ok149)	4% (n=27)	0% (n>100)
sel-5(RNAi)	32% (n=59)	ND
hda-1(RNAi); sel-5(RNAi)	54% (n=59)	ND

ND= Not Done

Table 5- Specification of π progeny-like cells in *hda-1* mutants

Genotype	Stage	n	% of π progeny-like cells					
			<6	6-7	>7	<6	6-7	>7
syIs80; L4440 (RNAi)	L4	32	9	91	0	22	78	0
syIs80; hda-1 (RNAi)	L4	49	61	35	4	73	27	0
cw2; syIs80	L4	15	33	67	0	53	47	0
e1795; syI80	L4	17	12	0	0	0	0	0
kuIs29; L4440 (RNAi)	L4	45	4	96	0	2	93	4
kuIs29; hda-1 (RNAi)	L4	59	19	44	37	29	58	14
cw2; kuIs29	L4	46	24	63	13	46	48	7

Table 6- Specification of π cells in *hda-1* mutants

Genotype	Stage	n	% of π like cells					
			<3	3	>3	<3	3	>3
syIs80; L4440 (RNAi)	L3	25	4	92	4	20	76	4
syIs80; hda-1 (RNAi)	L3	52	29	44	27	37	42	21
kuIs29; L4440 (RNAi)	L3	36	3	64	33	8	75	17
kuIs29; hda-1 (RNAi)	L3	36	6	36	58	8	39	53

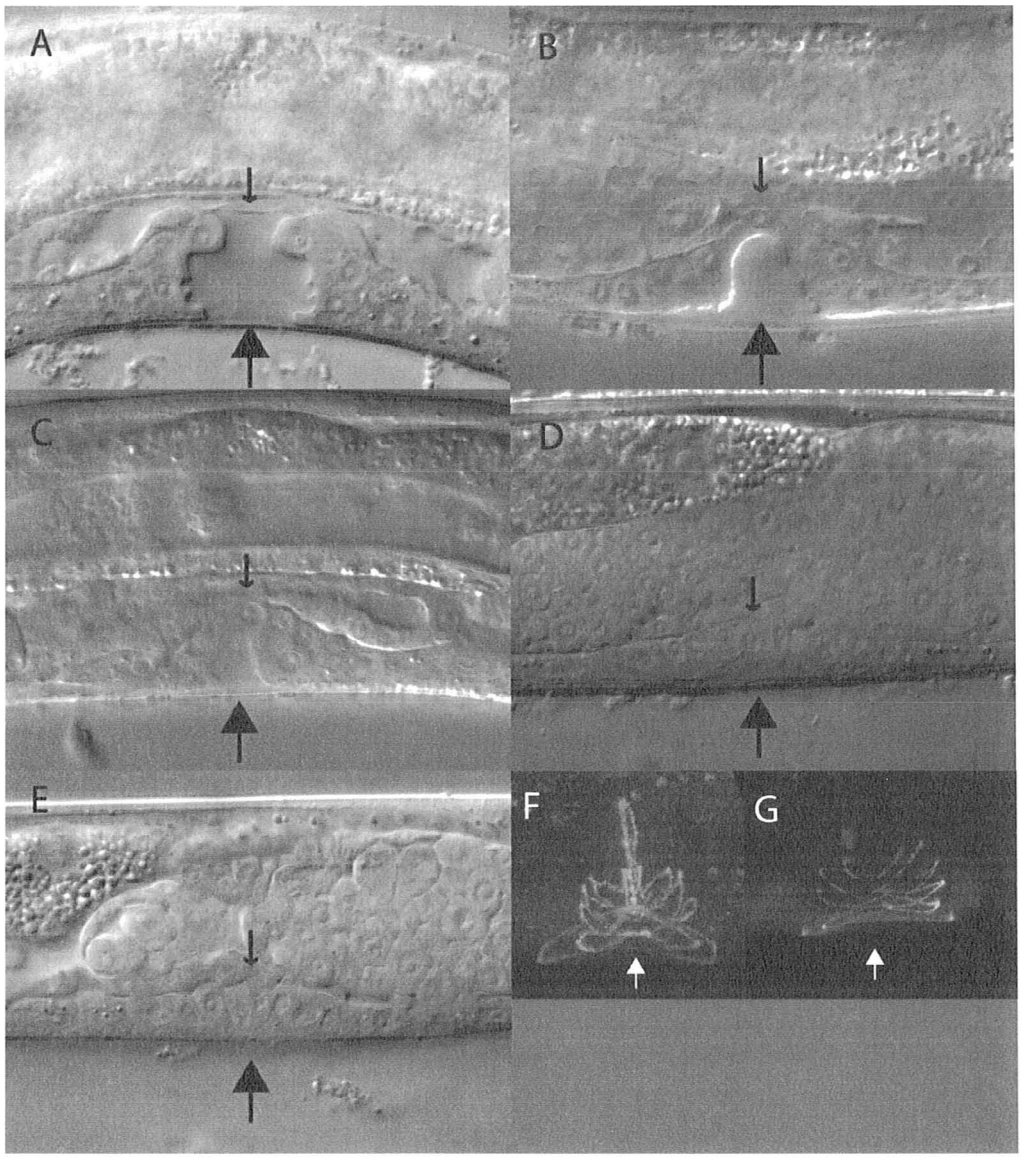
A
B
C
D
E
F
G

Figure 8- *hda-1* vulval mutant phenotypes

Large arrows point to the central vulval invagination. Small arrows point to the AC (if visible) or the utse. All animals are in the mid-L4 stage.

(A) Wildtype *C. elegans* vulva at the L4 stage. This animal has the typical 'Christmas tree like' vulval invagination. The AC has migrated away from the vulval apex and fused. The utse is formed in this animal, which is the thin membrane that connects the vulva to the uterus (indicated by the small arrow).

(B) Typical *hda-1(RNAi)* fed animal. An abnormal lopsided vulval invagination is present here. The AC has failed to migrate away from the vulval apex, but appears to have invaded through the basement membrane of the developing uterus.

(C) An *hda-1(cw2)* mutant is depicted here. The vulval invagination is much smaller than WT and *hda-1(RNAi)* fed animals, while the AC appears to be atop the vulval apex. The basement membrane between the uterus and the vulva is still intact.

(D) A typical *hda-1(e1795)* mutant. The vulva in these mutants fails to make a significant invagination and AC frequently fails to invade the basement membrane or migrate from the vulva. The gonad is also severely defective in these mutants.

(E) A *hda-1(cw2); hda-1(RNAi)* fed animal. *hda-1(RNAi)* in the *cw2* mutant increases the severity of the *hda-1* mutant defect to a similar level to *e1795*. The AC is not visible in this mutant, but it is clear that the basement membrane is still intact and the vulva has failed to make a significant invagination.

(F) *ajm-1::GFP* expression in a mid L4 wildtype animal.

(G) *ajm-1::GFP* expression in a mid L4 *hda-1(RNAi)* animal showing defective invagination and ring formation.

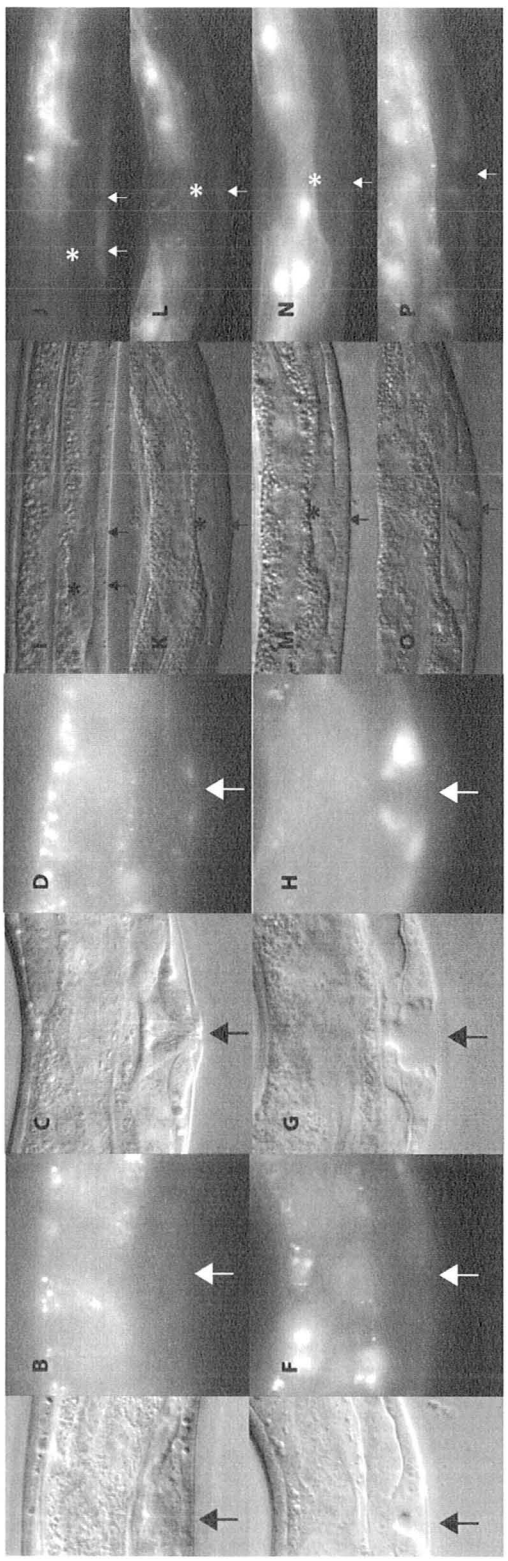
B
C
D
F
G
H
I
J
K
L
M
N
O
P

Figure 9- *hda-1* vulval expression

(A-D) *Cbr-hda-1::GFP* expression in *bhEx68* transgenic animals. Expression can be seen in the late L4 and Adult stages in the vulA cells

(E-H) *Cel-hda-1::GFP* expression in *bhEx72* transgenic animals. Hazy GFP expression can be seen in all vulval cell types in this early L4 animal (F). *hda-1::GFP* expression is also visible at the mid L4 stage in vulD/B1/B2/A cells in this focal plane.

(I-P) *sEx13706* expression in VPCs from the L3 stage through the mid-L4 stage. (I-J) are corresponding images of an L3 animal at the Pn.px stage. The * indicates placement of the AC directly above the P6.px cells. (K-N) are of late L3 animals. *hda-1* expression is clear in P(5-7).p and in the AC. (O-P) are the corresponding images of a mid L4 *sEx13706* animal expressing *hda-1* in vulA/B1/B2/D, along with the fused VPCs, P4.p and P.7p.

The large arrow indicates the central vulval invagination, while the * marks the AC.

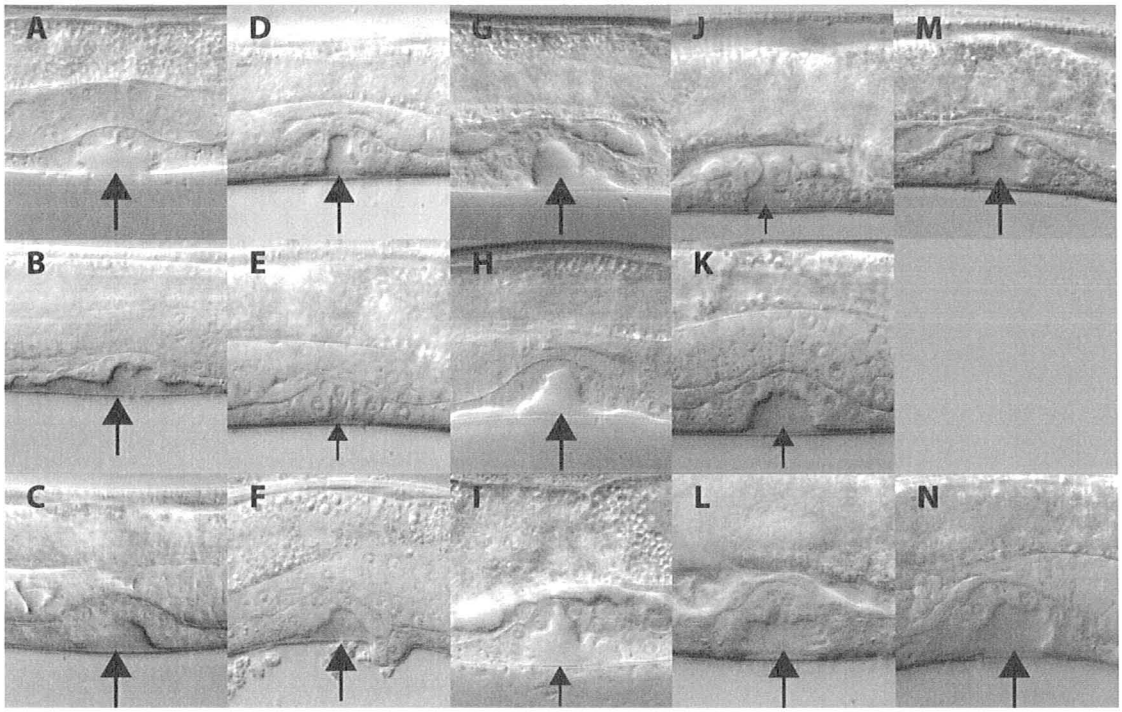

Figure 10- Putative *hda-1* target phenotype analysis

First Row: Mutant Phenotypes (except the last column, *nhr-91*, where no mutant exists)
Second Row: Mutant; *hda-1(RNAi)* Phenotypes
Third Row: target gene RNAi; *hda-1(RNAi)*

(A-C) *fos-1* analysis. The *fos-1(ar105)* mutant depicted in (A) has a vulval invagination defect and a clear failure of the AC to invade the basement membrane to form the utse. (B) *fos-1(ar105); hda-1(RNAi)* shows a much greater vulval invagination defect and retains the basement membrane invasion defect. (C) *fos-1(RNAi); hda-1(RNAi)* animals show a higher level of penetrance of the vulval invagination defect. Qualitatively the defect is similar to *hda-1(RNAi)* alone.

(D-F) *hbl-1* analysis. *hbl-1(mg285)* mutants have defective vulval invaginations which are affected by niether *hda-1(RNAi)*, nor *hbl-1(RNAi); hda-1(RNAi)*.

(G-I) *lin-29* analysis. Heterochronic *lin-29(n333)* mutants are known to have defects in vulval morphology which are not enhanced through *hda-1(RNAi)* in either the *lin-29(n333)* mutant or *lin-29(RNAi)* fed animals.

(J-L) *sel-5* analysis. *sel-5(ok149)* mutants have a slight vulval morphology defect which is evident in (J). *hda-1(RNAi)* treatment of these animals showed no difference in vulval defect penetrance from *hda-1(RNAi)* control animals.

(M-N) *nhr-91* analysis. *nhr-91(RNAi)* animals have a nearly WT morphology as exhibited in (M). Vulval defects in *nhr-91(RNAi); hda-1(RNAi)* animals were not enhanced when compared to *hda-1(RNAi)* animals alone.

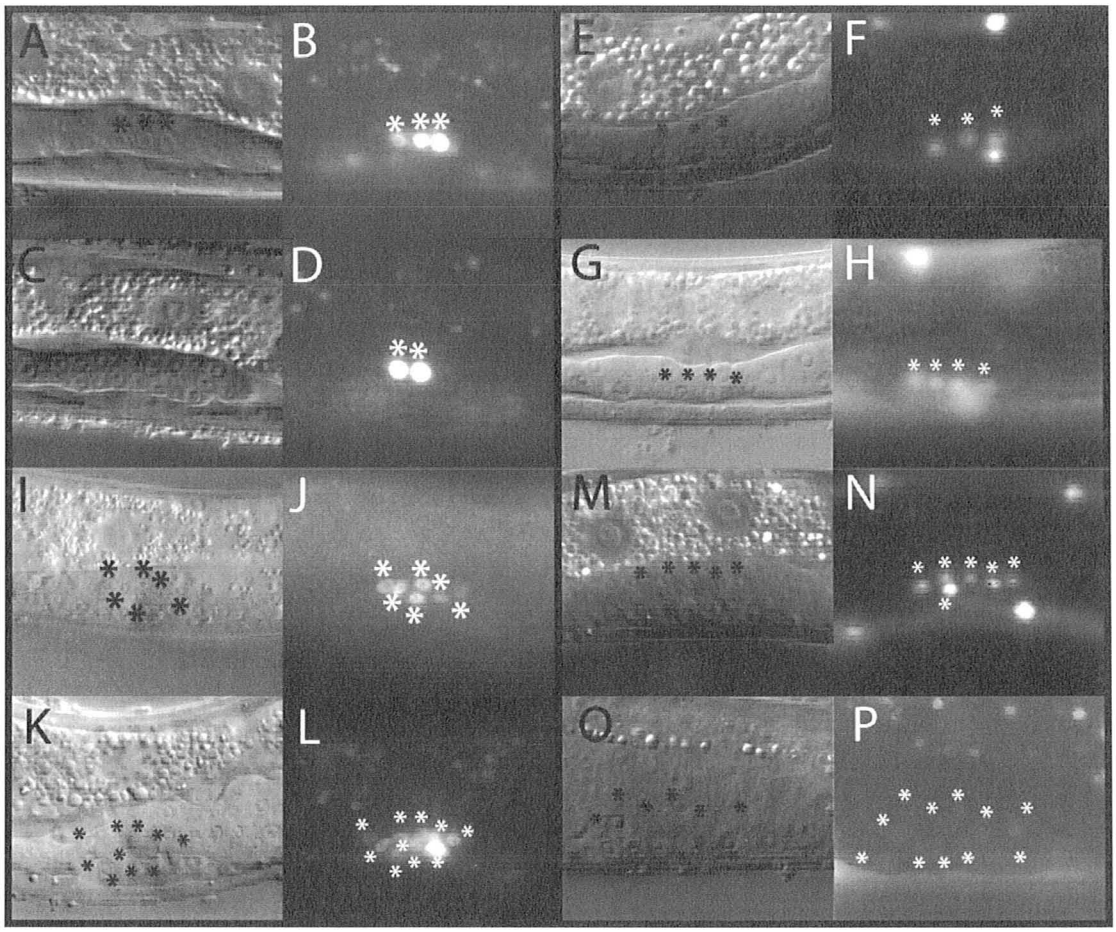

Figure 11- π cell specification in *kuIs29; hda-1(RNAi)* and *syIs80; hda-1(RNAi)* mutants

(A-D) L3 *kuIs29* expression. Wildtype expression of *egl-17::GFP* (A-B) can be seen in 3 prominent GFP expressing π cells marked by *. *kuIs29; hda-1(RNAi)* fed animals show abnormal *kuIs29* expression (C-D). This animal only has two π cells.
(E-H) L3 *syIs80* expression. Wildtype expression of *lin-11::GFP* (E-F) can be seen in 3 prominent GFP expressing π cells marked by *. *syIs80; hda-1(RNAi)* fed animals show abnormal *lin-11::GFP* expression (G-H). This animal has 4 π cells expressing *lin-11::GFP* at the L3 stage.
(I-L) L4 *kuIs29* expression. Wildtype expression of *egl-17::GFP* (I-J) can be seen in 6 prominent GFP expressing π progeny cells marked by *. (K-L) This *kuIs29; hda-1(RNAi)* fed animal shows *egl-17::GFP* expression in 10 π progeny-like cells.
(M-P) L4 *syIs80* expression. Wildtype expression of *lin-11::GFP* (M-N) can be seen in 6 prominent GFP expressing π progeny cells marked by *. (O-P) This *syIs80; hda-1(RNAi)* fed animal is faintly expressing *lin-11::GFP* in at least 11 π progeny-like cells.

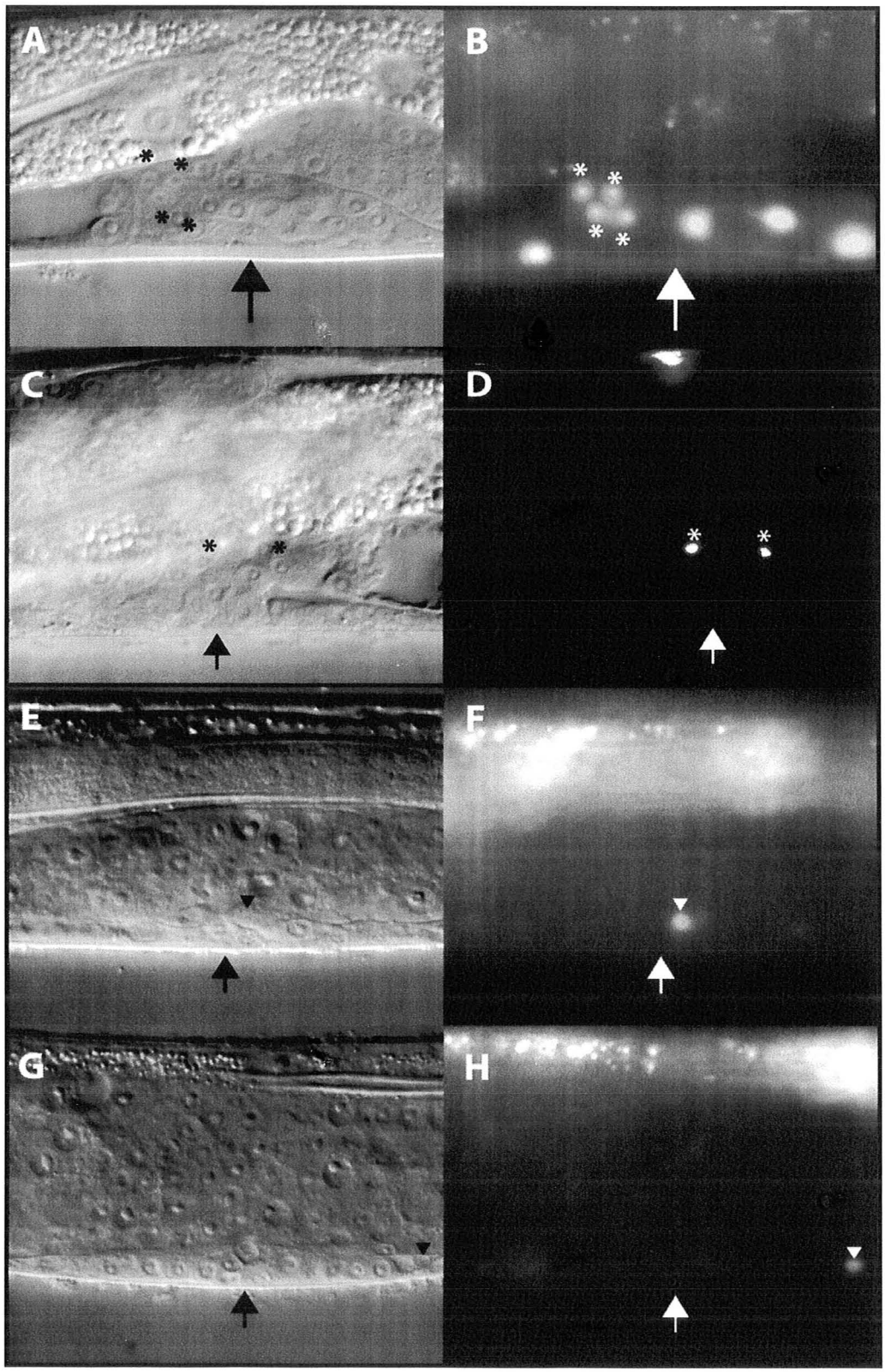
A
B
C
D
E
F
G
H

Figure 12- *hda-1(cw2); kuIs27* and *hda-1(e1795); syIs80* mutant expression

(A-D) *hda-1(cw2); kuIs27* animals showing abnormal *egl-17::GFP* expression.
(A-B) This L4 animal has a defective vulva typical of *cw2* mutants and is only expressing *egl-17::GFP* in 4 π progeny-like cells, indicated by *. Some misplaced ventral cord (VC) neurons are also fluorescing. The vulval invagination is indicated by the arrow.
(C-D) *egl-17::GFP* can only be seen in two π progeny-like cells in this L4 animal. Expression is also absent from the VC neurons.
(E-H) *hda-1(e1795); syIs80* L4 animals showing abnormal expression of *lin-11::GFP*. Expression is absent in both of these animals in most tissues.
(E-F) A single π progeny-like cell expresses in this mutant.
(G-H) *lin-11::GFP* expression in π progeny-like cells is absent in this animal. A single neuron is also fluorescing.

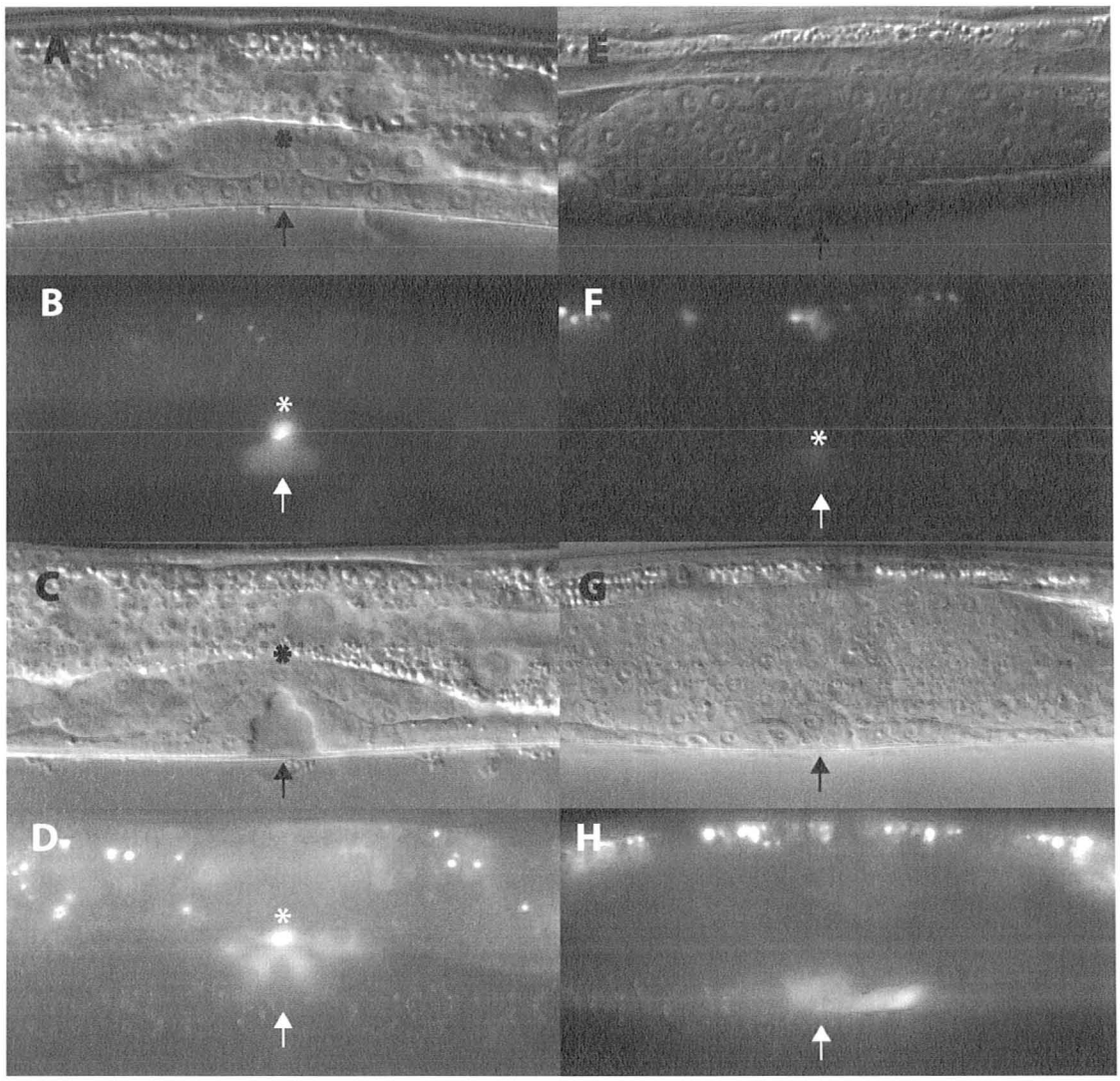

Figure 13- *syIs49 (zmp-1::GFP)* expression in *hda-1(e1795)* mutants

(A-D) Wildtype *zmp-1::GFP* expression can be seen fluorescing brightly in the AC in both the L3 (A-B) and L4
(C-D) stages as indicated by a *. At the L4 stage expression spreads to the neighbouring π progeny cells once the AC fuses with them. The vulval opening is indicated by an arrow.
(E-G) *hda-1(e1795); syIs49* animals show abnormal expression of *zmp-1::GFP*.
(E-F) AC expression is greatly reduced in this animal when compared to the wildtype (B).
(G-H) AC expression is not clear in this mutant at the L4 stage. Detectable expression seems to be coming from the vulval cells.

Chapter 4: Molecular Characterization of *pry-1*

Wnt signaling is known to be involved in maintain VPC competence throughout development by acting through the HOX gene *lin-39* (Sternberg, 2005). The conservation of this signaling pathway was of interest to us, so we used a sister species of *C. elegans* to facilitate a comparative study. Using a forward genetics approach, *C. briggsae* mutants were isolated that possessed a Muv phenotype. Of these mutants, 3 alleles failed to complement each other and were mapped to a single gene, *Cbr-pry-1*. Molecular characterization of this gene was required to understand the basis of its phenotype, which allows genetic interactions with known Wnt pathway genes to be tested.

4.1 Sequencing of the *Cbr-pry-1* Locus Reveals Mutations Corresponding to *sy5353* and *sy5411*

Previous work by B. Gupta and N. Bojanala has shown that *sy5353, sy5270,* and *sy5411* fail to complement each other, suggesting that they are alleles of *Cbr-pry-1*. To confirm this we sequenced the genomic region of *Cbr-pry-1* in all three alleles (Chapter 2: Materials and Methods). In the case of *sy5353* there is a G to A transition at the first base of intron 6 that is predicted to disrupt the splicing donor site. There are two in frame stop codons (TAA and TGA) within 40 bp (Figure 6) (Seetharaman, 2008; Seetharaman et al., 2010). The *sy5411* allele carries a GC insertion in exon 5 (+1761 from translational start site, flanking sequences TCGGCGCGC and CAGCCGTAC) that is expected to alter the reading frame leading to the introduction of two premature in frame codons (TGA and TAA) within 125 bp (Figure 6) (Seetharaman et al., 2010). With regards to the *sy5270*

allele, no mutation was found within any of the exons of *Cbr-pry-1*. It is conceivable that *sy5270* may be a regulatory mutation located upstream, downstream, or within an intron of the gene.

4.2 Overexpression of *pry-1* cDNA in *C. elegans* and *C. briggsae* Rescues the *pry-1* Mutant Phenotype

Further validation of *Cbr-pry-1(sy5353)* was necessary, along with confirmation of the *Cel-pry-1(mu38).* To achieve this we generated constructs that contained full length *pry-1* cDNAs for both *Cel-pry-1* and *Cbr-pry-1* under the control of a heat shock promoter and introduced this array into each mutant background. Overexpression of *Cbr-pry-1* cDNA (*pGLC29 hsp::Cbr-pry-1*) was shown to rescue the mutant phenotype in over half of the *sy5353* animals (53% wild type, n = 163, compared to 3% wild type, n = 39 in *sy5353* animals without heat shock) (Seetharaman, 2008; Seetharaman et al., 2010). Using the same heat shock promoter, we were able to rescue the mutant phenotype in *mu38* animals using both *Cel-pry-1* and *Cbr-pry-1* cDNA. Overexpression of *Cel-pry-1* cDNA (*pGLC37 hsp::Cel-pry-1)* was able to rescue the Muv phenotype in 91% (n=103) compared to 40% (n=96) in animals without heat shock (Seetharaman et al., 2010). A similar result was obtained by overexpressing *Cbr-pry-1* cDNA (*pGLC29)* in *mu38; bhEx81* animals, where 91% (n=76) of the heat shocked animals were rescued, compared to 36% (n=66) of *mu38; bhEx79* animals that were not heat shocked (Seetharaman et al., 2010). We also overexpressed *Cel-pry-1* cDNA (*pGLC37*) to rescue the mutant phenotype in nearly half of the heat shocked *sy5353; bhEx93* animals (46% wildtype,

n=142, compared to 21% wild type, n=142 in *sy5353* animals without heatshock) (Seetharaman et al., 2010).

4.3 *pry-1* Mutant Phenotype

An EMS screen was undertaken to identify mutations that cause the formation of ectopic vulva inductions leading to ectopic pseudo-vulvae in adults. Since mutants were chosen based on adult phenotypes it was pertinent to further characterize the ectopic vulva inductions at the mid-L4 stage. Since ectopic pseudo-vulvae can form in adults for a number of reasons (extra cell divisions, failure of VPCs to migrate correctly, lack of competence to respond to inductive signaling, etc) it was crucial to understand the nature of the ectopic inductions in *pry-1* mutants. Upon detailed analysis of the vulval invagination in mid-L4 stage *sy5353* animals we discovered that the vulva exhibited a defective morphological phenotype consistent with *Cel-pry-1(mu38)* animals (Figure 14) (Seetharaman et al., 2010). Closer analysis of *Cbr-pry-1(sy5353)* mutants revealed the presence of both an overinduced and underinduced vulva phenotype. Overinduced refers to the presence of ectopically induced VPCs in the larval stages, while underinduced refers to the lack of induction of P7.p specifically. Thus, it is possible for a single animal to display both of these phenotypes. Frequently in most *Cbr-pry-1* mutant animals P3.p, P4.p, and P8.p were ectopically induced, while P7.p remained uninduced (Table 9, Chapter 5) (Figure 14) (Seetharaman et al., 2010). A similar, albeit less penetrant phenotype is observed in *Cel-pry-1(mu38)* animals (Table 7) (Seetharaman et al., 2010). The apparent discrepancy in penetrance raises the question of whether *mu38* and *sy5353*

are truly genetic null alleles. To test this, *mu38* was placed over a deficiency, and the Muv penetrance was scored. eDf3 has been shown to delete the *pry-1* locus (M.C. Beckerle unpublished) and is known to be embryonic lethal, where heterozygous mothers lay dead eggs. The *pry-1(mu38)/eDf3* animals failed to show a Muv phenotype. This did not provide clear evidence as to what kind of allele *mu38* is, presumably due to a loss of the deficiency in the parental strain (Data not shown). Further testing of the strain is required to validate that the strain does carry the eDf3 deficiency that spans the *pry*-1 locus, such as PCR amplifying the region containing the deletion. An alternate approach could use qRT-PCR to measure the mRNA levels of the *pry-1* gene in both *C. elegans* and *C. briggsae*.

Previously it has been shown that placement of the AC will affect which VPCs receive the most inductive signal and are subsequently induced (Sternberg, 2005). To test whether the *pry-1* mutant phenotype was due to ectopic AC placement or formation, we scored AC placement in both *sy5353* and *mu38* animals. Both mutants showed typical AC placement above P6.p from L2 stage through to early L4 stage (Table 7) (Figure 14). These results are consistent with a similar phenotype that has been described previously in *C. elegans* (Gleason et al., 2002). From these results, along with our combination of rescue experiments, it is evident that *pry-1* is performing a similar role in both species.

4.4 *pry-1* Mutants have Posterior Pn.p Defects

Examination of uninduced posterior VPCs P(7-11).p in *Cbr-pry-1* mutants revealed a novel phenotype. Uninduced posterior VPCs in these mutants were significantly smaller in size compared to wildtype ($p<0.0001$) and adopted a P12.p-like morphology (Figure 14) (Seetharaman et al., 2010). Posterior VPCs in *Cbr-pry-1(s5353)* mutants were found to be, on average, 33% smaller than WT AF16 posterior VPCs (*sy5353* average VPC size= 6.9 mm, n=13; AF16 average VPC size= 10.2 mm, n=11. VPCs were measured as full screen printouts using a ruler, which maintained the ratio between the two genotypes). It is unclear whether these cells have adopted a P12.p-like fate through fate transformation. To further delve into this interesting phenotype we used GFP based cell junction markers, *ajm-1::GFP* and *dlg-1::GFP*, to assess whether these uninduced cells fuse to a major hypodermal syncitium, hyp7. AJM-1 (a novel coiled-coil protein) and DLG-1 (*Drosophila* Disc Large family) are localized to apical junctions (Bossinger et al., 2001; Koppen et al., 2001) and identify cells that do not fuse to the hyp7 (Sharma-Kishore et al., 1999) (Marie-Anne Felix, personal communication) which allows them to remain competent to respond to patterning signals. Uninduced posterior VPCs in *Cel-pry-1(mu38); ajm-1::GFP* animals are frequently unfused, which is comparable to *Cbr-pry-1(sy5353); dlg-1::GFP* animals where the uninduced posterior VPCs are also frequently unfused (Figure 15) (Seetharaman et al., 2010). In both species there was frequent GFP expression in unfused P7.p and P8.p, but unfused P(9-11).p were also observed (Table 8) (Seetharaman et al., 2010). These results suggest that Wnt signaling

plays an important role in maintaining VPC competence, but also provide a new function in that Wnt signaling is also involved in promoting cell proliferation and differentiation.

4.5 *Cbr-pry-1* Expression Pattern

The expression pattern of *Cel-pry-1* has been shown in previous work (Korswagen et al., 2002) and to complete a detailed analysis of the function of Wnt signaling in *C. elegans* and *C. briggsae* it was important to observe the *Cbr-pry-1* expression pattern. Three separate constructs were generated to dissect the 5' UTR of the *Cbr-pry-1* locus. Constructs containing a 5 kb, 3.8 kb, and 2.4 kb PCR fragment of the 5' UTR were subcloned into the Fire lab expression vector pPD95.69 (Figure 6) (Seetharaman et al., 2010). All three constructs show similar patterns of expression, although the level of fluorescence decreases as the size of the insert decreases. *Cbr-pry-1* expression is visible throughout development and begins in the embryo in numerous hypodermal cells, which is similar to *Cel-pry-1* expression that has been previously reported (Korswagen et al., 2002). Expression persists throughout the L1 and L2 stages and can be seen in many neurons in the ventral hypodermal region (Figure 16). In the late L2 stage expression is observed in all VPCs, which persists in the progeny of P(5-7).p until the late L4 stage, indicating that *Cbr-pry-1* may play a role in both VPC specification and vulval differentiation and morphogenesis (Figure 16) (Seetharaman et al., 2010). Throughout development there are numerous unidentified cells in the head, tail, body wall regions, and neuronal projections that run in a dorsal-ventral manner that express *Cbr-pry-1*, indicating that *pry-1* is likely required in multiple cell fate specification events (Figure

16) (Seetharaman et al., 2010). *pry-1::GFP* expression also persists through adulthood and can be observed in the adult vulva (Figure 16) (Seetharaman et al., 2010).

4.6 Summary and Discussion

This chapter discusses the molecular characterization of *pry-1* in both *C. elegans* and *C. briggsae*. First we isolated *C. briggsae* EMS mutants that display a Muv phenotype, and mapped three of these mutants to the *Cbr-pry-1* locus. Sequencing of these mutants was able to confirm that two of these alleles are indeed *Cbr-pry-1* mutants, while the mutation in the third allele has yet to be discovered. Furthermore, *pry-1* cDNA from both species was able to rescue mutants in both species in each different combination which confirms that the *pry-1* mutations found are causing the Muv phenotype, and that *pry-1* is conserved in *C. elegans* and *C. briggsae*. We further characterized the *pry-1* mutant phenotypes and this was found to be consistent between both *C. elegans and C. briggsae*. Next we determined the *Cbr-pry-1* expression pattern by dissecting the *Cbr-pry-1* promoter into three overlapping fragments and all GFP reporter lines showed the same pattern of expression. From this we can conclude that *pry-1* is likely conserved in both species, but further genetic analysis is required to confirm this hypothesis.

Table 7- Anchor Cell placement in pry-1 mutants

Genotype	Stage	n	Normal	Abnormal
pry-1(mu38)	**L2**	26	24	2
	L3	51	51	0
	Early L4	18	17	1
Cbr-pry-1(sy5353)	**L2**	20	20	0
	L3	23	23	0
	Early L4	23	20	3

Table 8- Cell fusion scoring in pry-1 mutants

Genotype	n	# of Unfused Cells								Overinduced
		P3.p	P4.p	P5.p	P6.p	P7.p	P8.p	P9.p	P10.p	
sy5353; dlg-1::GFP	28	21	17	28	28	26	25	20	18	27
mu38; ajm-1::GFP	28	4	0	28	28	27	7	8	2	4

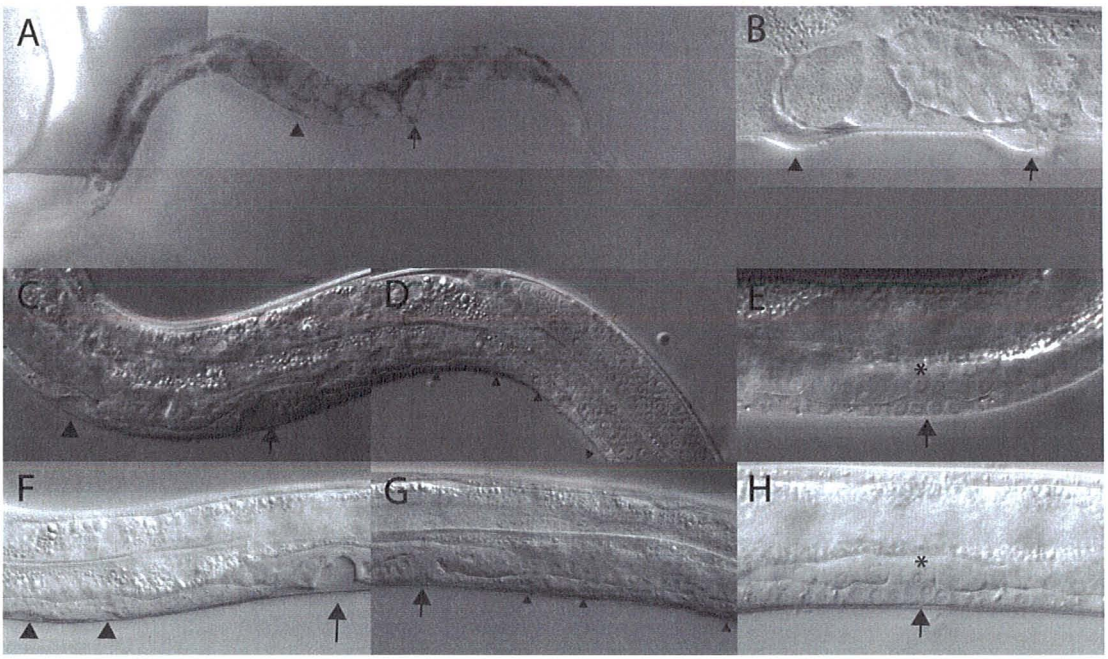

Figure 14- *pry-1* mutant phenotypes

Arrows point to the central vulval. Large arrowheads point to ectopic invaginations, while small arrowheads point to posterior Pn.ps. *'s mark the AC.

(A) An adult Muv *pry-1(mu38)* animal.
(B) A high magnification image of an adult Muv phenotype
(C) *Cbr-pry-1(sy5353)* L4 animal showing ectopic induction of P3.p
(D) *Cbr-pry-1(sy5353)* L4 animal showing uninduced posterior Pn.p cells that have acquired a P12.pa (neuronal) –like fate
(E) An L3 *Cbr-pry-1(sy5353)* animal showing WT AC placement
(F) A *pry-1(mu38)* animal displaying ectopic induction of both P3.p daughter cells
(G) Posterior Pn.p cells in *pry-1(mu38)* mutants do not acquire the P12.pa like fate observed in *Cbr-pry-1(sy5353)* animals
(H) WT AC placement in a *pry-1(mu38)* L3 animal

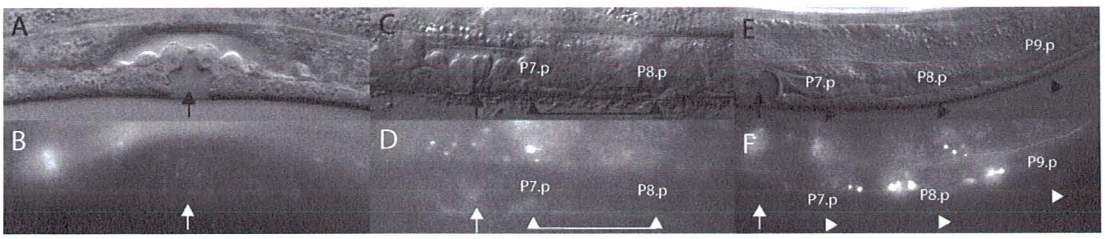

Figure 15- Posterior Pn.p cells are often unfused in *pry-1* mutants

Arrows indicate the central vulval invagination. Arrowheads indicate unfused cells.

(A-B) WT *ajm-1::GFP* expression in an N2 animal. Expression can only be seen in the unfused vulva toroidal rings
(C-D) In *pry-1(mu38)* mutants *ajm-1::GFP* expression can be seen extending from P7.p to P8.p indicating that neither of these Pn.p cells have fused to the hyp7.
(E-F) In *Cbr-pry-1(sy5353)* mutants *dlg-1::GFP* expression is detected in P(7-9).p indicating that these cells have not fuses appropriately with the hyp7.

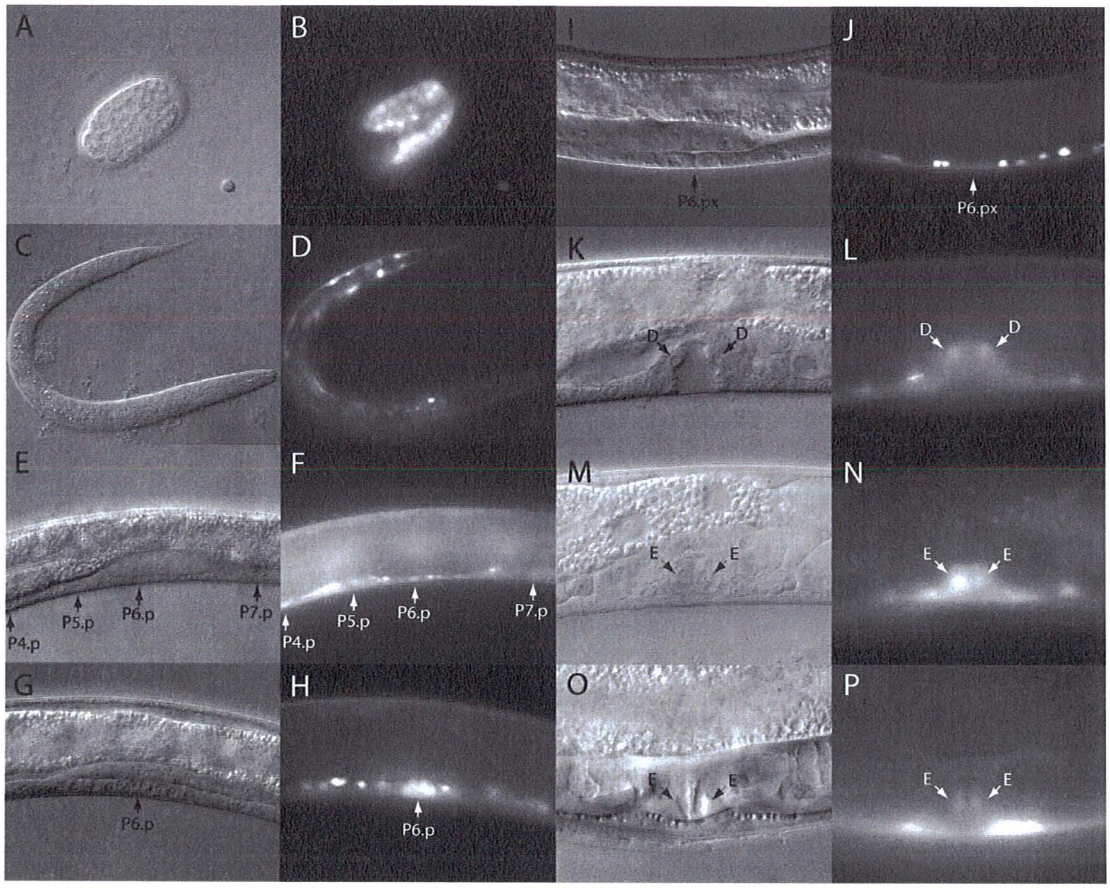

Figure 16- *pry-1::GFP* expression

pry-1::GFP is expressed throughout development, starting from embryogenesis (A-B), continuing through the L1 stage (C-D), the L2 stage (E-F), the L3 stages (G-J), and maintained in the L4 stage (K-M) through to the adult stages (M-P). *pry-1::GFP* expression can also been seen from the L2 stage through to the adult in vulval cells (E-P).

Chapter 5: Genetic Interactions of *pry-1* with Wnt Signaling Pathway Components and Targets

The molecular and phenotypic characterization of *Cbr-pry-1* allowed us to focus on determining its role in *C. briggsae* Wnt signaling, specifically in vulval development. It is important to investigate the role *Cbr-pry-1* plays in the Wnt signaling pathway. This will establish its position along the signaling cascade as well as provide a means to compare its function to its *C. elegans* counterpart. The interesting P7.p induction defect seems to be conserved and elucidation of this mechanism is important to fully understand the function of Wnt signaling in vulval development. Since many signaling pathways converge on each other during vulval development, studying how these pathways interact will be beneficial to establishing a signaling hierarchy within vulval development. From this analysis we may be able to identify specific targets of Wnt signaling that have been previously uncharacterized. To this end we use both genetic and RNAi approaches to study pathway interactions and downstream targets of Wnt signaling.

5.1 *Cbr-pry-1* Acts Upstream of *Cbr-pop-1* and *Cbr-lin-39*

Components of the Wnt signaling pathway involved in vulva development have been indentified and characterized in *C. elegans* (Eisenmann, 2005). Previous work has shown that *Cbr-pry-1* is a member of the *C. briggsae* Wnt signaling pathway (Seetharaman, 2008; Seetharaman et al., 2010). Through a series of RNAi experiments *Cbr-pry-1* was shown to act upstream of *Cbr-bar-1*, which is involved in vulva development, but was not epistatic to *Cbr-sys-1*, another β-catenin which as been shown

to be involved in gonadogenesis (Seetharaman, 2008; Seetharaman et al., 2010). Continuation of this pathway characterization has revealed that, *Cbr-pry-1* is a bona fide member of the Wnt signaling pathway in *C. briggsae*.

Using the RNAi approach, we focused on the role of the *tcf/lef* family member, *Cbr-pop-1*. We found that *Cbr-pry-1(sy5353); Cbr-pop-1(RNAi)* animals strongly suppressed the *pry-1* overinduced phenotype (Table 9). Similarly, *Cel-pry-1(mu38); Cel-pop-1(RNAi)* (Seetharaman, 2008; Seetharaman et al., 2010) and *Cel-pry-1(mu38); Cel-pop-1(hu9)* (constructed by B. Gupta) animals both showed a strong suppression of ectopic VPC induction (Table 9), indicating a conserved role of *pry-1-pop-1* mediated vulval development. To assess the cell fates associated with suppressed induction we determined how often VPCs in *Cbr-pry-1(sy5353); Cbr-pop-1(RNAi)* animals acquired a 3^{o} or F fate. VPCs in *Cbr-pry-1(sy5353); Cbr-pop-1(RNAi)* animals acquired the 3^{o} or F fate 33% of the time (n=90 VPCs), while control *Cbr-pry-1(sy5353); L4440 (RNAi)* animals acquired the 3^{o} or F fate 14% of the time (n=66 VPCs). While this suppression was not observed in P7.p or P8.p, it is clear that P(3-6).p fail to become induced more frequently when *Cbr-pop-1* is knocked down, which is indicative of the inability to respond to inductive signaling.

Studies in *C. elegans* have shown that Wnt signaling, through the HOX gene *lin-39,* plays a very important role in preventing the fusion of VPCs in the L2 stage, and then in the specification of VPC fates in the L3 stage (Eisenmann, 2005; Eisenmann et al.,

1998). Since this regulation is through *pry-1-pop-1* mediated Wnt signaling, we were interested in determining the role of *Cbr-lin-39*. Again, using the RNAi approach, we were able to show the conserved role of *lin-39* between *C. elegans* and *C. briggsae*. *Cbr-lin-39(RNAi)* animals show defects in cell fusion and specification similar to published results in *C. elegans* (Table 9) (Seetharaman et al., 2010). We also found that the overinduced phenotype was strongly suppressed in *Cbr-pry-1(sy5353); Cbr-lin-39(RNAi)* animals (Table 9) (Seetharaman et al., 2010). Again, we assessed the frequency of VPCs adopting a 3^{o} or F fate in *Cbr-pry-1(sy5353); Cbr-lin-39(RNAi)* animals. VPCs in *Cbr-pry-1(sy5353); Cbr-lin-39(RNAi)* animals acquired the 3^{o} or F fate 15% of the time (n=72 VPCs), while control *Cbr-pry-1(sy5353); L4440 (RNAi)* animals acquired the 3^{o} or F fate 14% of the time (n=66 VPCs) (Seetharaman et al., 2010). There is a slight, but statistically insignificant increase in the acquisition of the 3^{o} or F fate when *Cbr-lin-39* is knocked down. This result failed to show whether the suppression of the *pry*-1 phenotype is due to the acquisition of the 3^{o} or F and needs further confirmation. Nonetheless these results suggest that *Cbr-pry-1* has a conserved role in regulating cell fusion and specification as it does in *C. elegans*. The *pop-1* and *lin-39* data presented here indicate that the *C. briggsae* orthologs of these genes also act downstream of *Cbr-pry-1* in the same manner as the *C. elegans* Wnt signaling pathway.

5.2 Ectopically Induced VPCs in *pry-1* Mutants Adopt a 2^{o} Cell Fate

To determine the role of Wnt signaling in cell fate specification we utilized GFP-based molecular cell fate markers that are expressed in the progeny of VPCs that acquire

1^{o} and 2^{o} cell fates. Using six different reporter genes in *C. elegans* (*syg-2* – immunoglobulin superfamily, *daf-6* – *patched*-related, *dhs-31* – short-chain dehydrogenase/reductase, *egl-17* – *fibroblast growth factor (fgf)* family, *lin-11* – LIM homeobox family, and *ceh-2* – *Drosophila empty spiracles (ems)* homeodomain family) and two in *C. briggsae* (*Cbr-zmp-1* – zinc metalloproteinase family and *Cbr-egl-17*) that are faithfully expressed in subsets of 1^{o} or 2^{o} lineage of vulval cells, we were able to determine the cell fate of ectopically induced VPCs (Table 9) (Seetharaman et al., 2010). Various stages of vulval development were examined using the pertinent markers in order to demonstrate that the cell fates of ectopically induced VPCs were consistent at all larval stages. Typical patterns of expression, both in a cell specific and temporal manner, have been used in multiple studies to identify the fates of induced VPCs, which enabled us to assess the VPC fates in *pry-1* mutants (Burdine et al., 1998; Felix, 2007; Gupta et al., 2003; Inoue et al., 2002; Perens and Shaham, 2005; Shen et al., 2004) (Figure 17).

In *Cel-pry-1(mu38)* animals expression of 1^{o} lineage markers *egl-17::GFP(ayIs4)* (early/mid-L3 stage), *daf-6::YFP (bhEx53)* and *syg-2::GFP (wyEx3372)* (both mid/late-L4 stage) was localized to P6.p progeny and not detected in any of the ectopically induced VPCs (Figure 18) (Seetharaman et al., 2010). Contrary to the 1^{o} marker expression, the 2^{o} lineage markers *egl-17::GFP (ayIs4)*, *lin-11::GFP (syIs80)*, *ceh-2::GFP (syIs54)* (all mid/late-L4 stage) and *dhs-31::GFP (syIs101)* (old adult stage), were expressed in induced P5.p and P7.p along with all other ectopically induced VPCs (Figure 18) (Seetharaman et al., 2010). The analysis of *Cbr-pry-1(sy5353)* animals

revealed that, similar to *C. elegans*, the 2° lineage marker, *Cbr-egl-17::GFP* (*mfIs5*) (mid L4 stage), was expressed in the progeny of induced VPCs except P6.p (Figure 18) (Seetharaman et al., 2010). Furthermore, the 1° lineage cell marker, *Cbr-zmp-1::GFP (mfIs8)* (late L4 stage) was exclusively expressed in P6.p progeny and not present in any ectopically induced VPCs (Figure 18) (Seetharaman et al., 2010). An identical expression pattern of vulval cell fate markers in both *C. elegans* and *C. briggsae* indicates that the mechanism of Wnt signaling in 2° VPC fate specification is evolutionary conserved.

5.3 Activated Wnt Signaling Confers 2° Vulval Cell Fates in the Absence of a Gonad Derived Inductive Signal

The gonadal AC is the source of the LIN-3/EGF inductive signal that activates the Ras signaling pathway in VPCs, which confers 1° cell fate P6.p and that, in turn, activates the LIN-12/Notch signaling pathway to specify the 2° fate in the neighbouring P5.p and P7.p. It has also been shown that the Wnt ligands *mom-2* and *lin-44* are expressed in some gonadal cells, which may indicate that the gonad could be a source of the Wnt signal (Inoue et al., 2004). To assess the contribution of the gonad in VPC induction in *Cel-pry-1* mutants we ablated the gonadal precursor cells in the L1 stage, in *pry-1(mu38) ayIs4* animals and observed VPC fates in L3 and L4 stages. These ablations (performed by B. Gupta) revealed that 57% of induced cells (n=7) in laser operated animals adopted a 2° cell fate as judged by *egl-17::GFP* expression, while no induced cells (n=5) adopted a 1° cell fate (Seetharaman et al., 2010). Similar ablations in *Cbr-pry-1(sy5353); mfIs5* mutants performed by A. Seetharaman produced similar results (Seetharaman, 2008; Seetharaman et al., 2010). By removing the source of the inductive gonadal signal

through gonad ablation, we were able to show that Wnt signaling plays an instructive role in vulval development independent of the inductive signal.

5.4 LIN-12/Notch is not required in *pry-1* mutants to confer a 2° fate on ectopically induced VPCs

Previous studies have shown that LIN-12/Notch signaling is necessary and sufficient to confer a 2° fate on VPCs (Greenwald et al, 1983; Greenwald 2005; Sternberg 2005). Our results show that, through the use of molecular markers to assess cell fates, ectopic inductions in *pry-1* mutants acquire a 2° fate. These results, in conjunction with accepted views, formed the basis for us to study the role of LIN-12/Notch signaling in *pry-1* mediated VPC induction. To this end we used both RNAi and genetic approaches. *Cbr-lin-12(RNAi)* and *Cel-lin-12(RNAi)* in wildtype animals both resulted in a slight overinduction phenotype and abnormal vulval morphology (Table 9) (Seetharaman et al., 2010). When these RNAi construct containing bacteria were fed to *Cbr-pry-1(sy5353)* and *Cel-pry-1(mu38)* animals we found no suppression of the overinduced/underinduced phenotype (Seetharaman et al., 2010). These results may be due to the fact that *lin-12(RNAi)* does not work well in both species, which leads to a false positive result that activated Wnt signaling is acting to specify vulval fates in the absence of *lin-12*. To rigorously test this result *pry-1(mu38) ayIs4; lin-12(n676n909)* double mutants were generated. *lin-12(n676n909)* is a null allele and results in animals whose P(5-7).p adopt a 1° fate and form a large Pvl phenotype, but lack any other inductions (Figure 19). Crosses were set up and heterozygous clones were picked that possessed *egl-17::GFP* in order to assess the fate of induced cells (Materials and Methods). From these heterozygous

mothers, 26 putative homozygous *pry-1(mu38) ayIs4; lin-12(n676n909)* hermaphrodites were obtained. In two other attempts 12 more putative double mutants were obtained. All of the putative homozygous animals displayed a combination of Pvl and overinduced phenotypes (Seetharaman et al., 2010). While in the second set of putative double mutants some of the double mutants (n=6) were confirmed based on only morphology, and in 6 other cases we also examined *egl-17::GFP* expression in ectopically induced VPCs (Seetharaman et al., 2010). Finally, in the first set (n=26) the *lin-12* locus was sequenced to determine the presence of the *n676* mutation, further confirming the results. Of these sequenced putative double mutants 13 were found to be heterozygous for *n676*, 7 were found to be wild type, 3 were lost during PCR, and 1 was found to be homozygous for *n676* (Seetharaman et al., 2010). In summary, our results show that activated Wnt signaling in *pry-1* mutants confers a 2^{o} cell fate on ectopically induced VPCs in the absence of LIN-12/Notch signaling.

These experiments show that Wnt signaling can act independently of LIN-12/Notch to confer 2^{o} fates on induced VPCs. It is possible that LIN-12/Notch signaling is acting upstream of Wnt and feeding directly into the Wnt pathway to specify 2^{o} cell fates. It is known that *lin-12* acts through the HOX gene *lin-39* to specify vulval fates, while *pry-1* acts through the *tcf/lef* factor *pop-1*. If *lin-12* were to act upstream of Wnt signaling, then *pop-1(RNAi)* or the *pop-1(hu9)* mutant in conjunction with a *lin-12* weak gain of function mutation would suppress ectopic vulval inductions. *lin-12(n952)* provides a sensitized genetic background where only 2/3 of animals exhibit

overinduction, thus if *lin-12* signaling is upstream of Wnt signaling, *lin-39(RNAi)* and *pop-1(RNAi)* or the *pop-1(hu9)* double mutant will decrease the levels of overinduction. *lin-12(n952); lin-39(RNAi)* animals, as expected, strongly suppressed the *n952* overinduction phenotype, but *lin-12(n952); pop-1(RNAi)* and *lin-12(n952); pop-1(hu9)* failed to show this suppression (Table 9) (Seetharaman et al., 2010). These results support the hypothesis that LIN-12/Notch signaling is not acting upstream of the Wnt signaling pathway, but is acting in a parallel manner through *lin-39* to confer 2^{o} cell fates on VPCs.

Previous work has shown that *lip-1* (MAP Kinase Phosphatase) is a transcriptional target of *lin-12* and promotes the 2^{o} cell fate by antagonizing *mpk-1* (MAP Kinase) and subsequently, the 1^{o} fate (Berset et al., 2001). Thus, testing the role *lip-1* plays in VPC specification and induction was used to confirm that an activated Wnt signaling pathway can act independently of the LIN-12/Notch pathway in VPC specification. To accomplish this we took RNAi and genetic approaches. *Cel-lip-1(RNAi)* and *Cbr-lip-1(RNAi)* did not show any obvious defects in control animals, which was also the case when fed to the appropriate *pry-1* mutants (Table 9) (Seetharaman et al., 2010). No suppression or additional defects were observed in *lip-1(RNAi)* fed *pry-1* mutants (Table 9). The *lip-1(zh15)* mutant shows no obvious defects in vulval induction, much like the RNAi control animals, so to confirm these results we constructed a *Cel-pry-1(mu38) ayIs4; lip-1(zh15)* double mutant strain. Contrary to the expected result of a reduction in ectopic induction, we observed a significant increase in overinduced animals, where nearly all ectopically induced VPCs adopted a 2^{o} cell fate (Table 9) (Seetharaman et al., 2010). These data

provide strong support for the hypothesis that activated Wnt signaling can independently confer 2^{o} cell fates on induced VPCs.

5.5 Knockdown of *lin-12* and *lip-1* Promotes P7.p Induction in *pry-1* Mutants

Although no suppression of the overinduced phenotype or additional defects were observed in any of the *mu38 or sy5353 lin-12(RNAi)*, *lip-1(RNAi)*, or *lip-1(zh15)* double mutants, upon closer examination an interesting result was obtained. In each of the cases where *lin-12* or its transcriptional target *lip-1* was knocked down (or knocked out in the case of the *zh15* mutant) P7.p induction in *pry-1* mutants substantially increased (Table 9) (Seetharaman et al., 2010). This result is counterintuitive since *lin-12* null mutants form no 2^{o} fated cells, thus knockdowns of *lin-12* or *lip-1* would be expected to inhibit P7.p induction. In *Cel-pry-1(mu38),* P7.p is induced 82% of the time, while in *Cbr-pry-1(sy5353); mfIs42* P7.p is only induced 38% of the time (Table 9) (Seetharaman et al., 2010). Using these data as baselines we were able to compare P7.p induction to RNAi treated animals. In the case of *Cel-pry-1(mu38); lin-12 (RNAi)* there was a weak increase in P7.p induction (82% in *mu38* alone vs. 85% in *mu38; lin-12(RNAi)*) (Seetharaman et al., 2010). A more dramatic increase in P7.p induction was observed in *mu38; lip-1 (RNAi)* and *mu38; lip-1(zh15)* animals (82% vs 98% and 96%, respectively) (Table 9) (Seetharaman et al., 2010). Furthermore, each induced P7.p adopted a 2^{o} cell fate, as judged by *ayIs4* expression (100% n=60). The *lip-1(RNAi)* and *lip-1(zh15)* double mutants nearly restored P7.p induction to wildtype levels, while *lin-12(RNAi)* suppressed this phenotype to a lesser extent, which is expected since previous data suggest that *lin-*

12(RNAi) is not very efficient in *C. elegans*. In the case of *Cbr-pry-1(sy5353); lin-12 (RNAi)* there was a strong increase in P7.p induction compared to *sy5353* alone (38% vs. 83%) (Seetharaman et al., 2010). A similar level of increase was also observed in *sy5353; lip-1(RNAi)* animals (38% vs 71%) (Table 9) (Seetharaman et al., 2010). The promotion of P7.p induction in *Cbr-pry-1(sy5353)*; *lin-12(RNAi)* or *lip-1(RNAi)* shows a more dramatic increase than observed in *C. elegans* which may be due to the fact that the *sy5353* phenotype is much more severe.

5.6 Persistent LIN-12/Notch Signaling Upregulates *lip-1* Expression and Prevents P7.p Induction in *pry-1* Mutants

A promotion of P7.p induction in *lin-12* and *lip-1* knockdowns in both *C. elegans* and *C. briggsae pry-1* mutants encouraged us to delve further into the mechanism behind this counterintuitive result. Using *lip-1::GFP* reporter constructs, *zhIs4* in *C. elegans* and *mfIs29* in *C. briggsae*, we were able to assess the extent to which *lip-1* is expressed in both wildtype and *pry-1* mutant backgrounds. *zhIs4* expression has previously been characterized and is known to be expressed in VPCs from the L2 stage until late-L3 (Berset et al., 2001). Berset and colleagues have shown that *lip-1* expression increases in VPCs in response to a *lin-12* signal, thus identifying *lip-1* as a true *lin-12* transcriptional target (Berset et al., 2001). In *C. briggsae* wildtype *lip-1::GFP* expression (*mfIs29*) is first detectable in all VPCs, P(3-8).p, at the L2 stage (Figure 20) (Seetharaman et al., 2010). During the early L3 stage, *lip-1::GFP* expression was only visible in P5.p and P7.p (Figure 20) (Seetharaman et al., 2010). This pattern persisted through to mid-L3 stage (Pn.px) and was sometimes observed in P4.p and P8.p progeny. By the late L3–

early L4 stage *lip-1* expression was undetectable in P(5-7).p daughter cells. Berset et al (2001) described a similar dynamic expression pattern in *C. elegans* wildtype larvae. The expression of *lip-1::GFP* in *Cbr-pry-1(sy5353); mfIs29* animals was similar to wildtype at the early L2 stage, but differed in the level of expression in P7.p and P8.p (Seetharaman et al., 2010). P7.p and P8.p were observed to be fluorescing brighter than anterior VPCs at the L2 stage, while at the early L3 stage (Pn.p) fluorescence had faded in P3.p to P6.p but remained bright in P7.p and P8.p (69% n=26) (Figure 20) (Seetharaman et al., 2010). By the mid L3 stage, where the VPCs have divided to give two daughter cells (Pn.px), P7.p and P8.p were the only VPCs that had any detectable level of *lip-1* expression (Figure 20) (Seetharaman et al., 2010). In *Cel-pry-1(mu38); zhIs4* animals a similar pattern of expression was observed where L2 staged animals showed a higher level of fluorescence in P7.p compared to other VPCs (30% n=43) (Figure 20) (Seetharaman et al., 2010). The abnormal pattern of expression of *lip-1* in both *pry-1* mutants, taken into account with our results that when *lip-1* is inhibited, either through RNAi or mutation, P7.p induction is promoted, provides a molecular basis for the P7.p induction defect in *pry-1* mutants.

5.7 Reduction of MAP Kinase Activity in *pry-1(mu38)* Mutants Further Reduces P7.p Induction

As stated previously, *lip-1* antagonizes *mpk-1* in wildtype animals to inhibit the acquisition of a 1^{o} cell fate in P5.p and P7.p. To assess the role that *mpk-1* plays in P7.p induction we utilized a weak reduction of function mutant, *mpk-1(ku1)*. By using this particular mutant we were able to determine whether the level of P7.p induction was

affected in *pry-1(mu38)* animals when *lip-1-mpk-1* signaling was impaired. *Cel-mpk-1(ku1)* mutants are underinduced in only 2% of the animals, which usually results in P6.p failing to become induced (Wu and Han, 1994). We found that P7.p induction is significantly reduced in *pry-1(mu38); mpk-1(ku1)* double mutants (P>0.0001) when compared to *pry-1(mu38)* P7.p induction alone (Table 9). This result is in line with the *lip-1* data, since a reduction of P7.p induction is expected if *lip-1* is signaling through *mpk-1* in P7.p to regulate induction. In this scenario, removal of the *mpk-1* signal that would normally be antagonized by *lip-1* would be expected to further enhance the P7.p induction defect. This result suggests that persistent *lin-12-lip-1* signaling in an activated Wnt signaling background interacts with the Ras signaling pathway influence P7.p induction.

5.8 Summary and Discussion

After characterizing the molecular basis and the phenotype of the *pry-1* mutants, we sought to place *Cbr-pry-1* in the Wnt signaling pathway. Using RNAi we were able to determine that *Cbr-pry-1* is placed at the same point in the Wnt signaling pathway as *pry-1*. The specification of cell fate on ectopic invaginations is important to understand the genetic basis of Wnt mediated VPC specification. Using molecular markers we show that overinduced VPCs in *pry-1* mutants acquire a 2^{o} cell fate independent of the gonad derived and LIN-12/Notch mediated lateral signals. This result proved to be a novel way of assigning 2^{o} cell fate in *C. elegans* and *C. briggsae* vulval development. The *pry-1* phenotype shows an interesting P7.p induction defect, although the animals are frequently

Muv. This prompted us to attempt to characterize the mechanism behind this phenomenon. We found that LIN-12 mediated signaling was disrupting the proper temporal and level of expression of its transcriptional target the MAP kinase phosphatase *lip-1* in P7.p, which caused frequent P7.p induction failure. To confirm this result, *mpk-1* was analyzed in *pry-1* mutants, and indeed P7.p induction was accordingly decreased. These results display the complex signaling network that is the basis of vulval development where Ras, Notch, and Wnt signaling interact to ensure the proper formation of the vulva in the nematodes *C. elegans* and *C. briggsae*.

Previous work by numerous groups has shown a role for the HOX genes *mab-5* (*Antp/Ubx/Abd-A* family) and *egl-5* (*Abd-B* family) in the development of the posterior end of *C. elegans*. *mab-5* is known to be expressed in the posterior VPCs P7.p and P8.p and is involved in maintaining VPC competence by antagonizing *lin-39* function (Clandinin et al., 1997; Salser et al., 1993). This antagonism reduces the potential of P7.p and P8.p to respond to the inductive and lateral signal from the gonad and P6.p, respectively. Since P7.p in both species adopts an uninduced fate (and the entire posterior set of Pn.p's in *Cbr-pry-1* mutants adopt this fate), it is likely that this is due to lack of competence, which may be mediated by disrupted *mab-5* expression. Preliminary data using the RNAi approach in *C. briggsae* and *C. elegans* shows a slight increase in posterior VPC induction in *mab-5(RNAi)* knockdowns. Further along the posterior axis it is known that *egl-5* is expressed and important in patterning P12 lineage in the tail (Chisholm, 1991; Ferreira et al., 1999). Without *egl-5* expression the P12 lineage results

in the P12 cell being transformed to a P11 like fate, while overexpression of *egl-5* results in the formation of two P12 like cells (Chisholm, 1991; Jiang and Sternberg, 1998). It is known that *egl-5* acts downstream of the gonad derived (EGF) signaling pathway in P12 development (Jiang and Sternberg, 1998) and recent work has shown that in specific *egl-5 mab-5* double mutants, the Wnt signaling pathway can specify the P12 fate (Li et al., 2009). The transformation of the P12 lineage in the tail in *egl-5* mutants is very similar to the type of transformation seen in *Cbr-pry-1* mutants. Li and colleagues were able to show that there are layers of patterning systems in the posterior epidermis (2009). They were able to show that Wnt signaling underlies HOX genes in the patterning of the posterior epidermis(Li et al., 2009). Two more posterior HOX genes are also present in *C. elegans*, *php-3* and *nob-1*, which may also be playing a role in the development of posterior VPCs in both species (Van Auken et al., 2000; Wang et al., 1993). Thus, these posterior HOX genes, initially *mab-5* and *egl-5*, need to be further investigated in both *pry-1* mutants understand whether their function is altered and causing the posterior VPC and Pn.p defects.

Table 9- Vulval Induction analysis in mutant and RNAi treated animals

Genotype	RNAi Target	% Induced VPCs						% Overinduced	n
		P3.p	P4.p	P5.p	P6.p	P7.p	P8.p		
sy5353	-	39	82	100	100	17	21	93	44
mfIs42	-	0	0	100	100	100	0	0	Many
sy5353;mfIs42	-	58	86	100	100	38	20	98	50
mfIs42	*Cbr-pop-1*	0	0	33	47	30	0	0	30
sy5353;mfIs42	*Cbr-pop-1*	27	13	87	87	20	13	27	15
mfIs42	*Cbr-lin-39*	0	0	12	18	6	0	0	15
sy5353;mfIs42	*Cbr-lin-39*	25	50	100	100	25	7	42	12
mfIs42	*Cbr-lip-1*	0	0	100	100	100	0	0	25
sy5353;mfIs42	*Cbr-lip-1*	60	32	100	100	71	19	88	58
mu38	-	24	6	100	100	82	10	31	89
+	*lin-12*	0	0	100	100	100	0	0	50
mu38	*lin-12*	38	13	100	100	85	8	49	53
+	*lip-1*	0	0	100	100	100	0	0	100
mu38	*lip-1*	16	7	100	100	98	4	28	57
zh15	-	0	0	100	100	100	0	0	30
mu38;zh15	-	65	47	100	100	96	68	92	77
hu9	-	0	0	100	100	100	0	0	14
n952	-	9	91	100	91	91	82	100	11
hu9;n952	-	3	14	79	93	79	93	69	29
mu38;mpk-1	-	24	7	100	100	64	9	21	107

Table 10- Transgene expression patterns

Array	Transgene	Stage	Cell lineage marker
ayIs4	*egl-17::GFP*	Early L3	1^{o}
bhEx53	*daf-6::GFP*	Mid L4	1^{o}
mfIs8	*Cbr-zmp-1::GFP*	Late L4	1^{o}
wyEx3372	*syg-2::GFP*	Mid L4	1^{o}
ayIs4	*egl-17::GFP*	Mid L4	2^{o}
mfIs5	*Cbr-egl-17::GFP*	Mid L4	2^{o}
syIs80	*lin-11::GFP*	Mid L4	2^{o}
syIs54	*ceh-2::GFP*	Mid L4	2^{o}
syIs101	*dhs-31::GFP*	Old Adult	2^{o}

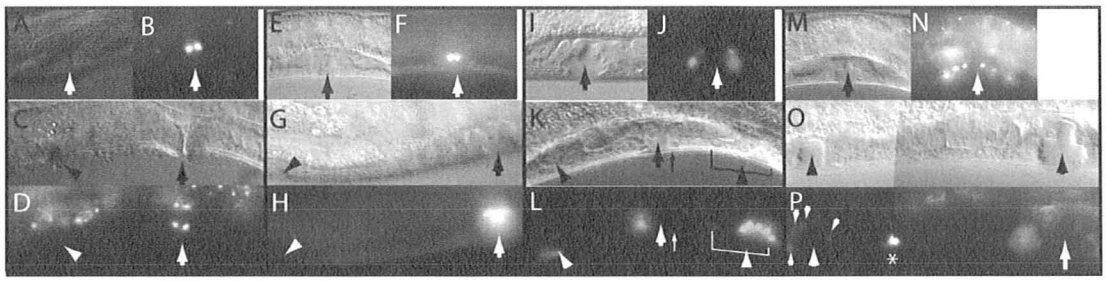

Figure 17- Sample expression of 1^{o} and 2^{o} molecular markers in *pry-1* mutants

Arrows point to the central vulval invagination. Arrowheads point to ectopically induced VPCs.

(A-B) Wildtype *Cbr-zmp-1::GFP* expression in 1^{o} cells
(C-D) *Cbr-zmp-1::GFP* expression is not detected in ectopically induced VPCs in *Cbr-pry-1(sy5353)* mutants
(E-F) Wild type *daf-6::GFP* expression in 1^{o} cells
(G-H) *daf-6::GFP* expression is not detected in ectopically induced VPCs in *pry-1(mu38)* mutants
(I-J) Wildtype *Cbr-egl-17::GFP* expression in 2^{o} cells
(K-L) *Cbr-egl-17::GFP* expression is detected in ectopically induced VPCs in *Cbr-pry-1(sy5353)* mutants
(M-N) Wildtype *lin-11::GFP* expression in 2^{o} cells
(O-P) *lin-11::GFP* expression is observed in ectopically induced VPCs in *pry-1(mu38)* mutants

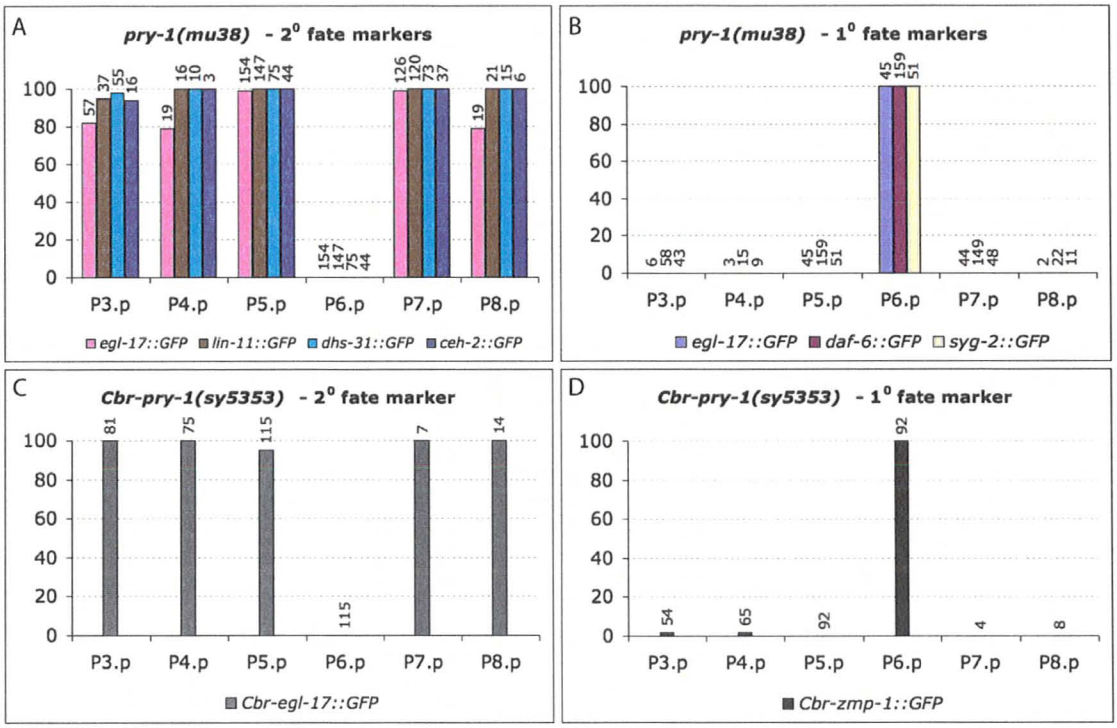

Figure 18- Expression analysis of vulval cell fate markers in *pry-1* mutants

The y-axis represents the percentage of VPCs expressing the marker. The number of animals examined for each VPC is given above the bar. The 2° lineage markers are expressed in the progeny of all but P6.p whereas 1° lineage markers are expressed in P6.p progeny only. (A) 20 lineage markers in *C. elegans – egl-17::GFP (ayIs4), lin-11::GFP (syIs80), dhs-31::GFP (syIs101), and ceh-2::GFP (syIs54). (B) 1° lineage markers in C. elegans – egl-17::GFP (ayIs4), daf-6::YFP (bhEx53), and syg-2::GFP (wyEx3372).* (C) 2° lineage marker *Cbr-egl-17::GFP (mfIs5)* in *C. briggsae*. (D) 1° lineage marker *Cbr-zmp-1::GFP (mfIs8)* in *C. briggsae*.

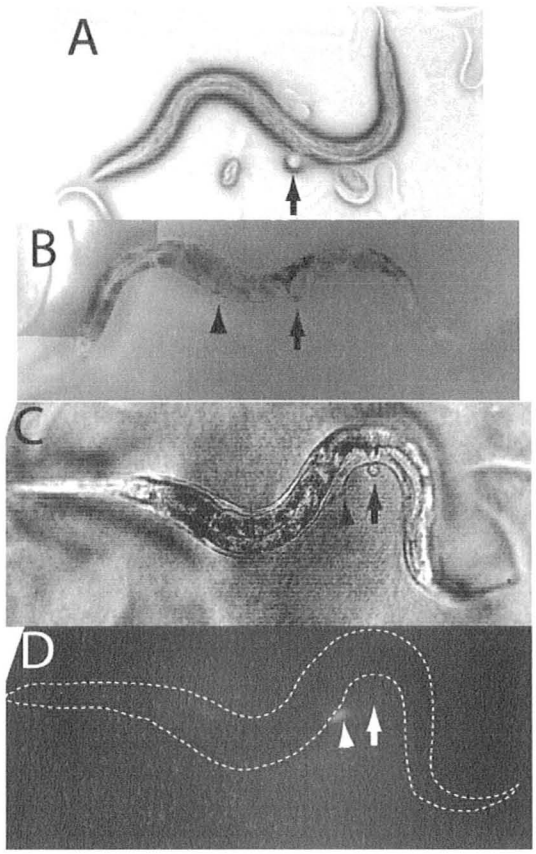

Figure 19- *lin-12* indpendent induction of VPCs in *pry-1* mutants

(A) A *lin-12(n676n909)* mutant. This animal has a typical *lin-12(0)* phenotype where P(5-7).p adopt 1° fates and form a large protrusion (Pvl) (Arrow).
(B) A *pry-1(mu38)* mutant. P4.p in this animal is ectopically induced to give a Muv phenotype. Central invagination is indicated by the arrow. Ectopic invagination is indicated by the arrowhead.
(C-D) A *pry-1(mu38); lin-12(n676n909)* double mutant. This animal shows ectopic pseudovulva (due to induced P4.p) and protruding vulva phenotypes. The *egl-17::GFP* expression can be seen in the progeny of P4.p (arrowhead).

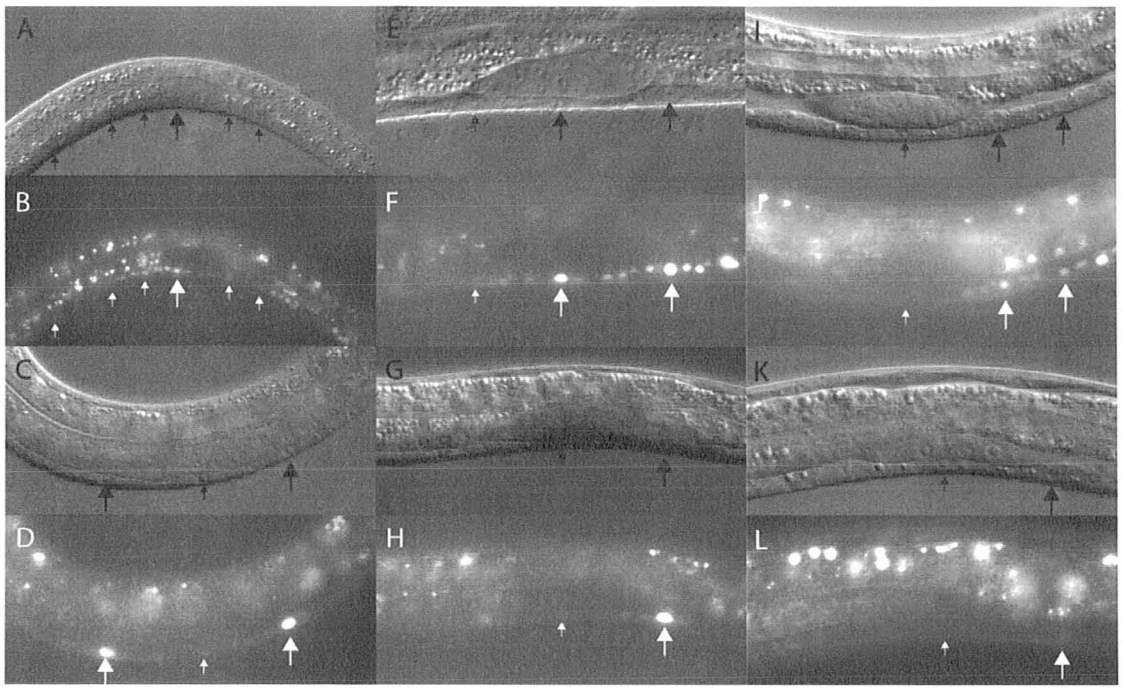

Figure 20- *lip-1::GFP* expression patterns in wild type and *pry-1* mutants

(A-D) Wildtype *lip-1::GFP* expression. (A-B) This early L2 animal has bright *lip-1::GFP* expression in P6.p (larger arrow), while faint reduced expression in all other VPCs (small arrows). (C-D) Bright *lip-1::GFP* expression can be seen in equal proportions in both P5.p and P7.p, while P6.p barely fluoresces.
(E-H) *pry-1(mu38); zhIs4 (lip-1::GFP)* animals. (E-F) In this L2 animal *lip-1::GFP* expression is clearly brighter in P6.p and P7.p (large arrows) compared to P5.p (small arrow). (G-H) This early L3 animal expresses *lip-1::GFP* brigntly in P7.p (large arrow), faintly in P6.p (small arrow), and does not express in P5.p.
(I-L) *Cbr-pry-1(sy5353); mfIs29 (lip-1::GFP)* animals. (I-J) An L2 animal expressing *lip-1::GFP* in P(7-8).p but not in any other VPCs. (K-L) Very faint expression can be seen in P7.p in this early L3 stage animal, while no expression is observed in any other VPCs.

Chapter 6- Conclusions and Future Directions

Complex layers of gene regulation and interaction that influence developmental processes are crucial to maintaining a precise developmental program in all animals. Multiple levels of regulation are necessary to ensure that when one process is perturbed the progression of development is not affected. The layers are also required to abort the progression of development if crucial components are missing or damaged. Using the model organisms *C. elegans* and *C. briggsae* allows for the study of gene regulation throughout development. Their striking similarity, yet substantial evolutionary divergence, allows for a comparative study of gene regulation in vulval development. The data presented in this paper is available in two separate publications regarding vulval development. First, the role of *hda-1* in vulval development is discussed in Cumbo et al., 2010. This manuscript is in preparation and is expected to be submitted to Developmental Biology in the summer of 2010. Second, the role of Wnt signaling in *C. elegans* and *C. briggsae* vulval development is discussed in Seetharaman and Cumbo et al., 2010. This manuscript has been accepted for publication in Developmental Biology and is currently in press.

6.1 The Histone Modifier, *hda-1*, Regulates Vulval Morphogenesis and Uterine Formation

One layer of regulation occurs at the chromatin level, where remodeling of chromatin through histone modifications either restricts or allows the access of transcription factors to specific genes. This regulation either promotes or inhibits the

transcription of genes, which in turn affects developmental processes within tissues, such as cell division, commitment, and migration. The histone deacetylase, *hda-1*, is a histone modifier and is known to affect gene regulation. Previous work shows that *hda-1* is involved in gonadogenesis and vulval development in *C. elegans*. Further examination of the *hda-1* mutant phenotype revealed a role for *hda-1* in utse formation and π cell specification. Using a microarray approach we were able to characterize a selected group of putative *hda-1* targets. This analysis revealed that *hda-1* regulates the expression of *fos-1b* in vulval development (assessed by V. Raghavan), and the transcription factors *lin-11* and *egl-13* in utse differentiation and π cell specification.

6.1.1 *hda-1* mutants show defects in vulval morphology and utse formation

This study shows that *hda-1* mutants have defects in vulval development, which include morphogenesis and cell specification defects. We show that *hda-1* is expressed in all vulval cell types and is necessary for vulval morphogenesis. Vulval morphogenesis defects range from mild in *cw2* mutants to severe in *e1795* mutants, where the size and shape of the vulval invagination is substantially affected. This analysis revealed a novel phenotype where the utse fails to form properly and the AC fails to invade the basement membrane. Using cell junction markers, we were able to determine that the 7 toroidal rings that form the adult vulva fail to fuse properly and are frequently missing. These results support the observations that *hda-1* regulates vulval morphogenesis and utse formation.

6.1.2 *hda-1* regulates the expression of *lin-11*, *egl-13*, and *zmp-1* in uterine development

To further examine the utse defects in *hda-1* mutants, I focused on three transcription factors known to be involved in utse formation, namely *lin-11, egl-13,* and *zmp-1*. *lin-11* and *egl-13* expression was greatly reduced in *hda-1* mutants, while animals that had faint expression were found to have supernumerary π like cells and π progeny-like cells, consistent with *hda-1* regulating these transcription factors in uterine formation. AC defects were also observed in *hda-1* mutants, thus *zmp-1::GFP* was used to assess AC fate. *zmp-1::GFP* expression was reduced in *hda-1* mutants and revealed that the AC failed to invade the basement membrane to form the utse and subsequently failed to migrate from the apex of the vulva. These results demonstrate that hda-1 is necessary for correct differentiation of AC, π cells, and π progeny, leading to the formation of a functional vulva-uterine connection.

6.1.3 Future Directions

To determine the mechanism of how *hda-1* influences vulva development will require further analysis of the targets identified from the microarray. Genetic interactions must be established using genetic mutants and not only RNAi. This is crucial because RNAi is known to be variable and may not work efficiently in all cases. It is also plausible that the targets identified in the microarray are stage specific since the microarray was performed with RNA obtained in the L2 stage (Cumbo et al., 2010; Joshi, 2008). In general testing the role of other NuRD complex components would prove

useful in understanding the role of chromatin remodeling in vulval development. Since many of the NuRD complex components are also SynMuvB genes, it would be interesting to characterize their functions in the context of vulval development and morphogenesis. An interesting avenue to test would be the role of *lag-2* in π specification and vulval development. Duforquc and colleagues have observed a derepression of LAG-2 in *hda-1* mutant animals, where their GFP based reporter was expressed throughout the animal in *hda-1* mutants, but was localized to only a few cells in the wildtype (2002). Since *lag-2* is known to influence *lin-12* signaling in uterine development, and *hda-1* mutants derepress *lag-2* and have uterine defects, it would be exciting to investigate the interaction of *hda-1* with the Notch pathway.

6.2 Wnt Signaling Confers Cell Fate on VPCs and Interacts with LIN-12/Notch in P7.p Specification

Gene regulation also occurs at the level of the signaling pathway, where activation or inhibition of signaling will affect the expression of target genes. Wnt signaling is known to play a crucial role in maintaining VPC competence in *C. elegans* and we have determined that this role is conserved in *C. briggsae*. We have placed *Cbr-pry-1* at the same level of *pry-1* in the Wnt signaling pathway and show that it interacts with *Cbr-pop-1* and *Cbr-lin-39* in the same was as *C. elegans*.

6.2.1 Activated Wnt signaling in *pry-1* mutants confers 2° cell fate

In *pry-1* mutants Wnt signaling is activated causing the unregulated expression of Wnt target genes and a Muv phenotype. Using cell fate markers we have shown that ectopic inductions in *pry-1* mutants in both *C. elegans* and *C. briggsae* adopt a 2° cell fate. Furthermore, the acquisition of the 2° cell fate is independent of the gonad derived and LIN-12/Notch mediated lateral signaling pathways. Using gonad ablation and *lin-12* null mutant analysis, we were able to confirm these results. Previously, the LIN-12/Notch signaling pathway has been shown to be necessary and sufficient to promote the 2° cell fate in VPCs and our results show that this can be achieved in an activated Wnt signaling background. An explanation for this result is that the two pathways have evolved to perform the same function, where LIN-12/Notch is dominant to Wnt signaling, but both are capable of promoting cell fate in VPCs, thus supporting the notion that gene regulation is controlled by layers of complex regulatory networks.

6.2.2 Wnt-LIN-12/Notch signaling interactions are involved in P7.p induction

Although *pry-1* mutants are Muv, P7.p frequently fails to be induced, while P3.p, P4.p, and P8.p are induced frequently induced to adopt a 2° cell fate. Using RNAi and double mutants to assess the molecular basis of P7.p induction in *pry-1* mutants revealed that Wnt interaction with LIN-12/Notch and its transcriptional target, *lip-1*, is crucial to P7.p induction. First, *lin-12* and *lip-1* RNAi or mutants in a *pry-1* mutant background is able to significantly increase the induction of P7.p. This indicates that *lin-12* and *lip-1*

expression works to inhibit P7.p induction in *pry-1* mutants. Second, *lip-1* expression is upregulated and persists in P7.p and P8.p through its normal range of expression. It has been shown that excessive *lin-12* signaling leads to upregulation of *lip-1*, and in this case, this upregulation in *pry-1* mutants is preventing the induction of P7.p. The precise mechanism of this action in P7.p vs the anterior VPCs is still unknown, but I have proposed a model that explains the role of Wnt signaling and its interaction with Notch signaling in VPC fate specification (Figure 21). Two plausible explanations can be considered to explain the failure of P7.p induction. One explanation is that *lip-1* persistently antagonizes *mpk-1* in P7.p, leading to the inability of *mpk-1* to promote induction. Yet another possibility is the misregulation of *lip-1* interferes with the expression of *lin-12* target genes, thus preventing P7.p induction.

6.2.3 Future Directions

These results support a genetic interaction between the Wnt and LIN-12/Notch signaling pathways. Further analysis of this interaction is required to elucidate the exact mechanism and its role in P7.p induction. To this end multiple approaches can be utilized to further test these results. A forward genetics approach looking for suppressors in *Cbr-pry-1* mutants would prove valuable to in examining the role of Wnt and Notch cross talk in P7.p induction and identifying new regulators of VPC induction. Another approach could use high throughput genomics and would help to identify interacting partners and targets of Wnt signaling in both vulval development and P7.p induction. Both of these techniques would allow for the dissection of the Wnt and Notch signaling pathways and

may prove to be useful in determining the mechanisms of cross talk between the two. These approaches will eventually lead to a better understanding of gene regulation and pathway cross talk in development. Ultimately, these results show that Wnt signaling plays similar roles in *C. elegans* and *C. briggsae* vulval development and the proper development of the vulva requires interaction of multiple signaling pathways.

6.3 Conclusion

C. elegans vulval development provides an elegant means to study multiple cell processes. Cell migration, division, specification, morphogenesis, and commitment are all major determinants in proper vulval development. These processes are regulated on multiple levels which control target gene expression, specifically through, chromatin modification and signaling networks. My thesis has attempted to elucidate the roles of *hda-1* and Wnt signaling in vulval development. Understanding how chromatin modifications and signaling pathway crosstalk affects vulval development has revealed novel processes in morphogenesis and induction. Conservation of these processes in other eukaryotes provides a unique way to study how perturbations in chromatin modification or cellular signaling can cause cancers and diseases in humans.

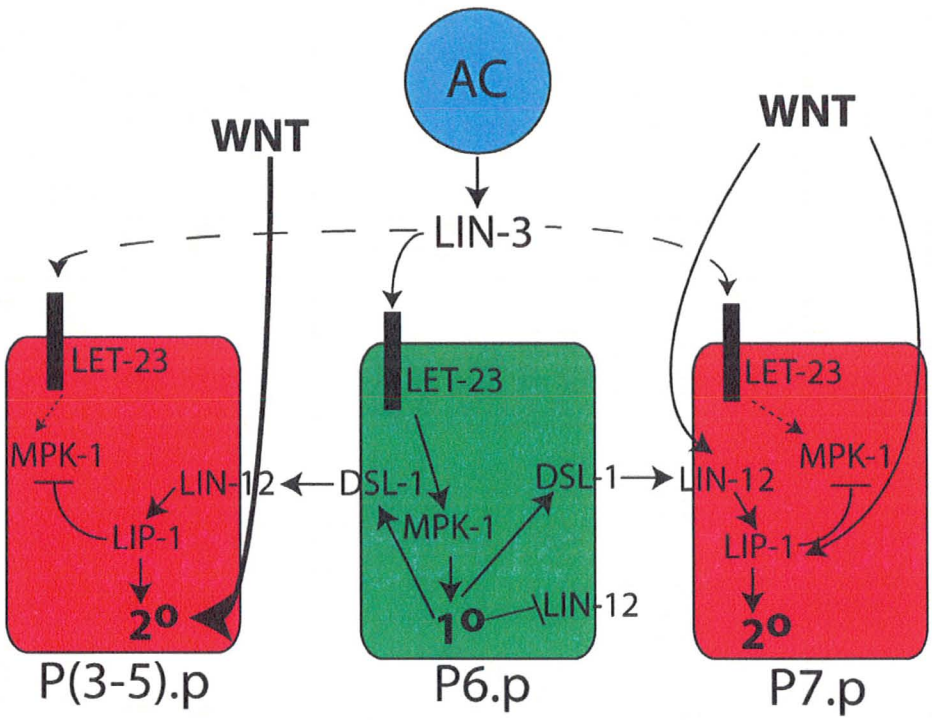

Figure 21-Complex Interactions of the Wnt, Ras, and Notch Pathways in VPC specification

Hashed arrows indicate a lower level of LIN-3 binding to the LET-23 receptor, which results in lower levels of MPK-1 signaling in the presumptive 2° VPCs.

Appendix

A1.1 Introduction to Tandem Affinity Purification

Tandem affinity purification (TAP) is a technique that was developed in yeast to isolate pure samples of protein-protein complexes (Rigaut et al., 1999). This method involves tagging a protein of interest with the TAP tag which can be used to purify native protein complexes (Rigaut et al., 1999). The TAP tag consists of two IgG binding domains from *Staphlococcus aureus* protein A (ProtA) and a calmodulin binding peptide (CBP) separated by a TEV protease cleavage site (Puig et al., 2001). This specific organization of binding sites separated by a cleavage site allows for a two step purification process. Initially the gene of interest-TAP construct must be created using either the C- or N-terminal tagged version, which are both commercially available. Once this construct has been created it needs to be introduced into the organism of interested and expressed at native levels. With regards to the purification process, first the ProtA domain binds tightly to an IgG matrix, which requires the use of the TEV protease to release the complex from the substrate. Second, the first eluate from the initial affinity purification is incubated with calmodulin coated beads in the presence of calcium (Puig et al., 2001). The column is washed to remove any contaminants and remaining TEV protease, then eluted in mild conditions with EGTA (Puig et al., 2001). The final eluate will contain pure protein of choice in complex with any other proteins bound when the original total protein isolate was obtained. This method reduces the possibility of false

positive binding partners through its two step tandem affinity purification and allows for near native conditions and levels of protein to be obtained since no overexpression is required. The eluted protein complex can be used for identification, functional, or structural studies (Puig et al., 2001). Identification of protein complexes has been particularly advanced using the TAP method through the use of mass spectrometry (MS) to identify proteins in complex with each other (Collins and Choudhary, 2008). Using MS to identify protein complexes using the TAP method has been successfully used in used in yeast, *E. coli*, and mammalian cell lines (Collins and Choudhary, 2008). These analyses have proved to be able to identify components of the TNFα/NF-κβ and WNT/β-catenin signaling pathways (Collins and Choudhary, 2008).

A1.2 hda-1p::hda-1::TAP analysis

The *hda-1p::hda-1::TAP* construct ***pGLC47*** was created as described in the materials and methods section. This construct, along with the rescue marker cDNA *unc-119*, were injected into *unc-119(ed4)* animals to obtain the transgenic line *bhEx77*. Animals were washed from 3-4 gravid plates with M9 and transferred to a 15 ml falcon tube. The worms were washed until all bacteria was cleared from the solution, then the pellet was resuspended in RIPA buffer for protein extraction. Using a microtip, the worm solution was sonicated for 20 seconds on ice followed by a 20 second rest on ice and repeated until the majority of the worms in the solution were lysed, as judged under a dissecting microscope (adapted from (Koelle, 2010). The total worm extracts were frozen at -80°C until needed. To verify the proper transcription and translation of the *hda-1::TAP* transgene, western blotting was utilized. Antibodies for HDA-1 and the IgG domain of

the TAP tag were obtained from Santa Cruz Biotechnology (Cat #s sc-5550 and sc-2004, respectively). A Bradford assay was utilized to account for varying protein concentrations in the N2 and *bhEx77* extracts, which can be used to ensure the loading of the same concentration of protein. Protein samples from both N2 and *bhEx77* animals were separated using SDS-PAGE electrophoresis and blotted with varying concentrations of anti-Cel-HDA-1 and anti-IgG. The size of the wildtype HDA-1 is 52.1 kD, TAP is 24.1 kD, so the HDA-1::TAP fusion protein should be 76.2 kD (Wormbase, 2010).

Initial blots identified the putative HDA-1::TAP fusion protein the *bhEx77* extracts with both the anti-HDA-1 and anti-TAP, but not in the N2 extract , while HDA-1 was identified in both extracts (Figure A1). The antibody concentrations were much too high initially, resulting in excess HDA-1 signal. Subsequent attempts to optimize the antibody concentrations failed to show the same results. HDA-1 was identified in all samples tested with anti-HDA-1, but smaller degradation products were also found (Figure A2). When the samples were blotted with anti-TAP, a band corresponding the size of HDA-1::TAP was identified in the N2 extracts, but not in the *bhEx77* extracts, which must be non-specific binding or sample contamination (Figure A2).

A1.3 Discussion

Initial blots were promising and showed the expected results, but further analysis was unable to produce similar results. This could be due to numerous factors involved in the preparation, storage, and loading of the protein. Antibody efficiency may have also played a role in obtaining inconsistent results. It is likely that the protein stored in the

RIPA buffer at -80°C degraded over time and resulted in variable results. This is evident since smaller products were clearly identified by anti-HDA-1 in blots after the initial tests. It is possible that anti-HDA-1 recognizes other non-specific proteins, but this has not been reported previously. The degradation of the sample would also result in degradation of the HDA-1::TAP fusion protein, which may already be unstable. The fact that initial blots with anti-TAP showed a clear band at 72 kD in the *bhEx77* extracts, but not the N2 extracts, indicates that the HDA-1::TAP fusion protein was intact immediately after protein extraction, and degraded after some time (Figure A2). Since the initial results were promising, this experiment should be repeated in order to obtain non-degraded protein extracts from both N2 and *bhEx77* animals in order to confirm the production of the HDA-1::TAP fusion protein. Once this is confirmed through western blotting, the protein extracts can be used to perform the tandem affinity purification protocol, and subsequently MS analysis.

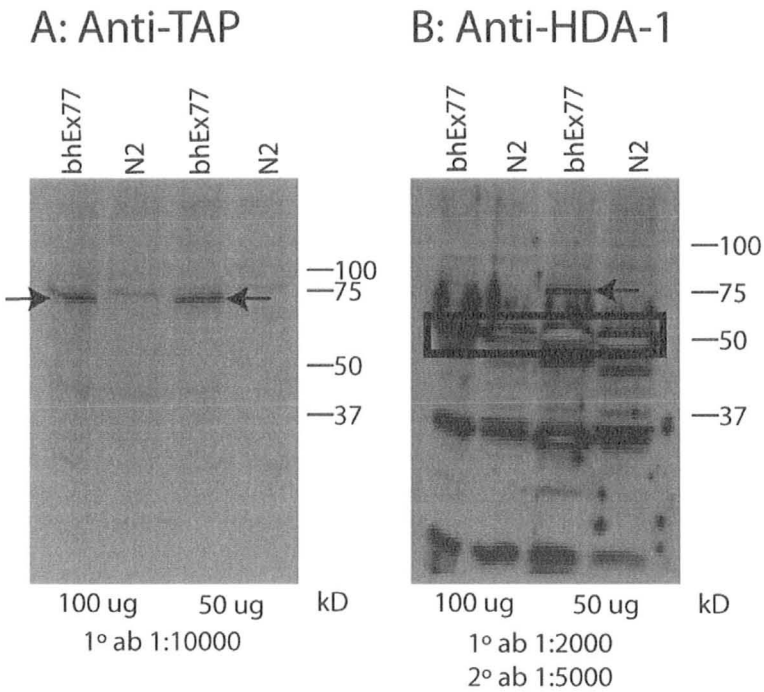

Figure A 1- Western blot analysis of HDA-1

(A) anti-TAP blot. HDA-1::TAP is identified on this blot in the *bhEx77* protein extract, but not the N2 extract. Specific binding of anti-TAP is indicated by the arrows. A non-specific band can be seen in the N2 lanes. 1° antibody dilution- 1:10000.

(B) anti-HDA-1 blot. HDA-1::TAP is only identified in the *bhEx77* protein extract lane, as indicated by the arrow. HDA-1 can be identified in both N2 and *bhEx77* protein extracts, which are contained in the box. 1° antibody dilution- 1:2000. 2° antibody dilution- 1:5000.

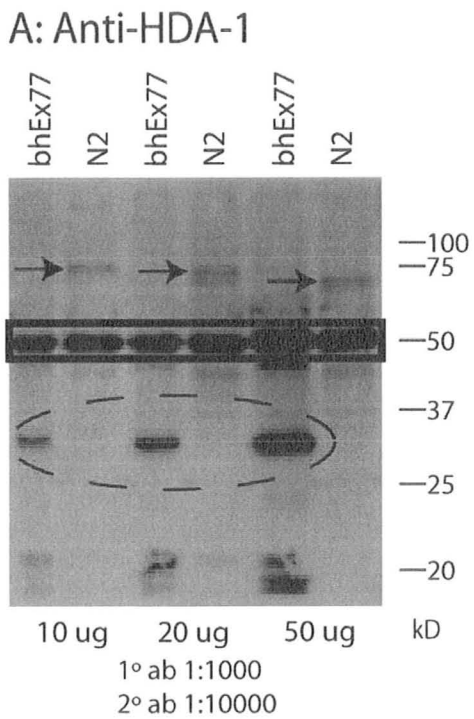

Figure A 2- HDA-1::TAP protein degradation

(A) Anti-HDA-1 blot. The dashed oval indicates the binding of anti-HDA-1 to a product that is approximately 30 kD in size. The strength of this signal indicates that this is most likely a degradation product. The boxed signal is endogenous wild type HDA-1. The arrows indicate the recognition of a protein product similar to the HDA-1::TAP fusion protein, but is in the N2 control lanes and not in the *bhEx77* lanes.

References

Avery, L., and Horvitz, H.R. (1987). A cell that dies during wild-type *C. elegans* development can function as a neuron in a ced-3 mutant. Cell *51*, 1071-1078.

Berset, T., Hoier, E.F., Battu, G., Canevascini, S., and Hajnal, A. (2001). Notch inhibition of RAS signaling through MAP kinase phosphatase LIP-1 during *C. elegans* vulval development. Science *291*, 1055-1058.

Bossinger, O., Klebes, A., Segbert, C., Theres, C., and Knust, E. (2001). Zonula adherens formation in Caenorhabditis elegans requires dlg-1, the homologue of the Drosophila gene discs large. Developmental biology *230*, 29-42.

Brenner, S. (1974). The genetics of Caenorhabditis elegans. Genetics *77*, 71-94.

Burdine, R.D., Branda, C.S., and Stern, M.J. (1998). EGL-17(FGF) expression coordinates the attraction of the migrating sex myoblasts with vulval induction in *C. elegans*. Development (Cambridge, England) *125*, 1083-1093.

Calvo, D., Victor, M., Gay, F., Sui, G., Luke, M.P., Dufourcq, P., Wen, G., Maduro, M., Rothman, J., and Shi, Y. (2001). A POP-1 repressor complex restricts inappropriate cell type-specific gene transcription during Caenorhabditis elegans embryogenesis. Embo J *20*, 7197-7208.

Chen, G., Fernandez, J., Mische, S., and Courey, A.J. (1999). A functional interaction between the histone deacetylase Rpd3 and the corepressor groucho in Drosophila development. Genes Dev *13*, 2218-2230.

Chen, N., and Greenwald, I. (2004). The lateral signal for LIN-12/Notch in *C. elegans* vulval development comprises redundant secreted and transmembrane DSL proteins. Developmental cell *6*, 183-192.

Chisholm, A. (1991). Control of cell fate in the tail region of *C. elegans* by the gene egl-5. Development (Cambridge, England) *111*, 921-932.

Clandinin, T.R., Katz, W.S., and Sternberg, P.W. (1997). Caenorhabditis elegans HOM-C genes regulate the response of vulval precursor cells to inductive signal. Developmental biology *182*, 150-161.

Collins, M.O., and Choudhary, J.S. (2008). Mapping multiprotein complexes by affinity purification and mass spectrometry. Curr Opin Biotechnol *19*, 324-330.

Conradt, B., and Xue, D. (2005). Programmed cell death. In WormBook, T.C.e.R. Community, ed. (WormBook).

Cui, M., Chen, J., Myers, T.R., Hwang, B.J., Sternberg, P.W., Greenwald, I., and Han, M. (2006). SynMuv genes redundantly inhibit lin-3/EGF expression to prevent inappropriate vulval induction in *C. elegans*. Developmental cell *10*, 667-672.

Cui, M., and Han, M. (2005). Roles of chromatin factors in *C. elegans* development. In WormBook, T.C.e.R. Community, ed. (WormBook).

Cumbo, P., Joshi, K., Raghavan, V., and Gupta, B.P. (2010). The *C. elegans* histone deacetylase *hda-1* controls morphogenesis of the vulva and uterine cells. Developmental biology *In preparation*.

Cutter, A.D. (2008). Divergence times in Caenorhabditis and Drosophila inferred from direct estimates of the neutral mutation rate. Mol Biol Evol *25*, 778-786.

Dufourcq, P., Victor, M., Gay, F., Calvo, D., Hodgkin, J., and Shi, Y. (2002). Functional requirement for histone deacetylase 1 in Caenorhabditis elegans gonadogenesis. Mol Cell Biol *22*, 3024-3034.

Eisenmann, D.M. (2005). Wnt signaling. In WormBook, T.C.e.R. Community, ed. (WormBook).

Eisenmann, D.M., and Kim, S.K. (1994). Signal transduction and cell fate specification during Caenorhabditis elegans vulval development. Curr Opin Genet Dev *4*, 508-516.

Eisenmann, D.M., Maloof, J.N., Simske, J.S., Kenyon, C., and Kim, S.K. (1998). The β-catenin homolog BAR-1 and LET-60 Ras coordinately regulate the Hox gene lin-39 during Caenorhabditis elegans vulval development. Development (Cambridge, England) *125*, 3667-3680.

Fares, H., and Greenwald, I. (1999). SEL-5, a serine/threonine kinase that facilitates lin-12 activity in Caenorhabditis elegans. Genetics *153*, 1641-1654.

Fay, D.S., Stanley, H.M., Han, M., and Wood, W.B. (1999). A Caenorhabditis elegans homologue of hunchback is required for late stages of development but not early embryonic patterning. Developmental biology *205*, 240-253.

Fay, D.S., and Yochem, J. (2007). The SynMuv genes of Caenorhabditis elegans in vulval development and beyond. Developmental biology *306*, 1-9.

Felix, M.A. (2007). Cryptic quantitative evolution of the vulva intercellular signaling network in Caenorhabditis. Curr Biol *17*, 103-114.

Ferguson, E.L., and Horvitz, H.R. (1985). Identification and characterization of 22 genes that affect the vulval cell lineages of the nematode Caenorhabditis elegans. Genetics *110*, 17-72.

Ferreira, H., Zhang, Y., Zhao, C., and Emmons, S. (1999). Patterning of Caenorhabditis elegans Posterior Structures by the Abdominal-B Homolog, egl-5. Developmental biology *207*, 215 - 228.

Fischle, W., Dequiedt, F., Fillion, M., Hendzel, M.J., Voelter, W., and Verdin, E., eds. (2001). Human HDAC7 histone deacetylase activity is associated with HDAC3 in vivo (United States).

Gao, L., Cueto, M.A., Asselbergs, F., and Atadja, P., eds. (2002). Cloning and functional characterization of HDAC11, a novel member of the human histone deacetylase family (United States).

Gissendanner, C.R., Crossgrove, K., Kraus, K.A., Maina, C.V., and Sluder, A.E. (2004). Expression and function of conserved nuclear receptor genes in Caenorhabditis elegans. Developmental biology *266*, 399-416.

Gleason, J.E., Korswagen, H.C., and Eisenmann, D.M. (2002). Activation of Wnt signaling bypasses the requirement for RTK/Ras signaling during *C. elegans* vulval induction. Genes Dev *16*, 1281-1290.

Gleason, J.E., Szyleyko, E.A., and Eisenmann, D.M. (2006). Multiple redundant Wnt signaling components function in two processes during *C. elegans* vulval development. Developmental biology *298*, 442-457.

Greenwald, I. (2005). Introduction to signal transduction. In WormBook, T.C.e.R. Community, ed. (WormBook).

Greenwald, I.S., Sternberg, P.W., and Horvitz, H.R. (1983). The lin-12 locus specifies cell fates in Caenorhabditis elegans. Cell *34*, 435-444.

Gregoretti, I.V., Lee, Y.M., and Goodson, H.V. (2004). Molecular evolution of the histone deacetylase family: functional implications of phylogenetic analysis. J Mol Biol *338*, 17-31.

Guerry, F., Marti, C.O., Zhang, Y., Moroni, P.S., Jaquiery, E., and Muller, F. (2007). The Mi-2 nucleosome-remodeling protein LET-418 is targeted via LIN-1/ETS to the promoter of lin-39/Hox during vulval development in *C. elegans*. Developmental biology *306*, 469-479.

Gupta, B.P., and Sternberg, P.W. (2002). Tissue-specific regulation of the LIM homeobox gene lin-11 during development of the Caenorhabditis elegans egg-laying system. Developmental biology *247*, 102-115.

Gupta, B.P., Wang, M., and Sternberg, P.W. (2003). The *C. elegans* LIM homeobox gene lin-11 specifies multiple cell fates during vulval development. Development (Cambridge, England) *130*, 2589-2601.

Hanna-Rose, W., and Han, M. (1999). COG-2, a sox domain protein necessary for establishing a functional vulval-uterine connection in Caenorhabditis elegans. Development (Cambridge, England) *126*, 169-179.

Hansen, M., Hsu, A.L., Dillin, A., and Kenyon, C. (2005). New genes tied to endocrine, metabolic, and dietary regulation of lifespan from a Caenorhabditis elegans genomic RNAi screen. PLoS Genet *1*, 119-128.

Harrison, M.M., Ceol, C.J., Lu, X., and Horvitz, H.R. (2006). Some *C. elegans* class B synthetic multivulva proteins encode a conserved LIN-35 Rb-containing complex distinct from a NuRD-like complex. Proc Natl Acad Sci U S A *103*, 16782-16787.

Herman, M. (2001). *C. elegans* POP-1/TCF functions in a canonical Wnt pathway that controls cell migration and in a noncanonical Wnt pathway that controls cell polarity. Development (Cambridge, England) *128*, 581-590.

Hillier, L.W., Miller, R.D., Baird, S.E., Chinwalla, A., Fulton, L.A., Koboldt, D.C., and Waterston, R.H. (2007). Comparison of *C. elegans* and *C. briggsae* Genome Sequences Reveals Extensive Conservation of Chromosome Organization and Synteny. PLoS Biol *5*, e167.

Horvitz, H.R., and Sulston, J.E. (1980). Isolation and genetic characterization of cell-lineage mutants of the nematode Caenorhabditis elegans. Genetics *96*, 435-454.

Hunt-Newbury, R., Viveiros, R., Johnsen, R., Mah, A., Anastas, D., Fang, L., Halfnight, E., Lee, D., Lin, J., Lorch, A., *et al.*, eds. (2007). High-throughput in vivo analysis of gene expression in Caenorhabditis elegans (United States).

Hwang, B.J., Meruelo, A.D., and Sternberg, P.W. (2007). *C. elegans* EVI1 proto-oncogene, EGL-43, is necessary for Notch-mediated cell fate specification and regulates cell invasion. Development (Cambridge, England) *134*, 669-679.

Imai, S., Armstrong, C.M., Kaeberlein, M., and Guarente, L. (2000). Transcriptional silencing and longevity protein Sir2 is an NAD-dependent histone deacetylase. Nature *403*, 795-800.

Inoue, T., Oz, H.S., Wiland, D., Gharib, S., Deshpande, R., Hill, R.J., Katz, W.S., and Sternberg, P.W. (2004). *C. elegans* LIN-18 is a Ryk ortholog and functions in parallel to LIN-17/Frizzled in Wnt signaling. Cell *118*, 795-806.

Inoue, T., Sherwood, D.R., Aspock, G., Butler, J.A., Gupta, B.P., Kirouac, M., Wang, M., Lee, P.Y., Kramer, J.M., Hope, I., *et al.* (2002). Gene expression markers for Caenorhabditis elegans vulval cells. Mech Dev *119 Suppl 1*, S203-209.

Inoue, T., Wang, M., Ririe, T.O., Fernandes, J.S., and Sternberg, P.W. (2005). Transcriptional network underlying Caenorhabditis elegans vulval development. Proc Natl Acad Sci U S A *102*, 4972-4977.

Jiang, L.I., and Sternberg, P.W. (1998). Interactions of EGF, Wnt and HOM-C genes specify the P12 neuroectoblast fate in *C. elegans*. Development (Cambridge, England) *125*, 2337-2347.

Johnstone, R.W. (2002). Histone-deacetylase inhibitors: novel drugs for the treatment of cancer. Nat Rev Drug Discov *1*, 287-299.

Joshi, K. (2008). The Role of Class I Histone Deacetylaze HDA-1 in Vulval Morphogenesis in Nematodes *C. elegans* and *C. briggsae*. In Biology (Hamilton, McMaster University), pp. 200.

Kim, H. (2007). In Biology (Hamilton, McMaster University).

Kimble, J. (1981). Alterations in cell lineage following laser ablation of cells in the somatic gonad of Caenorhabditis elegans. Developmental biology *87*, 286-300.

Kimble, J., and Hirsh, D. (1979). The postembryonic cell lineages of the hermaphrodite and male gonads in Caenorhabditis elegans. Developmental biology *70*, 396-417.

Koboldt, D.C., Staisch, J., Thillainathan, B., Haines, K., Baird, S.E., Chamberlin, H.M., Haag, E.S., Miller, R.D., and Gupta, B.P., eds. (2010). A toolkit for rapid gene mapping in the nematode Caenorhabditis briggsae (England).

Koelle, M. (2010). Koelle Lab Protocols, M. Koelle, ed.

Koppen, M., Simske, J.S., Sims, P.A., Firestein, B.L., Hall, D.H., Radice, A.D., Rongo, C., and Hardin, J.D. (2001). Cooperative regulation of AJM-1 controls junctional integrity in Caenorhabditis elegans epithelia. Nat Cell Biol *3*, 983-991.

Korswagen, H.C., Coudreuse, D.Y., Betist, M.C., van de Water, S., Zivkovic, D., and Clevers, H.C. (2002). The Axin-like protein PRY-1 is a negative regulator of a canonical Wnt pathway in *C. elegans*. Genes Dev *16*, 1291-1302.

Lemire, B. (2005). Mitochondrial genetics. In WormBook, T.C.e.R. Community, ed. (WormBook).

Li, X., Kulkarni, R.P., Hill, R.J., and Chamberlin, H.M., eds. (2009). HOM-C genes, Wnt signaling and axial patterning in the *C. elegans* posterior ventral epidermis (United States).

Lints, R., and Hall, D.H. (2008). Reproductive system. In WormAtlas.

Lu, X., and Horvitz, H.R. (1998). lin-35 and lin-53, two genes that antagonize a *C. elegans* Ras pathway, encode proteins similar to Rb and its binding protein RbAp48. Cell *95*, 981-991.

Maduro, M., and Pilgrim, D. (1995). Identification and cloning of unc-119, a gene expressed in the Caenorhabditis elegans nervous system. Genetics *141*, 977-988.

Maloof, J.N., and Kenyon, C. (1998). The Hox gene lin-39 is required during *C. elegans* vulval induction to select the outcome of Ras signaling. Development (Cambridge, England) *125*, 181-190.

Maloof, J.N., Whangbo, J., Harris, J.M., Jongeward, G.D., and Kenyon, C. (1999). A Wnt signaling pathway controls hox gene expression and neuroblast migration in *C. elegans*. Development (Cambridge, England) *126*, 37-49.

Marri, S., and Gupta, B.P. (2008). Dissection of lin-11 enhancer regions in Caenorhabditis elegans and other nematodes. Developmental biology, in press.

Mello, C.C., Kramer, J.M., Stinchcomb, D., and Ambros, V. (1991). Efficient gene transfer in C.elegans: extrachromosomal maintenance and integration of transforming sequences. EMBO J *10*, 3959-3970.

Miskowski, J., Li, Y., and Kimble, J. (2001). The sys-1 gene and sexual dimorphism during gonadogenesis in Caenorhabditis elegans. Developmental biology *230*, 61-73.

Myster, S.H., Cavallo, R., Anderson, C.T., Fox, D.T., and Peifer, M., eds. (2003). Drosophila p120catenin plays a supporting role in cell adhesion but is not an essential adherens junction component (United States).

Newman, A.P., Acton, G.Z., Hartwieg, E., Horvitz, H.R., and Sternberg, P.W. (1999). The lin-11 LIM domain transcription factor is necessary for morphogenesis of *C. elegans* uterine cells. Development (Cambridge, England) *126*, 5319-5326.

Newman, A.P., Inoue, T., Wang, M., and Sternberg, P.W. (2000). The Caenorhabditis elegans heterochronic gene lin-29 coordinates the vulval-uterine-epidermal connections. Curr Biol *10*, 1479-1488.

Newman, A.P., White, J.G., and Sternberg, P.W. (1995). The Caenorhabditis elegans lin-12 gene mediates induction of ventral uterine specialization by the anchor cell. Development (Cambridge, England) *121*, 263-271.

Oommen, K.S., and Newman, A.P. (2007). Co-regulation by Notch and Fos is required for cell fate specification of intermediate precursors during *C. elegans* uterine development. Development (Cambridge, England) *134*, 3999-4009.

Perens, E.A., and Shaham, S. (2005). *C. elegans* daf-6 encodes a patched-related protein required for lumen formation. Developmental cell *8*, 893-906.

Peterson, C.L., and Laniel, M.A., eds. (2004). Histones and histone modifications (England).

Pettitt, J., Cox, E.A., Broadbent, I.D., Flett, A., and Hardin, J. (2003). The Caenorhabditis elegans p120 catenin homologue, JAC-1, modulates cadherin-catenin function during epidermal morphogenesis. J Cell Biol *162*, 15-22.

Portman, D.S. (2005). Profiling *C. elegans* gene expression with DNA microarrays. In WormBook, T.C.e.R. Community, ed. (WormBook).

Priess, J.R. (1994). Establishment of initial asymmetry in early Caenorhabditis elegans embryos. Curr Opin Genet Dev *4*, 563-568.

Puig, O., Caspary, F., Rigaut, G., Rutz, B., Bouveret, E., Bragado-Nilsson, E., Wilm, M., and Seraphin, B. (2001). The Tandem Affinity Purification (TAP) Method: A General Procedure of Protein Complex Purification. Methods *24*, 218-229.

Rigaut, G., Shevchenko, A., Rutz, B., Wilm, M., Mann, M., and Seraphin, B. (1999). A generic protein purification method for protein complex characterization and proteome exploration. *17*, 1030-1032.

Rocheleau, C.E., Downs, W.D., Lin, R., Wittmann, C., Bei, Y., Cha, Y.H., Ali, M., Priess, J.R., and Mello, C.C. (1997). Wnt signaling and an APC-related gene specify endoderm in early *C. elegans* embryos. Cell *90*, 707-716.

Rocheleau, C.E., Yasuda, J., Shin, T.H., Lin, R., Sawa, H., Okano, H., Priess, J.R., Davis, R.J., and Mello, C.C. (1999). WRM-1 activates the LIT-1 protein kinase to transduce anterior/posterior polarity signals in *C. elegans*. Cell *97*, 717-726.

Salser, S.J., and Kenyon, C. (1992). Activation of a *C. elegans* Antennapedia homologue in migrating cells controls their direction of migration. Nature *355*, 255-258.

Salser, S.J., Loer, C.M., and Kenyon, C. (1993). Multiple HOM-C gene interactions specify cell fates in the nematode central nervous system. Genes Dev *7*, 1714-1724.

Seetharaman, A. (2008). Evolution of the Wnt Signal Transduction Pathway in *C. briggsae* Vulval Development. In Biology (Hamilton, ON. Canada, McMaster University), pp. 1-116.

Seetharaman, A., Cumbo, P., Bojanala, N., and Gupta, B. (2010). Conserved mechanism of Wnt signaling function in the specification of vulval precursor fates in *C.elegans* and *C. briggsae*. Developmental biology *In press*.

Seydoux, G., and Greenwald, I. (1989). Cell autonomy of lin-12 function in a cell fate decision in *C. elegans*. Cell *57*, 1237-1245.

Seydoux, G., Savage, C., and Greenwald, I. (1993). Isolation and characterization of mutations causing abnormal eversion of the vulva in Caenorhabditis elegans. Developmental biology *157*, 423-436.

Sharma-Kishore, R., White, J.G., Southgate, E., and Podbilewicz, B. (1999). Formation of the vulva in Caenorhabditis elegans: a paradigm for organogenesis. Development (Cambridge, England) *126*, 691-699.

Shaye, D.D., and Greenwald, I. (2002). Endocytosis-mediated downregulation of LIN-12/Notch upon Ras activation in Caenorhabditis elegans. Nature *420*, 686-690.

Shaye, D.D., and Greenwald, I. (2005). LIN-12/Notch trafficking and regulation of DSL ligand activity during vulval induction in Caenorhabditis elegans. Development (Cambridge, England) *132*, 5081-5092.

Shen, K., Fetter, R.D., and Bargmann, C.I. (2004). Synaptic specificity is generated by the synaptic guidepost protein SYG-2 and its receptor, SYG-1. Cell *116*, 869-881.

Sherwood, D.R., Butler, J.A., Kramer, J.M., and Sternberg, P.W. (2005). FOS-1 promotes basement-membrane removal during anchor-cell invasion in *C. elegans*. Cell *121*, 951-962.

Sherwood, D.R., and Sternberg, P.W. (2003). Anchor cell invasion into the vulval epithelium in *C. elegans*. Developmental cell *5*, 21-31.

Shi, Y., and Mello, C. (1998). A CBP/p300 homolog specifies multiple differentiation pathways in Caenorhabditis elegans. Genes Dev *12*, 943-955.

Siegfried, K.R., and Kimble, J. (2002). POP-1 controls axis formation during early gonadogenesis in *C. elegans*. Development (Cambridge, England) *129*, 443-453.

Solari, F., and Ahringer, J. (2000). NURD-complex genes antagonise Ras-induced vulval development in Caenorhabditis elegans. Curr Biol *10*, 223-226.

Stein, L.D., Bao, Z., Blasiar, D., Blumenthal, T., Brent, M.R., Chen, N., Chinwalla, A., Clarke, L., Clee, C., Coghlan, A., *et al.* (2003). The genome sequence of Caenorhabditis briggsae: a platform for comparative genomics. PLoS Biol *1*, E45.

Sternberg, P., and Horvitz, H. (1986). Pattern formation during vulval development in *C. elegans*. Cell *44*, 761 - 772.

Sternberg, P.W. (2005). Vulval development. In WormBook, T.C.e.R. Community, ed. (WormBook).

Sternberg, P.W., and Horvitz, H.R. (1988). lin-17 mutations of Caenorhabditis elegans disrupt certain asymmetric cell divisions. Developmental biology *130*, 67-73.

Sulston, J., and Horvitz, H. (1977a). Post-embryonic cell lineages of the nematode, Caenorhabditis elegans. Developmental biology *56*, 110 - 156.

Sulston, J.E., and Horvitz, H.R. (1977b). Post-embryonic cell lineages of the nematode, Caenorhabditis elegans. Developmental biology *56*, 110-156.

Sulston, J.E., and Horvitz, H.R. (1981). Abnormal cell lineages in mutants of the nematode Caenorhabditis elegans. Developmental biology *82*, 41-55.

Sulston, J.E., Schierenberg, E., White, J.G., and Thomson, J.N. (1983). The embryonic cell lineage of the nematode Caenorhabditis elegans. Developmental biology *100*, 64-119.

Sulston, J.E., and White, J.G. (1980). Regulation and cell autonomy during postembryonic development of Caenorhabditis elegans. Developmental biology *78*, 577-597.

Sundaram, M.V. (2005). RTK/Ras/MAPK signaling. In WormBook, T.C.e.R. Community, ed. (WormBook).

Thorpe, C.J., Schlesinger, A., Carter, J.C., and Bowerman, B. (1997). Wnt signaling polarizes an early *C. elegans* blastomere to distinguish endoderm from mesoderm. Cell *90*, 695-705.

Van Auken, K., Weaver, D.C., Edgar, L.G., and Wood, W.B. (2000). Caenorhabditis elegans embryonic axial patterning requires two recently discovered posterior-group Hox genes. Proc Natl Acad Sci U S A *97*, 4499-4503.

von Zelewsky, T., Palladino, F., Brunschwig, K., Tobler, H., Hajnal, A., and Muller, F. (2000). The *C. elegans* Mi-2 chromatin-remodelling proteins function in vulval cell fate determination. Development (Cambridge, England) *127*, 5277-5284.

Wang, B.B., Muller-Immergluck, M.M., Austin, J., Robinson, N.T., Chisholm, A., and Kenyon, C. (1993). A homeotic gene cluster patterns the anteroposterior body axis of *C. elegans*. Cell *74*, 29-42.

Winston, W.M., Sutherlin, M., Wright, A.J., Feinberg, E.H., and Hunter, C.P. (2007). Caenorhabditis elegans SID-2 is required for environmental RNA interference. Proc Natl Acad Sci U S A *104*, 10565-10570.

Wormbase (2010). WormBase web site, http://www.wormbase.org, release WS215, date 2010.

Wu, Y., and Han, M. (1994). Suppression of activated Let-60 ras protein defines a role of Caenorhabditis elegans Sur-1 MAP kinase in vulval differentiation. Genes Dev *8*, 147-159.

Xue, Y., Wong, J., Moreno, G.T., Young, M.K., Cote, J., and Wang, W., eds. (1998). NURD, a novel complex with both ATP-dependent chromatin-remodeling and histone deacetylase activities (United States).

Yoo, A.S., Bais, C., and Greenwald, I. (2004). Crosstalk between the EGFR and LIN-12/Notch pathways in *C. elegans* vulval development. Science *303*, 663-666.

Yu, H., Seah, A., Herman, M.A., Ferguson, E.L., Horvitz, H.R., and Sternberg, P.W., eds. (2009). Wnt and EGF pathways act together to induce *C. elegans* male hook development (United States).

Zhao, Z., Flibotte, S., Murray, J.I., Blick, D., Boyle, T.J., Gupta, B., Moerman, D.G., and Waterston, R.H., eds. (2010). New tools for investigating the comparative biology of Caenorhabditis briggsae and *C. elegans* (United States).

Zinovyeva, A.Y., Graham, S.M., Cloud, V.J., and Forrester, W.C. (2006). The *C. elegans* histone deacetylase HDA-1 is required for cell migration and axon pathfinding. Developmental biology *289*, 229-242.